Diplomarbeit

Vestibulo- ocular Responses to Off-Vertical Axis rotation during normal and altered gravity conditions- Review and Feasibility Study

eingereicht von

Yougeen Rezk

zur Erlangung des akademischen Grades

Doktor der gesamten Heilkunde

(Dr. med. univ.)

an der

Medizinischen Universität Graz

ausgeführt am

Institut für Physiologie

unter der Anleitung von

Daniel M. Merfeld, Ph.D. Professor of Otology and Laryngology

(Harvard Medical School – Massachusetts Eye and Ear Infirmary)

und

ao. Uni.-Prof. Dipl.-Ing. Dr.tech. Eugen Gallasch

Graz, 10 Juli 2015

Eidesstattliche Erklärung

Ich erkläre ehrenwörtlich, dass ich die vorliegende Arbeit selbstständig und ohne fremde Hilfe verfasst habe, andere als die angegebenen Quellen nicht verwendet habe und die den benutzten Quellen wörtlich oder inhaltlich entnommenen Stellen als solche kenntlich gemacht habe.

Graz, am 10 Juli 2015 *Yougen Rezk eh*

Acknowledgements

This diploma thesis has grown out of an application for a research project, which I created for the European Space Agency (ESA) and submitted to the former Austrian Space Agency (ASA). The experimental proposal included, was also presented at the International Space University during the Space Studies Program in 2011.

During the time working on that project, I was lucky enough to come in touch with interesting and inspiring people among them my mentor and thesis advisor at the Medical University of Graz Prof. Eugen Gallasch who helped me through this process therefore, thank you! In the last couple of years, I had to travel, to work and to get involved in the latest research activities in the field of neurovestibular research. That was just possible through the generous support of great and well-known researchers in this area. In this context, I would like to thank all my mentors and colleagues at the life science department of the International Space University. Among them Prof. Gilles Clément who has helped me with great advice. I would also have to thank Dr. Bernard Cohen at the Mount Sinai Hospital for his mentorship and his patience.

Special thanks to Prof. Daniel Merfeld, at the Massachusetts Eye and Ear Infirmary, who is not just my thesis advisor but has also become a great supporter through the entire working process of nearly a decade.

Table of Contents

List of Abbreviations

CW	Clockwise
CCW	Counter Clockwise
CCD	Charge-Coupled Device
CNS	Central Nerve System
EOG	Electrooculography
GIA	Gravito-Inertial-Accerletion
GIF	Gravito-Inertial-Force
lVOR	Linear Vestibulo-Ocular Reflex
OCAR	Off-Center Axis Rotation
OKAN	Optokinetic After Nystagmus
OKN	Optokinetic Nystagmus
OVAR	Off-Vertical Axis Rotation
rVOR	Rotational Vestibulo-Ocular Reflex
SCC	Semicircular Canal
SPV	Slow Phase of Velocity
SV	Subjective Vertical
VEMP	Vestibular Evoked Myogenic Potential
VOG	Video-Oculography
VOR	Vestibulo-Ocular Reflex

List of Figures

List of Tables

Zusammenfassung

Das vestibuläre System trägt maßgeblich dazu bei uns in einer gravitationsbedingten Kraftumwelt stabil zu bewegen und dabei unsere visuelle Orientierung zu unterstützen. Das periphere vestibuläre System besteht dabei aus fünf rezeptiven Strukturen zur Registrierung von Kopfbewegungen in allen drei Hauptbewegungsachsen: den zwei Otolithenorganen zur Aufnahme von Lageinformation und Linearbeschleunigungen, und den drei Bogengängen zur Aufnahme von Winkelbeschleunigungen. Sowohl Otolith- als auch Bogengangafferenzen interagieren um kombinierte Augenbewegungen zu generieren. Zahlreiche Studien auf Basis von dreidimensionalen Augenbewegungen wurden unternommen mit dem Ziel bessere Modellvorstellungen über die Zusammenhänge zwischen Gravitation, Kopfbewegungsreiz und den daraus resultierenden Augenbewegungen zu entwickeln. In diesem Zusammenhang wurden im Speziellen die Kanal-Otolith Interaktionen während der sogenannten Schrägachsenrotation (OVAR) genauer charakterisiert.

Ziel dieser Diplomarbeit ist eine Zusammenfassung der Studien bezugnehmend auf Normo- Hyper- und Hypogravitationsbedingungen. Zu diesem Zweck ist die vorliegende Arbeit in drei Teile gegliedert: Der erste Teil soll einen physiologischen und klinischen Überblick in Hinblick auf das vestibulo-okulomotorische System vermitteln. Zweiter Teil der Arbeit hat vergangene Schrägachsenrotation Studien im Fokus. Dieser bildet den erklärenden Übergang zum dritten Teil, einem Studienvorschlag für eine Parabelflug-Mission zur Untersuchung dreidimensionaler Augenbewegungen unter alternierenden Gravitationsbedingungen.

Abstract

The vestibular system consists of two components that cooperate to indicate our orientation and movement in space: the otoliths and the semicircular canals. While the canals respond to rotational movements the otoliths, in contrast, are responsible for the determination of our orientation in gravity. The otolith signals interact with the signals from the canals to generate combined eye movements. Studies on three dimensional eye movements during off-vertical axis rotation (OVAR), combined with model-based analysis have been done in order to characterize these canal-otolith interactions. The goal of this thesis is to review these studies with respect to hypo- and hyper-gravity. Based on the mentioned the present thesis consists of three main parts: The first part, gives a correlated physiology and clinical overview of the vestibulo-ocular system. The second part focuses on OVAR studies done in the past, which forms a transition to the third part of this thesis, a feasibility study for a parabolic flight campaign of the European Space Agency.

1 Introduction

1.1 Sensory functions

To obtain accurate information about our body position towards gravity we need a highly precise and adapted system. The physiological mechanisms and neural pathways supporting that system are only made possible by the interaction of very specialized sensory organs. The vestibular apparatus plays an important key role in this context. It is part of the sensory motor system, which controls daily actions like the adjustment of body orientation, locomotion, and accurate eye movements. This controlling system needs neuro-sensory information from vestibular, vision and proprioceptive organs. As signals from the vestibular and proprioceptive organs alter very much under changing gravity conditions, space neuroscientists wonder about the following question:

"***What is the relative contribution of gravity to these sensory and motor functions?***"

(Clément 2003, p. 91)

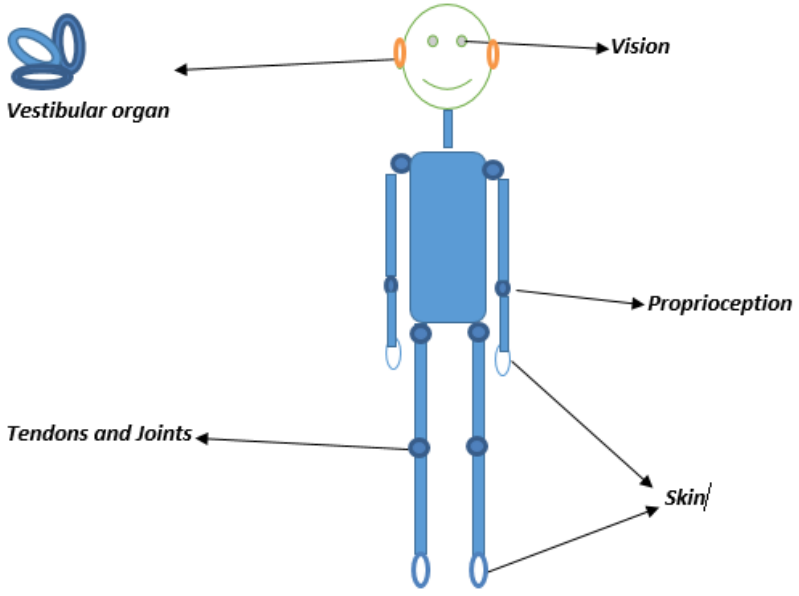

Figure 1: *Sensory Systems,* draft adapted from 'Fundamentals of Space medicine' (Clément 2003, p. 91)

1.2 OVAR

A variety of vestibular stimulation forms where used to answer the previous question. Among them, a vestibular stimulation method often referred to as Off-Vertical Axis Rotation (OVAR). During OVAR the rotatory axis is no longer parallel to the gravity vector like during the rotational VOR described in section 1.5 (see Figure 2 below). OVAR is considered an interesting stimulation form as it combines stimulation of the semicircular canals and otolith organs. However, when studying the literature off vertical axis rotation has proven to be mainly useful as a test of otolith function (Highstein, Fay & Popper 2004, p. 262). (see also chapter 2)

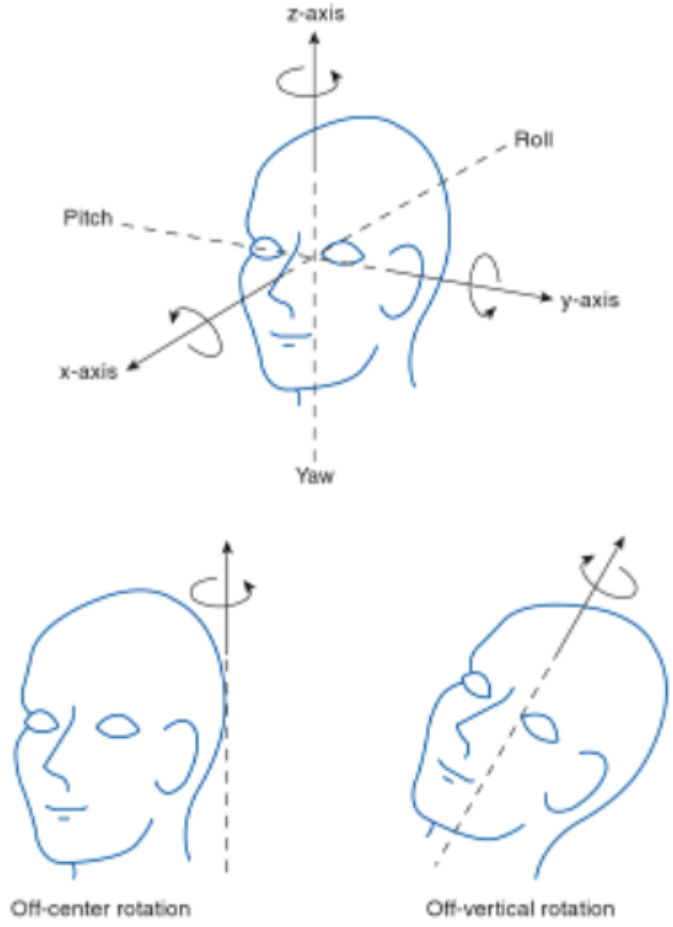

Figure 2: *Illustration of Rotational Axis.* From 'Clinical Neurophysiology of the Vestibular System' (Baloh., Honrubi & Kerber 2010, p. 190)

1.3 Vestibular System

1.3.1 **Vestibular Apparatus**

The vestibular apparatus is located in the petrous (pars petrosa) of the temporal bone (os temporale) at the base of the skull (see below Figure 3). It is composed of nerve cells that detect linear and angular accelerations. The semicircular canals (SCCs) are positioned in a 90-degree angle to one another in all three dimensions. SCCs are filled with a fluid called endolymph. During rotational head movements (angular acceleration) the endolymphs move, which leads to a stimulation of the canal in the plane of movement. This is the functional base for the detection of angular acceleration (Cohen & Gizzi 2002).

On the other hand, the vestibular apparatus also consists of a system for sensing linear acceleration, which is called otolith organ. There are two subsystems of the otolith organ. The utricle (horizontal acceleration) and the saccule (vertical acceleration) (Klinke & Silbernagl 2001, p. 596). A changing gravity vector would mainly affect this specific part of the vestibular organ. (Planel 2004, p. 71).

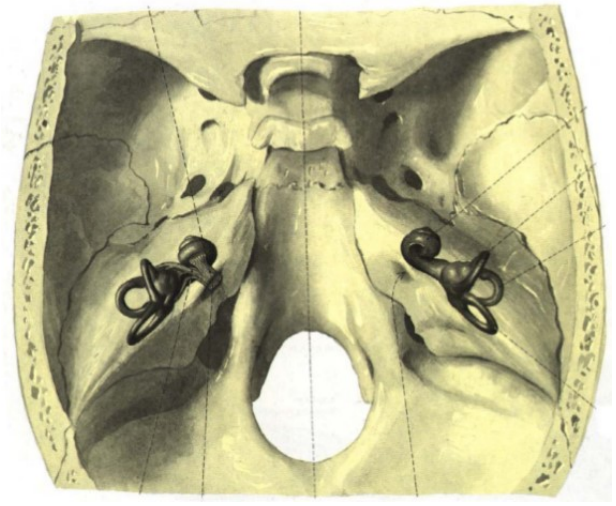

Figure 3: *Skull base location of the vestibular organ*. From ‚Der vestibulo-okuläre Reflex (VOR) und seine klinische Bedeutung', slide 11. (Straumann 2014) Taken from: http://slideplayer.org/slide/1341039/

1.3.1.1 Otolith Organs

The macula organs are the secondary sensory epithelia of the vestibular organs. Their main purpose is to register the gravitation (linear acceleration of 9.81 m / s2). There are two macula organs, called macula sacculi and macula utriculi (Klinke & Silbernagl 2001, p. 597). The sacculus and utriculus are located in a cavity of a forecourt, which lies between the cochlea and the semicircular canals. (see below Figure 4) The ductus utriculosaccularis is the connection through which sacculus and utriculus are connected with each other. When seen through the microscope, macula sacculi and macula utriculi are pelvic-shaped discs which stand roughly vertically on each other (Goldberg et al. 2012, p.8). Both the utricle and the saccule have an epithelium, consisting of the following layers: an upper otolith layer, a lower gelatinous layer attached to the macula. (see illustration below Figure 4) Macula organs contain hair cells called stereocilia and kinocilia, which dive into a gelatinous mass. On top of the sensory cells thin processes reach into the gelatinous membrane' (Planel 2004, p. 71). Otoliths are very fine crystalloid sensors consisting of calcium carbonate (Baloh & Honrubia 2011, p. 47). These otolith crystals have a higher density than the gelatinous surrounding (Klinke & Silbernagl 2001, p.599). Therefore, they accelerate relatively more and are thereby able to shift the otolithic membrane during head movements. As stereocilia are spatially unequally oriented, different acceleration vectors can be sensed. Sensory cells detect these shearing forces by a microscopically fine bending in the stereocilia. Therefore, straight translational movements and divergences of the head positions with respect to the vertical axis can be perceived through the otoliths (Highstein, Fay & Popper 2004, p. 181).

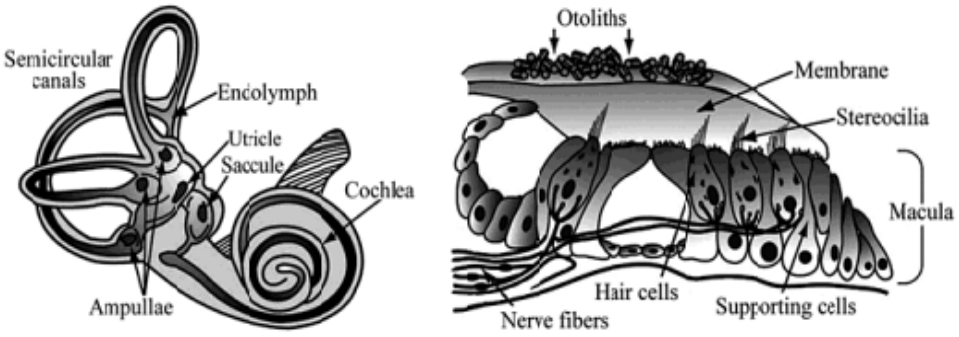

Figure 4: (*left) vestibular organ* and *the three layers of the otolith organ (right)*. From 'Fundamentals of Space Physiology' (Clément 2011, p. 99)

The principal function of the saccule is providing accurate perception of the vertical position, whereas the utricle is of importance when it comes to detecting horizontal accelerating and decelerating movements. The curved shape of the saccule also allows censoring movements that are exactly in vertical or horizontal planes (Saborowski 2001, p. 24). (see below Figure 5) A number of studies have demonstrated the major influence otoliths have on static and dynamic contribution on sensomotoric physiology (Bockisch, Straumann & Haslwanter 2005; Darlot & Denise 1988; Harris 1988; Haslwanter, Jaeger, Mayr & Fetter 2000). In space, for example the function of the macula utriculi and sacculi is strongly disturbed, which often results in misperception and in motion sickness symptoms (Clément 2003, p. 92).

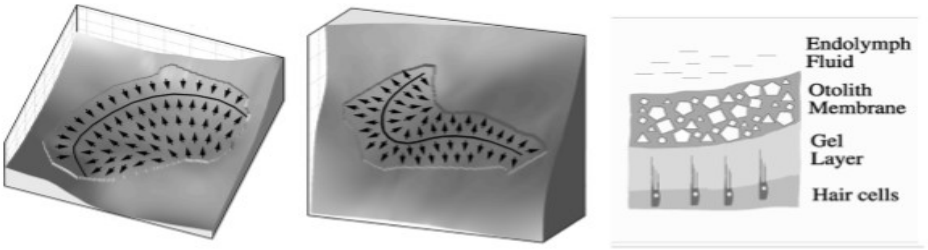

Figure 5: The *otholith organs* are responsible for sensing linear acceleration. *The utricle (left)* is approximately horizontally oriented; *the saccule (center).* From 'Sensory Systems Physiology & Computer Simulations' (Haslwanter et al. 2014, p. 120)

1.3.1.2 Semicircular Canals

The semicircular canal system detects angular acceleration. These canals are filled with a fluid called endolymph. The following figure also shows that the cupula is a biosensor switch located in the semicircular canals. Three cupula deflection states lead to different perception of dynamic physiological signals. The cupula can be in a resting position, in excitation or in inhibition deflection mode (Klinke & Silbernagl 2001, p. 599). Of course, these states depend on the direction of rotation. The movements of the endolymph in relation to the semicircular tube activate the cupula during rotational head movements. Resulting signals are bundled and sent through the vestibular ramus of the vestibulocochlear nerve to further processing regions (nuclei) of the brainstem (Klinke & Silbernagl 2001, p. 599-600).

1.4 Pathways

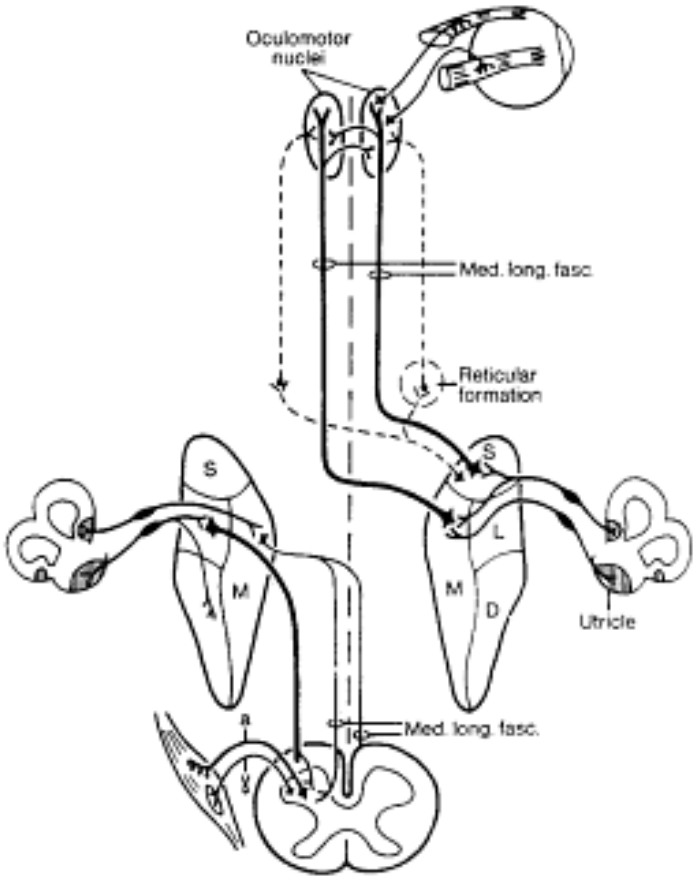

Figure 6: Interaction of the *vestibulo-ocular reflex (VOR)* and *the vestibulospinal reflex (VSR).* From 'Das Gleichgewicht' (Scherer 1997, p. 16)

Signals resulting from afferent sensing cells located in macula and cupula are further sent to the vestibular nerve and then processed in the ipsilateral vestibular nuclei. There are four vestibular nuclei: the medial (Schwalbe), labeled (M) the lateral (Deiters), labeled (L) the superior (Bechterew), labeled (S) and the inferior nucleus (Roller) labeled (D) (Johst 2001). (see beside Figure 6) Inhibiting pathways between these nuclei regulate the sensitivity of the contralateral side. The medial longitudinal fasciculus consists of excitation and inhibiting pathways to ipsi- and contralateral oculomotor nuclei. Secondary vestibular pathways run from the vestibular nuclei to the medulla, reticular formation to the cerebellum and to the external eye muscles (Klinike & Silbernagl 2001, p. 692). (see above Figure 6) The lateral vestibular nucleus (Deiter) further sends signals through the lateral vestibulospinal tract, to the ipsilateral motor neurons of the extensor and to the lumbosacral medulla segments. This tract signals stimulate the alpha and gamma moto neurons, in addition to the reticolospinal fibers. Motor neurons support extensors of the legs and flexors of the arms (antigravity muscles), so that the body can keep translated with respect to gravity (Klinke & Silbernagl 2001, p. 653-671).

Nerve fibers coming from the medial nucleus and superior nucleus run to the nuclei of the eye muscles (nucleus of abducens nerve, nucleus of trochlear nerve, nucleus of oculomotor nerve). (see next page Figure 7) There are as well connections to the thalamus (ventral lateral nucleus). The vestibular apparatus works as a sensor input for modifying interactions between neck muscles and eye muscles (Goldberg et al. 2012, p. 6-8). (see Figure 6) Mechanoreceptors of the human body perceive influences from the surrounding; based on this information CNS adapts the movement and posture of the limps in relation to gravity and to each other. These proprioceptive mechanic receptors are also called extra vestibular receptors. They allow us a perception of spatial perception and belong to the somatosensory system. Mechanoreceptors are located in the skin and enteroreceptors are located in the depth of the human body. Enteroreceptors are mainly proprioceptors, which can be found in muscles, tendons and joins. The proprioceptors of the muscles are also known as muscle spindles, which are sensors registering stretching states of the affected muscles. These spindles contain gamma motoneurons of the anterior horn through contraction of these; the gamma motoneurons can modulate the sensitivity of the stretching status. Afferent signals of muscles and their tendons are registered, and combined processing takes place in the integrative parts of the brain stem (see in Figure 6). Resulting information is further sent to the vestibular nuclei and the brain cortex (Klinke & Silbernagl 2001, p. 601-602) [1]. The nuclei of the brainstem are considered to have neuronal integral functions and are therefore the major assembling location of central processing synapses and responsible for the vestibular-oculomotor coordination. The connection explained shows the principle of how the brain is able to stir and coordinate eye, head and limb movements. However, depending on where the firing rates are coming from (whether from the canals or otoliths), signals are sent to the specific nuclei. Signals resulting from the excitation of sensory cells in the macula organs run through the vestibular ganglion, the radix vestibularis and to the vestibular nuclei, located in the medulla oblongata. The radix vestibularis divides path at the lateral nucleus (Deiter) the nerve runs further to the superior nucleus (Bechterew), medial nucleus (Schwalbe) and inferior nucleus (Fanghäne et al. 2003, p. 473). Signals from the semicircular canals are mainly sent to the superior and medial vestibular nucleus (see next page in Figure 7). The nerve fibers coming from the medial nucleus run to the vestibuluspinal tract, where they bifurcate to the cervical part of the medulla.

[1] For further reading: Klinke, R., & Silbernagl, S. (2001). Lehrbuch der Physiologie. In R. Klinke & S. Silbernagl Sensomotorische Systeme: Körperhaltung, Bewegung und Blickmotorick (3. ed., pp. 562, 669-685). Thieme.

The monosynaptic motor neurons located here induce contractions of the neck muscles (Fanghäne et al. 2003, p. 473-475). The physiological pathways of this tract have proven to be very useful for clinical diagnostics (Luft 2011). The lateral vestibular nucleus receives inhibiting afferents from the utricle, the cerebellum and the medulla. The inferior vestibular nucleus receives fibers from the semicircular canals as well as from the utricle and saccule. Additionally, this nucleus receives information from the cerebellar vermis. The majority of the efferent pathways run through the vestibulospinal and vestibuloreticular tract (Klinke & Silbernagl 2001, p. 600-602). Fibers going to the superior and medial vestibular nucleus run to the medial longitudinal fasciculus; from here they go to the front part of the pons, located under the middle line of the fourth ventricle. The medial longitudinal fasciculus connects the vestibular nuclei with eye movement processing nuclei in the middle brain and with the motoric apparatus of the cervical medulla (Fanghäne et al. 2003, p. 474-477). (see below Figure 7)

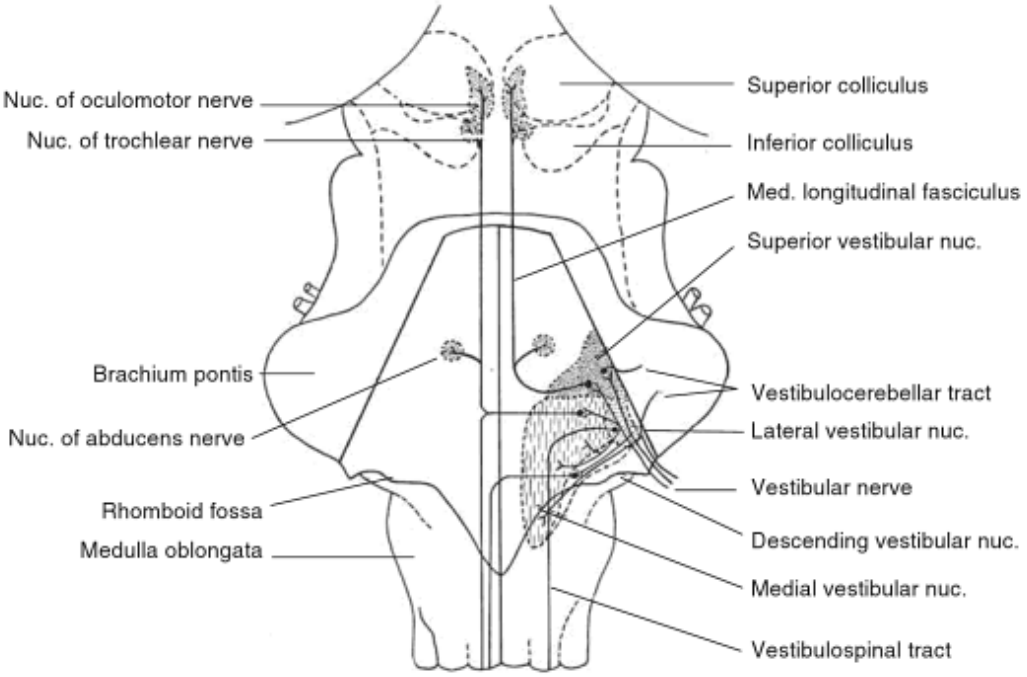

Figure 7: Shows the *communication pathways of the vestibular nuclei.* Taken from 'The Vestibular System A Sixth Sense' (Goldberg et al 2012, p. 6)

1.5 Vestibulo-Ocular Reflex

Beside eye mechanics and the physiology of the eye, the research of reflex arcs and their resulting eye movements are of major importance for clinical diagnostics. These reflex circuits are e.g. activated for stirring the eyeball during head movements. Consequently, it is crucial to gain a profound knowledge of these neural mechanisms in order to get a better integrative understanding of the involved brain regions. A deeper understanding of these neuronal signal processes is of importance when it comes to diagnosing neuro-vestibular disorders and their localization. In this context, the vestibulo-ocular reflex is of importance to discuss.

1.5.1 **Description of the Vestibulo-Ocular Reflex**

To keep a sharp view of our surroundings during rotational head movements the brain has to manage two specific tasks. First, it has to hold the gaze and second, it needs to determine the appropriate angle of movement needed for achieving this gaze direction. The gain of the VOR is the quotient resulting by dividing angular changes of eye movements into angular changes of head movements.

$$\text{Gain} = \frac{\Delta\text{Eye}}{\Delta\text{Head}}$$

Such compensation mechanisms are particularly important while rotating around yaw axis because the eye has to focus on a different image per degree of rotation. The vestibulo-ocular reflex generates such compensatory eye movements (see Figure 9). As every head rotation stimulates an eye movement in the opposite direction, the following three-neuron reflex arc is highly important in this respect. Angular (de)acceleration signals coming from the semicircular canals are sent through the vestibular nerve to the vestibular nuclei. These signals are then translated into inhibiting and stimulating signals and are further sent to the motor neurons of the six extra ocular eye muscles (Klinke & Silbernagl 2001, p. 692).

The Vestibulo-Ocular Reflex Arc

This neuronal reflex is a neurophysiological signal processing mechanism and consists of three neurons. In this context the following nuclei have integrative functions: First, is the vestibular nucleus located in the brainstem, second is the abducens nucleus and the third is the oculomotor nucleus (Klinke & Silbernagl 2001, p. 692-693). (see next page Figure 9) During rotational testing e.g. vestibulo-ocular reflex (see below Figure 8); head torsion reaches a 10 to 20 degree angle, so an ocular nystagmus appears. There are two components of the nystagmus. A fast phase of velocity and compensatory eye movement also referred to as the slow phase of velocity (SPV). The three-neuron vestibulo-ocular reflex arc was first described by Lorente de Nó in 1933 and was later confirmed by Szentàgothai in 1950 (Highstein, Fay & Poppe 2004, p. 241).

Illustration:

Test situation **VOR**:

Figure 8: Shows *test subject in experimental Situation (VOR)*. Taken with permission from EKIDA GmbH

Illustration of the Vestibulo-Ocular Reflex Arc

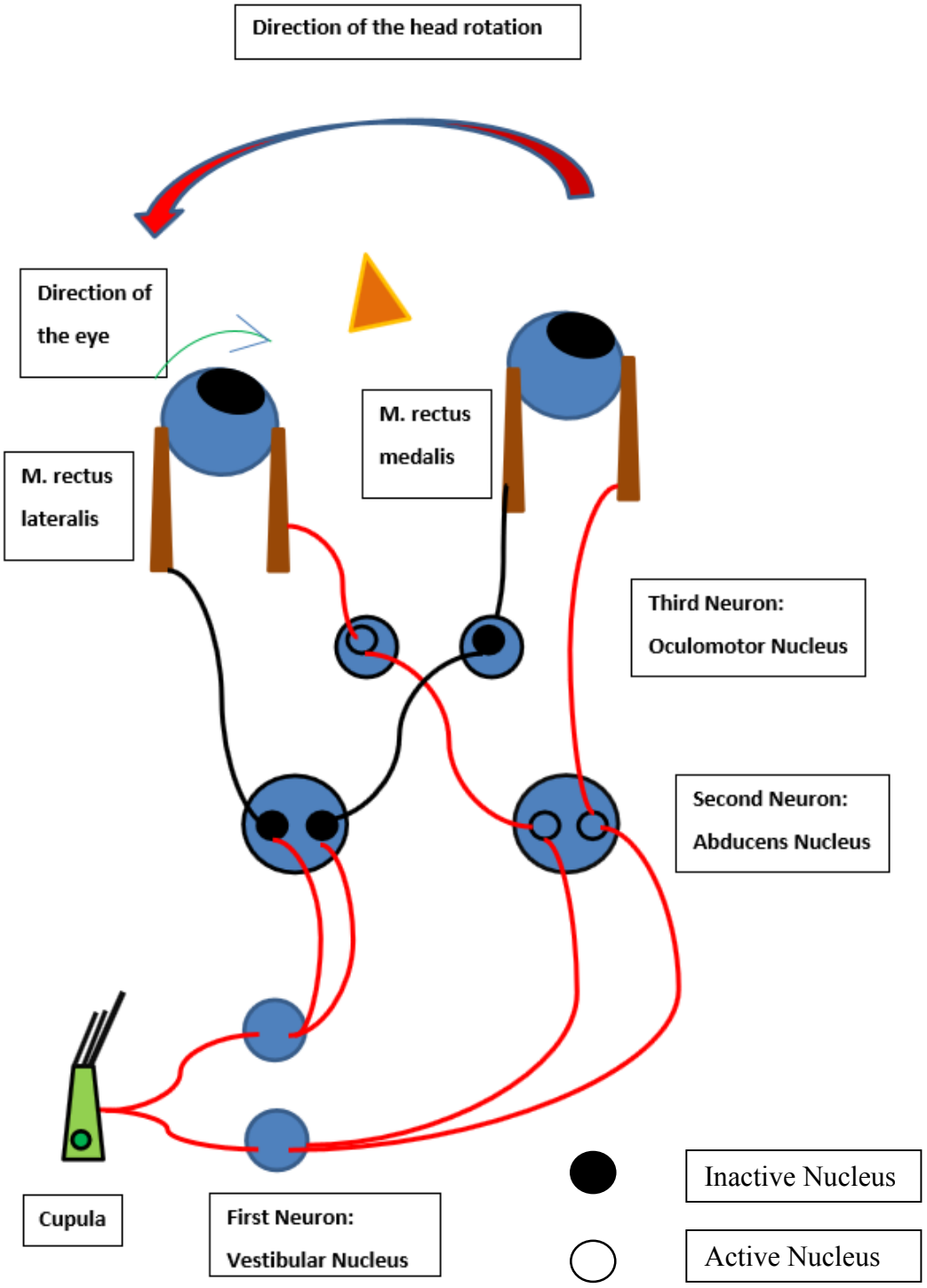

Figure 9: *Arc of the VOR.* Adapted from 'Lehrbuch der Physiologie' (Klinke & Silbernagl 2001, p. 692)

Neural circuits were clarified through recordings and investigations of electric potentials coming from the vestibular and oculomotor nuclei cells after semicircular canal stimulation (Cohen & Suzuki 1963; Cohen 1974; Uchino & Suzuki 1983). These tests have also shown variations in different species (Cohen 1974; Baloh et al. 2011, p. 75).

These experiments have shown that a stimulation of the horizontal semicircular canals results in a di-synaptic activation of the contralateral medial rectus muscles and a di-synaptic inhibition of the ipsilateral lateral rectus muscle (see below Table 1). In contrast to this, stimulating the anterior semicircular canal activates the contralateral superior rectus muscle and the inferior oblique muscle in addition to a di-synaptic inhibition of the ipsilateral superior oblique muscle and the inferior rectus muscle. Stimuli in the posterior canal lead to activations in the contralateral superior oblique muscle and the inferior rectus muscle, while the ipsilateral superior rectus muscle und the inferior oblique muscle receive inhibiting signals (Uchino & Suzuki 1983; Baloh et al. 2011, p. 75). For graphical illustration, (see Figure 10 on the next page).

Semicircular Canal	**Activation**	**Inhibition**
Horizontal	Ipsilateral medial rectus muscle. Contralateral lateral rectus muscle.	Ipsilateral lateral rectus muscle. Contralateral medial rectus muscle.
Anterior	Ipsilateral superior rectus muscle. Contralateral inferior oblique muscle.	Contralateral superior oblique muscle. Ipsilateral inferior rectus muscle.
Posterior	Ipsilateral superior oblique muscle. Contralateral inferior rectus muscle.	Ipsilateral inferior rectus muscle. Contralateral superior oblique muscle.

Table 1: Shows *activated and inhibited eye muscles* in correspondence to the *stimulated Semicircular Canal*. Adapted from 'Clinical Neurophysiology of the Vestibular System.' (Baloh, Honrubi & Kerber 2011, p. 75)

Neural Pathways of the Vestibulo-Ocular Reflex

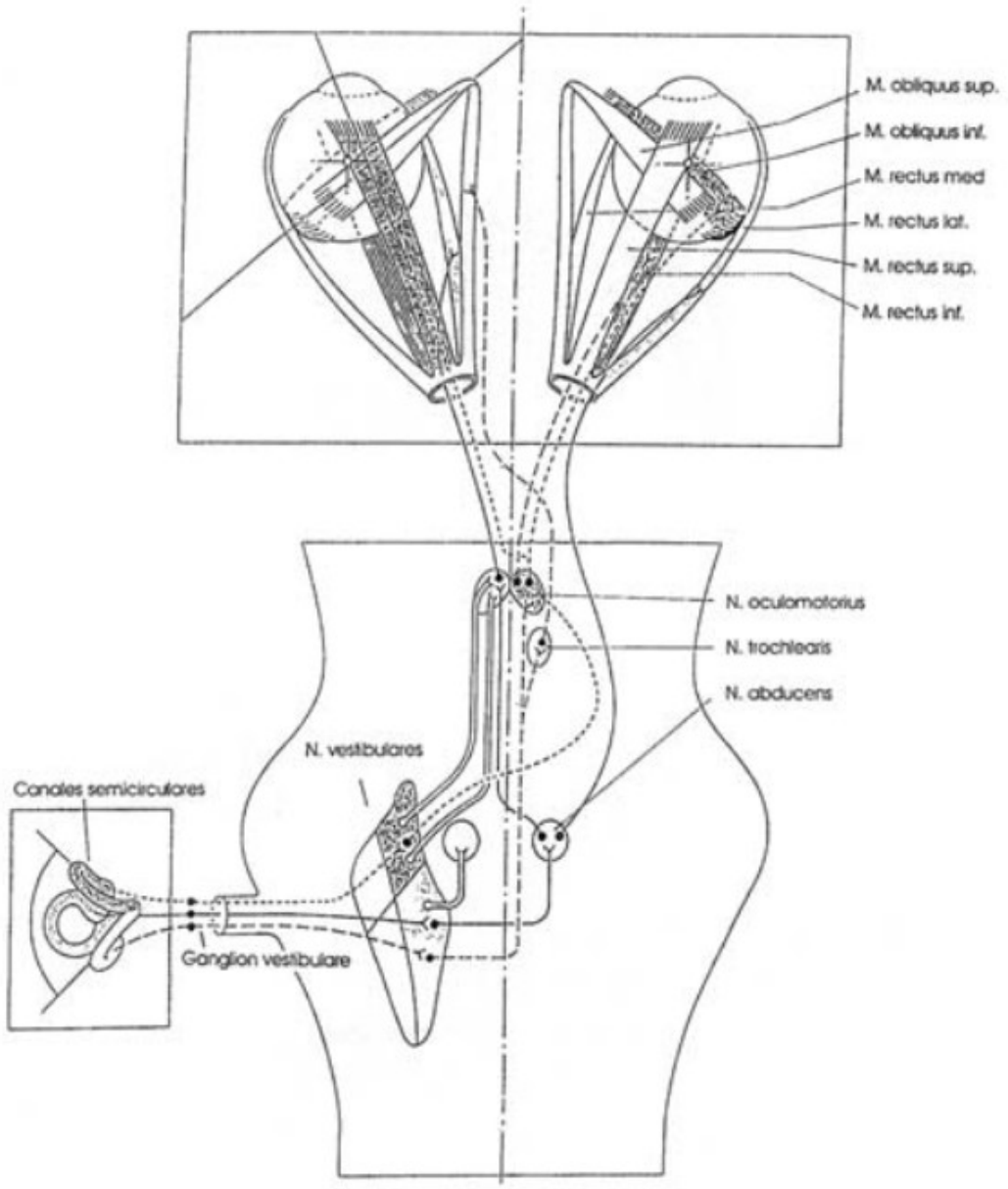

Figure 10: *Central processing pathways vestibular organ, nuclei and eye muscles*. From 'Neuere Aspekte des vestibulo-okulären Reflexes.' (Clarke 1995, p. 14)

1.6 Velocity storage phenomenon

The velocity storage is a well-established explanation model for rotational head movements. When a subject is accelerated on a rotatory device, for example, the compensatory eye movements last significantly longer than the mechanical stimulation. The three-neuron complex cannot explain this phenomenon. The term "velocity storage mechanism" describes a neural integrator storing and prolonging signals coming from the periphery vestibular organ (Raphan et al. 1979). Lately there have been interesting patient studies focusing on the relation between velocity storage mechanism and motion perception (Bertolini et al. 2012). The illustration below (Figure 11) explains the composition of the velocity storage mechanism and describes it in form of a positive feedback model.

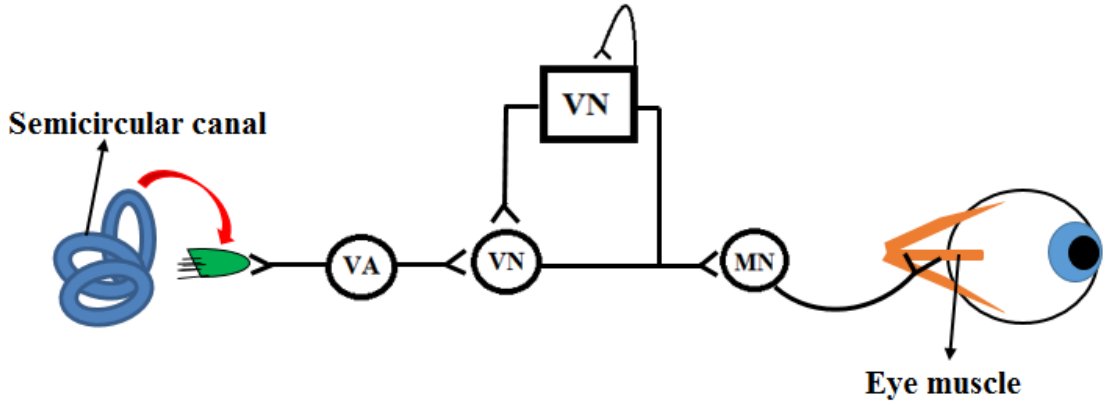

Figure 11: *The velocity storage.* Adapted from 'Tutorial on Neural Systems Modeling' (Anastasio 2010, p. 44)

Vestibular afferences coming from the semicircular canal (SCC), labeled (VA) are sent to the vestibular nuclei, labeled (VN). The vestibular nuclei have crucial functions, like the integration and processing of different sensory information (see chapter 1.6). However, these neurons also have a major influence on the prolongation of the nystagmus. As they already code for the extension of the time constant after receiving the original firing pulse e.g. from the SCC. Exemplary, in humans, the cupula decline is ≈ 4 s and the time constant is 12-20 s (Luxon, Furman, Martini & Stephens 2002). As a result, the prolonged signal is translated into eye movements by the motoric neuron, labeled (MN) in the figure above.

In 1991 Hess and Dieringer studied 3-D eye movements of the linear vestibulo-ocular reflex in rats. Eye movements of rats where recorded with search coil technique during sinusoidal acceleration in tilt angels from 15 to 360 degrees with respect to the acceleration vector. The most important findings were that there was a strict correspondence between the direction of acceleration and vestibulo-ocular responses. More specific accelerations types e.g. along the diagonal body axes have shown a maximum in vertical and torsional eye movements. These findings have supported the hypothesis that there is a synergistic effect during linear acceleration between the afferent nerves of the macula and the vertical semicircular canals (Hess & Dieringer, cited in Waltmann 2004). Büttner showed in 1978 that after optokinetic stimulation the ocular kinetic time response lasts for about 12-20 seconds. This is in contrast to the time response of 4-6 seconds response found by recording the potentials from the vestibular nerve (Büttner & Waespe, cited in Waltmann 2004). This delay led to the idea that there must be some sort of positive feedback system, a central loop, which is often referred to as "velocity storage mechanism". This was investigated and described in monkeys (Raphan et al. 1977), and later in humans (Raphan et al. 1979; Waespe & Schwarz, cited in Waltmann 2004). In 1971, Goldberg and Fernández showed changes in the time constant of the velocity storage in different species. For instance in humans it is 1.68 times longer than in monkeys. The velocity storage integrator has shown that there is an optimal frequency range in which head movements translate into eye movements. This range indicates a stable relation between the vestibular stimulus and the resulting time vector of the nystagmus. The frequency optimum of the semicircular canals is between 0.5 and 5 Hz whereas the optimums range of the otolith organs is between 0 and 2 Hz (Goldberg & Fernández, cited in Waltmann 2004).

1.7 Classical Tests

1.7.1 Investigation methods of central vestibular system

The optokinetic reflex

Optokinetic and vestibular reflexes are complementing each other. The optokinetic reflex is induced e.g. by walking so that moving surrounding objects are focused on the fovea centralis, to provide a stabilization reference. Direction and velocity of an image are sensed and coded by motion sensors called glia cells located in the retina (Klinke & Silbernagl 2001, p. 693).

Saccades

This form of eye movements is fast (700°/s), exact and happens while shifting from one object to another. Saccades can also be found in the nystagmus of the VOR, also known as the fast phase of velocity (Scherer 1997, p. 24). They are preprogrammed and ballistic and can therefore not be changed as soon as they start. Vertical and horizontal components of saccades are generated in the neural network of the brainstem. The paramedian pontine reticular formation is responsible for the horizontal eye movements (Scherer 1997, p. 29) whereas torsional and vertical components are generated through the so called mesencephalic reticular formation (Klinke & Silbernagl 2001, p. 694-695).

Refectory Saccades

This form occurs as soon as an object is sensed in the periphery of the optical field (Klinke & Silbernagl 2001, p. 695).

Arbitrary Saccades

For the visual exploration of our surroundings, this form of saccades generated by the cerebral cortex is of major importance. Arbitrary saccades are responsible for positioning the fovea of the eye to a specific image of interest while simultaneously suppressing refectory saccades. Therefore this reflex plays a clinical key role in patients with cortical lesions; specifically damaged cortical regions would lead to a suppression disability of the refectory saccades (Klinke & Silbernagl 2001, p. 695). Interesting experiments have tested modulate effects of transcranial magnetic stimulation on the generation of saccadic eye movements (Jenkinson & Miall 2010).

Conjugated eye movements

The cortex stirs eye pursuits of moving objects in a constant distant. This form of eye movements is smooth, therefore also called "smooth pursuit eye movements" and should not show any forms of saccades. Conjugated eye movements are important for the fixation of moving objects on the retina's fovea (Scherer 1997, p. 29).

Vergence

If in contrast to the conjugated eye movements the distance between the eyes and the object changes, the brain has to calculate different vision angles for both eyes, and the resulting eye movements are called, vergence. This kind of eye movement is the major reason why binocular vision creates a 3-dimensional perception (Klinke & Silbernagl 2001, p. 696-697).

Combined movements of eyes and head

Fast eye movements exceeding 10 degrees are combined with head movements, these compensatory saccadic eye movements are the fundamental basic for the vestibulo-ocular reflex (VOR). Saccade eyeball motions happen fast, and are followed by compensational head movements. This very well coordinated process leads to following useful compensation: fovea reaches its goal fast, fovea keeps focusing the image although head movement is still there, eye movements get back to the original position and all other sense organs (eye, ear, nose) get aligned with the direction of gaze (Klinke & Silbernagl 2001, p. 697).

The important role of the vestibular nuclei

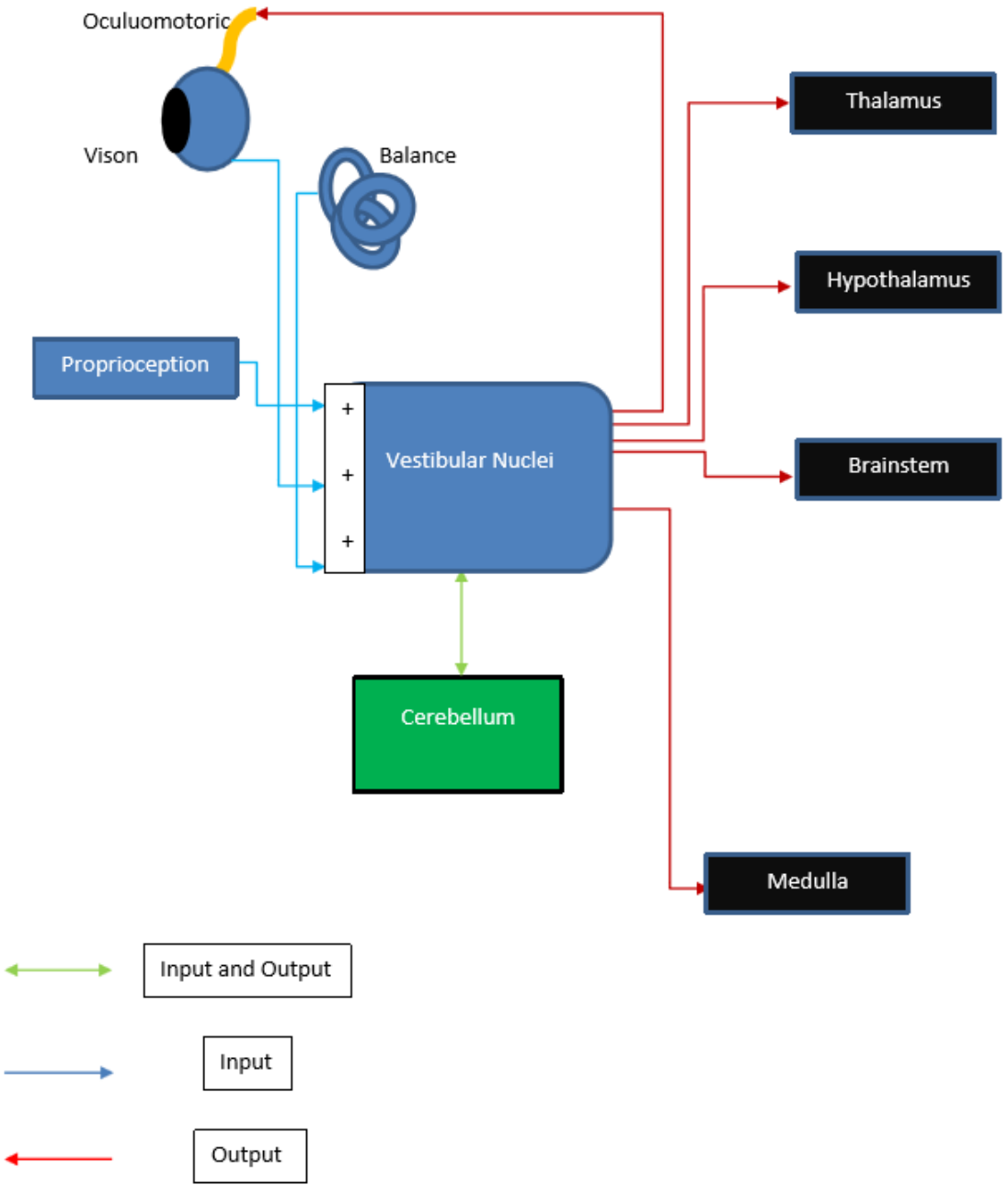

Figure 12: Shows the *vestibular nuclei* and their integrative functions. Adapted from 'Die anatomische Lokalisation des VEMP-Reflexes im Hirnstamm**.** (Luft 2011, p. 13) Originally taken from (Schünke et al. 2006)

1.7.2 Investigation methods of the periphery vestibular system

For clinical diagnostics, a combination of anamnesis and eye movement protocols are indispensable. Especially as the classification of vestibular symptoms is not easy, it is strongly related to clinical disciplines, comorbidities and other patient specific symptoms (Bisdorf et al. 2009). Anamnesis often gives information about the sort of dizziness and the pathologic mechanisms behind the patient's symptoms. Peripheral vestibular disorders for example often show symptoms of dizziness with a tendency to a specific direction. On the other hand, central vestibular disorders show unspecific symptoms and are therefore more difficult to diagnose. Typical diagnosing procedures are e.g. the Romberg test or Unterberger's stepping test (Scherer 1997, p. 100). However, the investigation and diagnosis of the specific canals and functional subsystems of the peripheral vestibular organ remains a challenging task. Therefore, functional tests have become indispensable.

Tests of the Semicircular Canals

Vestibular disorders can be diagnosed by using Frenzel goggles and by detecting spontaneous eye movements called nystagmus. A combination of a video-oculography (VOG) and an electro-oculography (EOG) device makes more accurate eye movement investigations possible. Unilateral semicircular canal investigation is possible with the caloric test (Clarke 1995, p. 23-25).

The caloric test

This test mainly activates the sensory cells of the horizontal canal and of the utricle (Klinke & Silbernagl 2001, p. 596). The labyrinth is activated by warm (44°C) and cold (30°C) water irrigation of the external auditory canal. This procedure leads to a change in the resting membrane potential of the vestibular nerve and as a result to a nystagmus (Scherer 1997, p. 196).

Rotatory tests

As seen above in section 1.5 rotatory tests have effects on both sides of the periphery vestibular systems. The vestibulo-ocular reflex is the basic mechanism behind the head trust test. The head trust test is the only bedside test for (SCCs) possible in clinical routine and is therefore of major importance. The test person has to fix a point, while the physician rotates the head quickly about 10 to 20° to the left and to right. Pathologic head trust tests show correction saccades (Baloh et al. 2011, p. 153). (see below Figure 13)

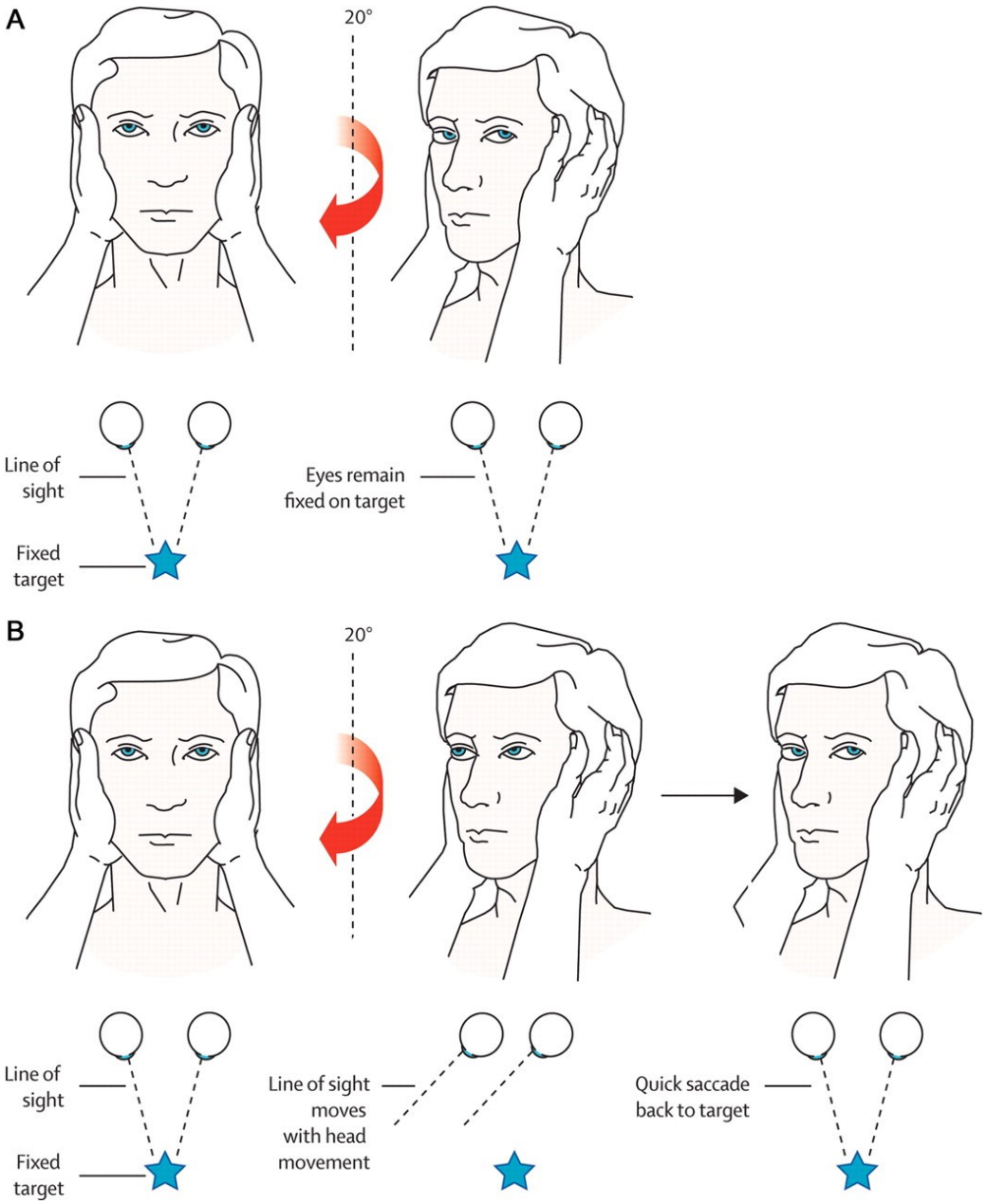

Figure 13: The *head trust* test shows the physiological response (A) and the pathologic correction *saccades* (B). Illustration taken from "The evaluation of a patient with dizziness" (Kerber & Baloh 2011, p. 27)

Tests of the Utricle

The utricle ocular reflex and the subjective vertical (SV) are tests of utricle function, especially the utricle ocular reflex gives information about the periphery vestibular organ while accelerating a test person towards a horizontal line.
The utricle ocular reflex should be examined with a video-oculography (VOG) device as resulting eye movements have torsional components called ocular counter-rolling (Clarke 1995). The perception of the subjective vertical test subject fixes a vertical light bar in translational and 20° tilted position. The SV test is an indicator of higher integrative cerebral regions like the vestibular cortex and the thalamus (Dieterich & Brandt, cited in Clarke 2001).

Vestibular Evoked Myogenic Potential (VEMP)

As mentioned in section 1.3, the saccule is a part of the vestibular system responsible for detecting gravitational acceleration changes. VEMP is based on a di-synaptic reflex arc, starting from the macula organs of the inner ear and innervating the motoric neurons of the sternocleidomastoid muscle. Acoustic stimuli lead to an excitation of the macula saccule, and as a result, the di-synaptic arc leads to micro contractions of the sternocleidomastoid muscles. These are the so-called vestibular evoked myogenic potentials, which are sensed via electrodes. Therefore, VEMP has proven to be a selective test of the saccule (Colebatch & Halmagyi 1992).

Historical Review of VEMP

During the 1920s, Tuillo showed in animal models that when applying acoustic stimuli, a combination of eye and head movements occurs (Scherer 1997, p. 390-395). In 1958 Geisler, Frishkopf and Rosenblith registered electrical potentials by applying acoustic stimuli. They have recorded potentials, which were called “inion response”. They assumed that these responses are of cortical origin (Geisler et al., cited in Heinemann 2014). Bickford and his group later postulated that these electrical responses are the result of muscular activation (Bickford et al., cited in Heinemann 2014).

From there on research projects mainly focused on stimulations of the vestibular organ (Cody & Bickford; Townsend & Cody, cited in Heinemann 2014). Experiments on cats where done by Greiner and colleagues in 1967 as well as Spiegel and his group in 1968 (Scherer 1997, p. 287). A number of studies led to the assumption that acoustic evoked potentials stimulate the saccule (Colebatch & Halmagyi 1992; Colebatch et al., cited in Luft 2011). This was finally confirmed by studies done by Murofushi and Curthoys (Murofushi & Curthoys, cited in Heinemann 2014). Knowing that one needed to find a more stable way to induce this reflex, the inion response proved not to be reliable. Colebatch et al. identified the sternocleidomastoid muscle as a valid muscle for reproducing a reliable muscular activation during VEMP (Colebatch et al., Heinemann 2014). VEMPs show biphasic waveforms with negative (n) and positive (p) peaks. Positive is equivalent to an inhibition while negative is equivalent to an excitation (Colebatch & Rothwell, cited in Luft 2011). Two potential complexes have been identified: the earlier one has a vestibular origin (saccule), the other complex appears later and is still the subject of research (Huang et al.; Colebatch et al., cited in Heinemann 2014). Amplitudes of the potential show individual differences, e.g. in the tonus of the muscles as well as in the intensity and frequency of the applied acoustic stimulation (Colebatch et al.; Lim et al., cited in Heinemann 2014) (see Figure 14). The latency of the primary potentials was subject of a couple of studies (Welgampola & Colebatch, cited in Luft 2011). Today VEMPs have shown clinical relevance for the examination of the utricule function (oVEMP) and saccule function (cVEMP) (Brandt, Dieterich & Strupp 2012, p. 26-29). (see beside, Figure 14)

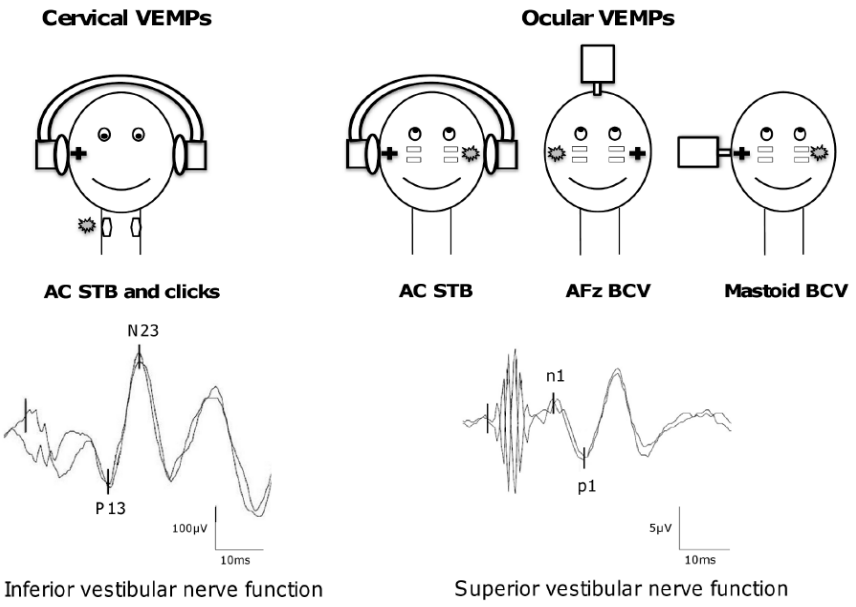

Figure 14: *Cervical VEMPs* (saccular function) are induced by air-conducted sounds e.g. 500 Hz short-tone bursts (AC STB) or clicks. *Ocular VEMPs* (utricular function) are evoked by AC STB, bone-conducted vibration AFz (AFz BCV) or at the mastoid (mastoid BCV). Illustration taken from 'The Role of Cervical and Ocular Vestibular Evoked Myogenic Potentials in the Assessment of Patients with Vestibular Schwannomas.' (Chiarovano et al 2014, p. 2)

Otolith function test with rotatory chair

The modulation function of the otolic organs in connection to rotation chair tests where tested in in different experimental forms. The procedure of tilting a test person in the phase of the VOR after nystagmus is called “tilt suppression”. As it is a test of otolith function “tilt suppression” shows, some significant changes in its time constant of the after-nystagmus (see below Figure 15). Consequently, this phenomenon was investigated in the context of the velocity storage mechanism (see section 1.6) (Brantberg, Fransson & Bergenius 1996). Previously Waespe et al. used tilt suppression in monkeys to investigate modulations of the nodulus and ouvula. Lesions of the nodulus and uvula lead to a loss of the monkeys ability to suppress the postrotatory VOR in tilted position (Waespe, Cohen & Raphan 1985). These results indicate that postrotatory time constant during tilt suppression could be a valid diagnosing parameter in patients with central lesions or disorders. Later Brantberg and collegues studied the effect of head tilt in patients after complete unilateral vestibular neurectomy. Investigations included tilting manuever during VOR postrotatory phase and tilting during optokinetic after-nystagmus (OKAN). Among other findings a shortened VOR time constant, as well as a shortened post-rotatory “head tilt” VOR time constant was observed. OKAN responses were mostly manifested (Brantberg et al. 1996).

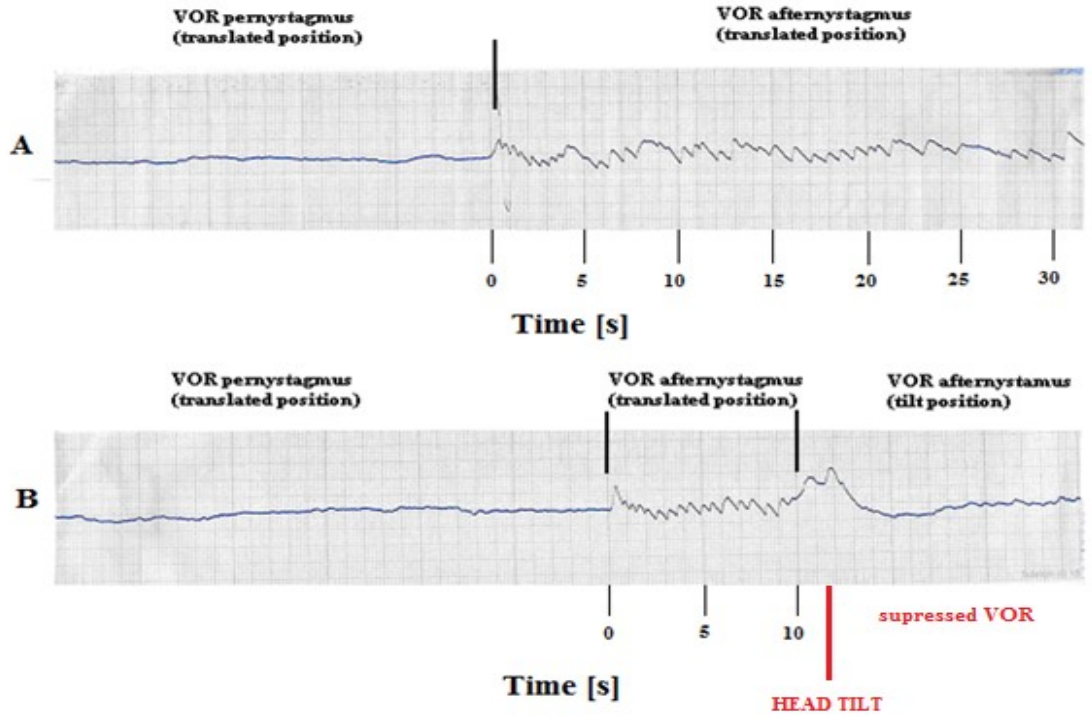

Figure 15: Demonstration of the *“tilt suppression”* phenomenon. Notice *the nystagmus in (A) shows the VOR per - and afternytagmus (head translated position). (B) When head tilts in the phase of the VOR after nystagmus, VOR time constant is shortened (VOR suppression)* compared to *(A).* (Own measurements**)**

2 Literature review on OVAR

2.1 Off-Vertical Axis Rotation

Off-vertical axis rotation is performed while the test subjects are seated in a conventional Barany chair. Then the chair is tilted so that the rotatory axis is tilted with respect to the gravity vector (Scherer 1997, p. 267) (see Figure 16). This rotation form is used mainly for research purposes, and is particularly useful to demonstrate orienting reflexes around y, x and z-axis (Highstein et al. 2004, p. 264). See OVAR axis illustration in section 1.2.

Illustration:

Experimental situation **OVAR**:

Figure 16: Shows *test subject in experimental Situation (OVAR)*. Image taken from Neuro Kinetics, Inc.

2.2 Eye movements during Off-Vertical Axis Rotation

2.2.1 Axis of eye motion

Eye movements are mechanical translations resulting from neuro-electrical signals. These signals could be of neuro-vestibular origin like those mentioned in the first chapter. However, the vector of eye movements is strictly depended on the activated nuclei. This process translates electrical signal codes into 3-D eye movements through the extra ocular muscles. Studies on three dimensional eye movements during off-vertical axis rotation (OVAR), combined with model-based analysis have been done in order to characterize these canal-otolith interactions. In this context, parameters like the direction and temporal properties of the resulting OVAR nystagmus are of interest. Generated 3-D eye movements are the result of activated nerves and lead to elevation and depression around horizontal y-axis; abduction and adduction around vertical x-axis and excyclotorsion and incyclotorsion around torsional z-axis (see below Figure 17).

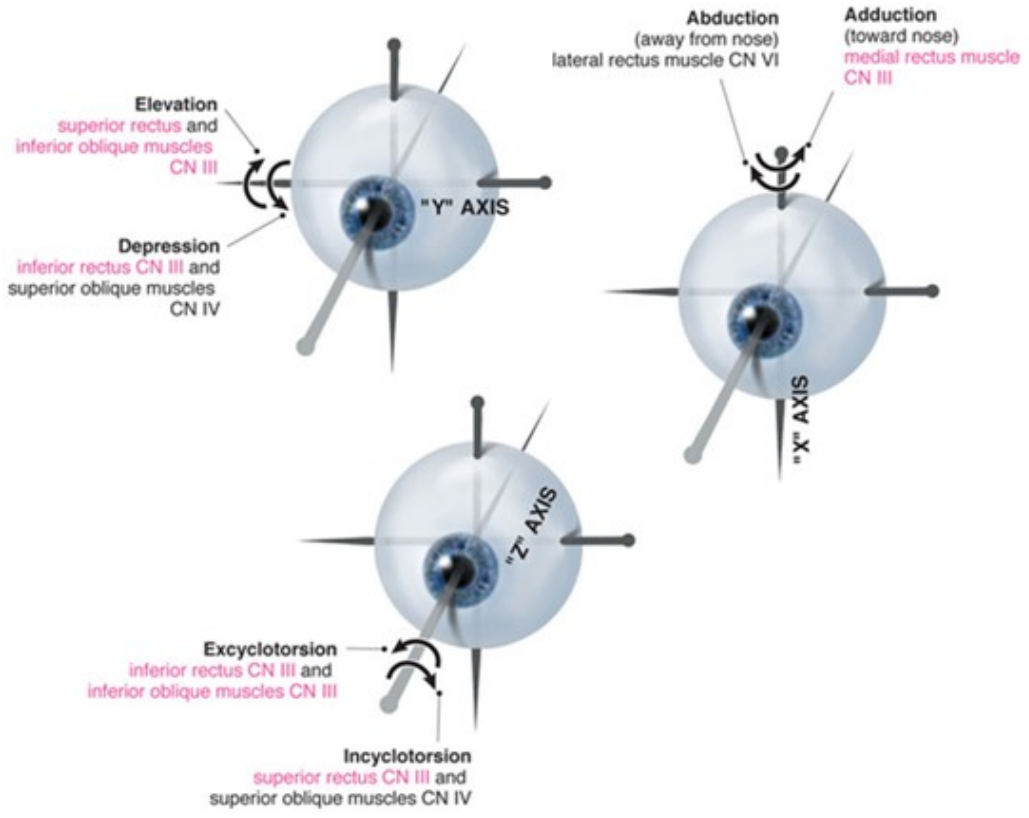

Figure 17*: Right eye movements around the "X", "Y" and "Z" axes.* From http://www.bmc.med.utoronto.ca/cranialnerves/illustrations-by-chapter/oculomotor-iii

2.2.2 Nystagmus following OVAR

Due to a rotation around a tilted rotational z-axis during OVAR, semicircular canals get stimulated while the macula organs are stimulated because of the continuous change of the gravity vector. More precisely, after a time constant of approximately 20 seconds of continuous steady OVAR rotation, horizontal eye movements decay like illustrated in the figure below in form of an exponential function (Haslwanter 2000) (see Figure 18). The thick lines are equivalent to the mean slow phase of velocity (SPV) with wave shaped oscillations around them. These oscillations are the result of a still active otolith input. From there on the nystagmus, reaches the so-called "steady state" phase (Scherer 1997, p. 267).

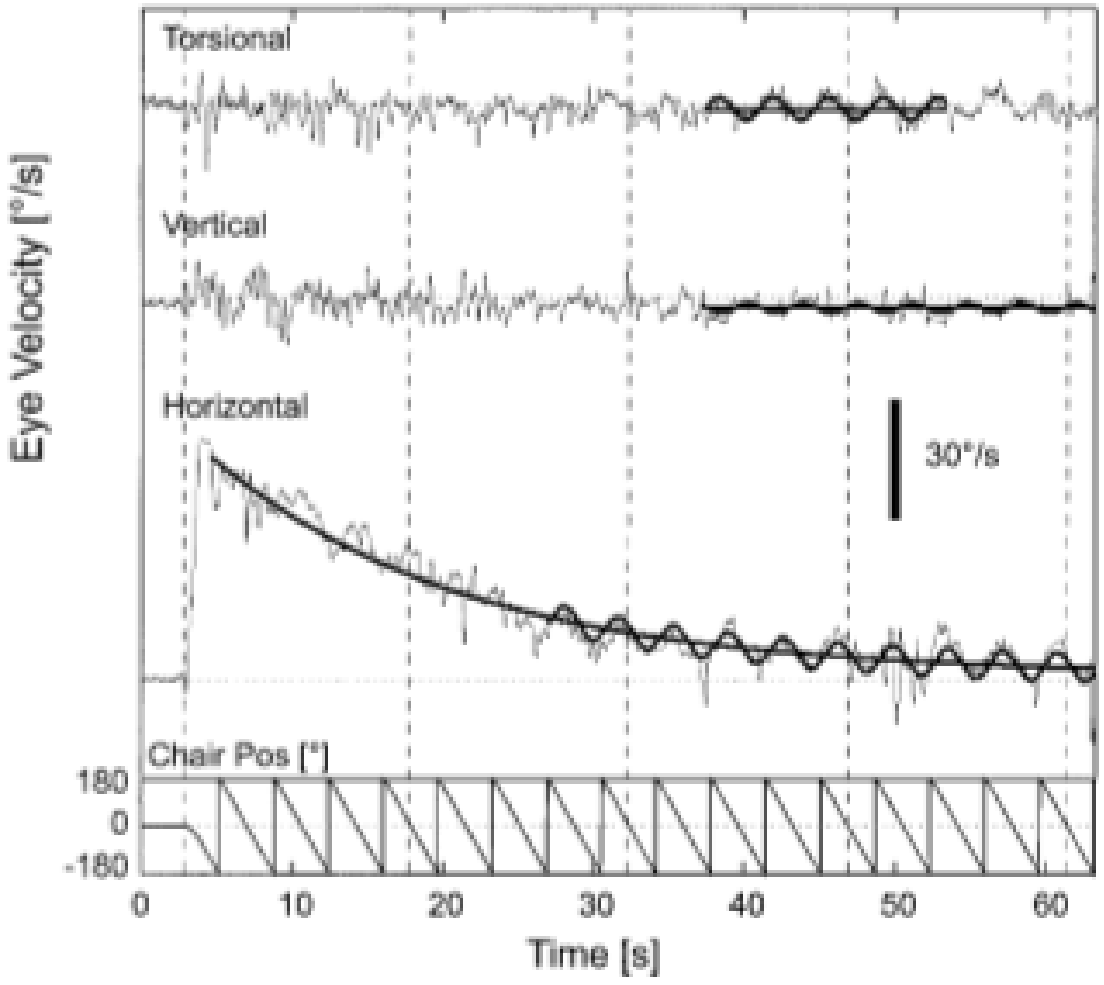

Figure 18: *OVAR Nystagmus horizontal decay, persistent vertical and torsional components.* Plot taken from 'Three-dimensional eye-movement responses to off-vertical axis rotations in humans.'(Haslwanter, Jaeger, Mayr & Fetter 2000, p. 98)

2.2.3 OVAR "Steady State"

In the "steady state" phase, the semicircular canals indicate no rotation while the otolith organs are still stimulated by a sinusoidal oscillation of the gravity vector around the head (Haslwanter et al 2000). This dynamic stimulation of the otolith organs keeps the nystagmus going (Goldberg et al. 2012, p.260-264) (see Figure 19). Combined afferences of otoliths and SCC are used to estimate orientation and movement with respect to the gravity vector (Kushiro et al. 2002). The illustration below illustrates torsional, vertical and horizontal eye movements (thin grey lines) generated by OVAR. Through specific signal processing techniques, saccades (fast phases of velocity), where removed from the nystagmus. As a result we see, the thicker lines also called the "desaccaded data" (Haslwanter et al 2000).

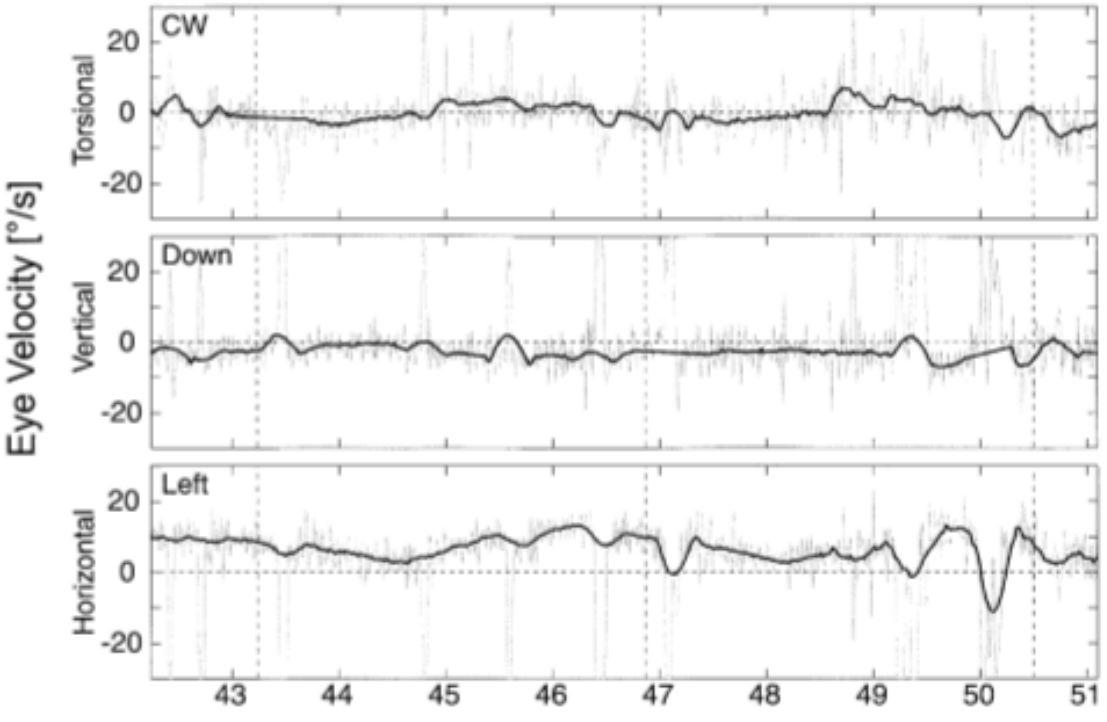

Figure 19: *Horizontal, vertical and torsional eye movements* generated by *Off- Vertical Axis Rotation*. Plot taken from 'Three-dimensional eye-movement responses to off-vertical axis rotations in humans.' (Haslwanter, Jaeger, Mayr & Fetter 2000, p. 98)

2.3 OVAR during normal gravity

2.3.1 OVAR – Historical Review

Pre-stimulation forms of OVAR were reported in the 1960s. In the so-called barbeque rotation test, test persons are rotated in a 90-degree angle to the gravity vector. The occurring eye responses have confirmed that the deflection of the cupula is not related to gravity (Benson et al; Correia & Guedry; Guedry, cited in Clarke 1995). "Formerly, Guedry (1965, 1974) and Benson (Benson & Bodin 1966; Benson 1974) discovered that OVAR induces a continuously horizontal nystagmus with superimposed oscillations. Later Young and Henn (1975) found out that there are modulations in eye velocity and eye position as well" (Highstein et al. 2004, p.262). As the nystagmus doesn't vanish, there is a certain bias component of the baseline as long as rotational velocity keeps steady (Highstein et al. 2004, p. 264). Additionally, the velocity of the slow phase of velocity (SPV) component of the nystagmus shows a waving pattern its frequency is in direct correspondence to the rotational velocity (Scherer 1997, p. 267). This waved pattern is also often referred to as the modulation component of OVAR continuous nystagmus (Clarke 1995). Per and after nystagmus can be modulated by otoliths (Schöne cited in Clarke 1995). A phenomenon that was also explained in context of the tilt suppression maneuver (dumping) (Benson 1974, cited in Clarke 1995). Therefore, a number of mathematical models appeared to suggest central processing mechanisms behind rotatory and translational head movements (Glasauer 1992). Harris et al. investigated the priority of information coming from SCC and otoliths (Scherer 1997, p. 267). In 1986, Harris compared the nystagmus of two experimental orders, VOR after nystagmus and OVAR with decreased velocity. Normally VOR after nystagmus changes its direction after stopping. On the contrary, the OVAR nystagmus decreased due to the decrease of the rotatory velocity but the nystagmus direction did not change. As it is the same direction of the otoliths, it was concluded that information coming from the otoliths have more dominance than those from the SCC' (Scherer 1997, p. 277).

Later modeling approaches have become more interesting. For example, a very successful model of Merfeld describes ocular responses to otolith-canal interactions (Merfeld 1999). This model is the only one of its kind as it integrates signals from semicircular canals and otoliths during arbitrary movements (Haslwanter et al. 2000). Haslwanter later compared OVAR eye responses to Merfeld's model, and found out that the predictive character was limited to a tilt axis of 45 degrees (Haslwanter et al. 2000).

Unfortunately, only little is known about OVAR possibilities of clinical application (Furman, Koizuka & Schor 2000). However, several attempts seemed to be promising to apply OVAR stimulation to clinical practice (Furman et al. 1992; Furman et al. 1993) as well as other canal-otolith interaction stimulation paradigms (Lewis et al 2011a; Lewis et al. 2011b) .

Off Vertical Axis in Animals

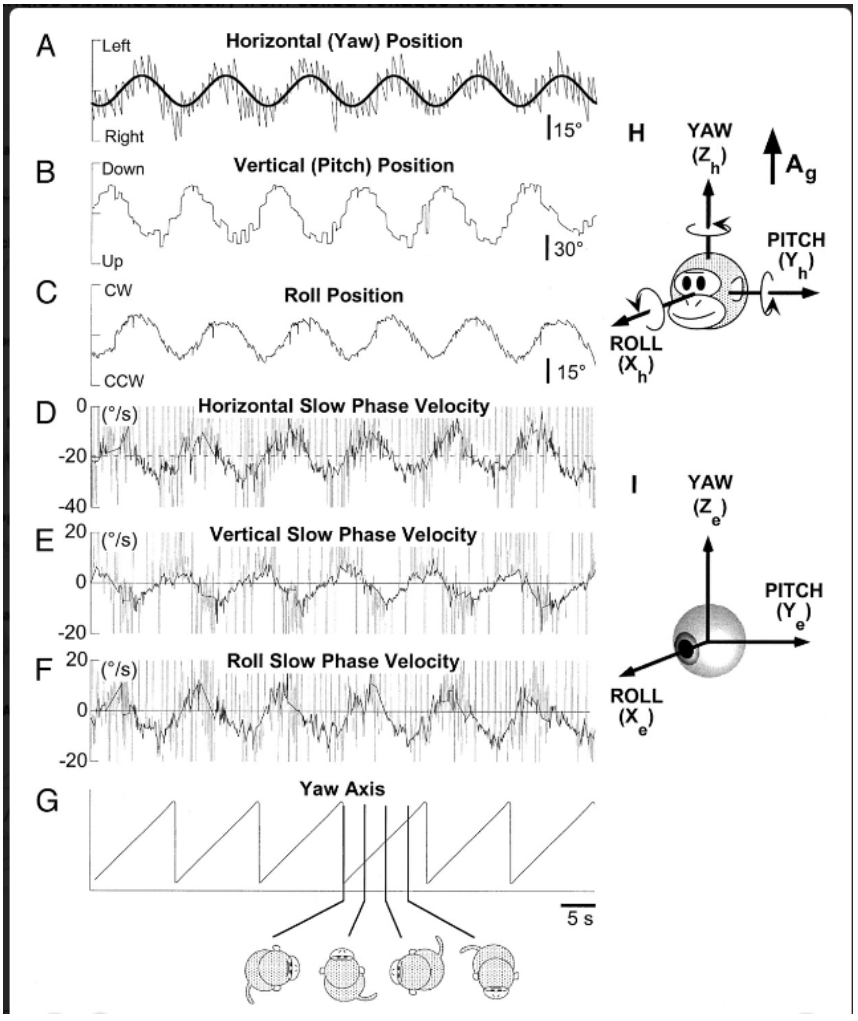

Figure 20: *Horizontal, vertical, and roll eye positions (A–C).* Image taken from 'Compensatory and orienting eye movements induced by off-vertical axis rotation (OVAR) in monkeys.' (Kushiro et al 2002, p.2447)

The effects of dynamic sensory interactions of otoliths and canal and their resulting influences on horizontal, vertical, and torsional eye movements have been investigated in both animals (Raphan et al. 1981; Hess & Dieringer 1990; Kushiro et al. 2002) and humans (Haslwanter et al. 2000). In different species OVAR has revealed very valuable mechanisms of the central vestibular system e.g. in cats (Harris 1987; Darlot & Denise 1988) in monkeys (Kushiro et al. 2002). Unilateral vestibular loss has shown asymmetries in animals while rotating around tilted z-axis (Chan & Cheung; cited in Clarke 1995). The same was true in patients with unilateral vestibular loss (Furman & Baloh; cited in Clarke 1995). The figure above shows a nystagmus induced by OVAR in a monkey form Kushiro and colleagues 2002. Horizontal, vertical and torsional eye movements were recorded. (see above Figure 20)

2.3.2 Motion sickness during OVAR

There have been several attempts to investigate motion sickness symptoms resulting from OVAR. Dai et al. undertook one of these by investigating if there were a relation between the degrees of tilt and different rotation velocities. The experiments showed that subjects reported a motion sickness maximum when rotating with a speed of 60°/s around a tilted axis of 30 degrees. However, there was also no connection recorded between motion sickness maximum and the modulation of the test subject's eye velocity (Dai et al. 2010).

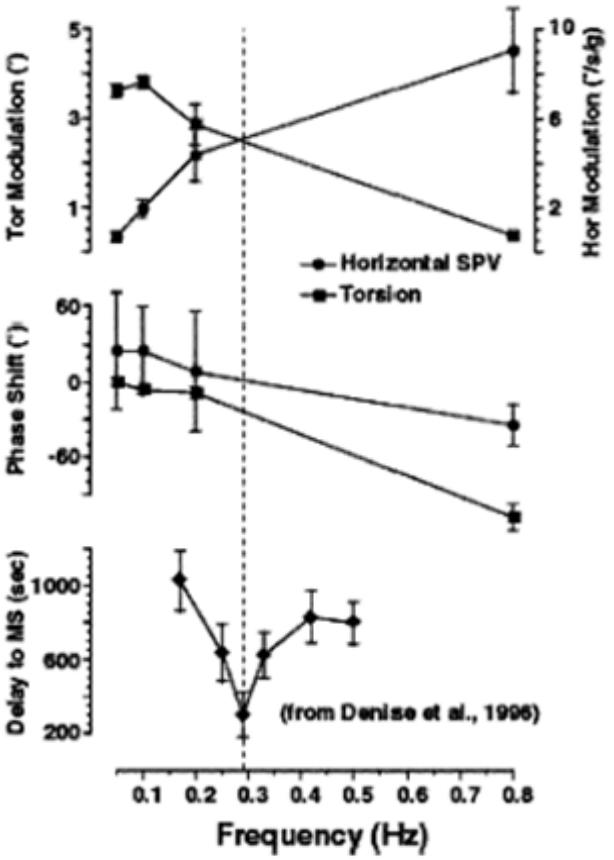

Figure 21: "Otolith–ocular responses and motion sickness as a function of frequency. The response amplitude and phase shift (positive is leading) for torsion (squares) and horizontal SPV (circles) are shown as a function of frequency (mean 1 SEM). Note how the peak of motion sickness susceptibility (dashed line) during OVAR at the same tilt angle (adapted with permission from occurs in the region where torsional and horizontal SPV modulation responses crossover. "(Wood 2002, p. 42) Plot taken from 'Human otolith-ocular reflexes during off-vertical axis rotation: effect of frequency on tilt-translation ambiguity and motion sickness. ' (Wood 2002, p. 42)

In 2002, Wood examined the modulation of otolith-mediated tilt (torsion) and translation (horizontal slow phase velocity (SPV)) of OVAR ocular reflexes during constant velocity. He found an apparent crossover in the torsional and horizontal responses (Wood 2002). However, these ocular responses are in correlation with the frequency region (0.05-0.8Hz) of increased susceptibility to motion sickness (Denise, Etard, Zupan & Darlot 1996). (see above Figure 21) Conclusively this crossover phenomenon could be a very useful parameter in future motion sickness studies. (see section 4.2.1)

2.4 Space experiments of importance for OVAR

2.4.1 Velocity storage and Canal-Otoliths interaction

The ***velocity storage mechanism*** plays a major role. First through its models based on previously done stimulation forms one could predict per and post-rotatory spatial components of eye movements. The velocity storage system can be activated by many types of stimuli (canal, otolith, vision) and through a three-dimensional gravity depended structure; the system is capable of storing information to produce eye movements in all planes (Cohen et al. 2001; Honrubia 2011, p. 86). These results lead to the hypothesis that the after-nystagmus in response to OVAR, rotation, and OKN are all produced by the same central neural mechanism, i.e., by velocity storage in the central vestibular system.

OKN and VOR were also tested in parabolic flights (Dizio & Lackner 1992). Below there are their most important findings:

- 'Horizontal OKAN and vestibular nystagmus both have no effect of G level on their initial or peak slow phase velocities (SPV).
- SPV of OKAN decay rates were quicker in 0G and 1.8G than in 1G.
- Vertical vestibular nystagmus also showed no effect of G level on peak velocity but decayed quicker in 0G relative to 1G. '(Dizio & Lackner 1992).

These-findings confirm that there is a common velocity storage mechanism for optical and vestibular stimulation that shortens the time constant of the decay rate in correspondence to the magnitude of G (Dizio & Lackner 1991; Dizio & Lackner 1992).

Paul Dizio and James Lackner investigated the velocity storage mechanism in connection with motion sickness susceptibility during parabolic flight (Dizio & Lackner 1991).

Their most important findings are listed below:

- "a shortened decay time constant of the slow phase velocity of post-rotary nystagmus under 1G
- a decrease of time constant reduction elicited in OG and 1.8G but was not correlated with sickness
- the extent of time constant reduction elicited by head tilts in 1G was significantly correlated with sickness
- Changes in the extent of time constant reduction in OG and 1.8G over repeated tests." (Dizio & Lackner 1991)

Symptoms of motion sickness were categorized based on the criteria of Ashton Graybiel (1968) (Dizio et al. 1991). (see later Table 2)

2.4.2 Einstein's "Equivalence Principle"

Although Einstein himself never participated in vestibular research, he made a relevant contribution. The theoretical basis behind Einstein's theory of general relativity is in this respect of importance. The so-called "Equivalence Principle" states that linear accelerometer sensors are not able to distinguish between linear acceleration and gravity. Consequently, our linear acceleration sensors, the otoliths, are not able to provide the brain exact information in order to distinguish acceleration from head tilt with respect to gravity (Clément 2003, p. 96).

A number of relevant studies where done to reveal the neural mechanisms the central nerve system (CNS) uses in order to solve the ambiguous information provided by the otoliths (Merfeld et al. 1999; Angelaki, Wei & Merfeld 2001; Merfeld 2003; Merfeld et al. 2005a; Merfeld et al. 2005b; Wood et al. 2007). However, otoliths induced afferences are the result of the combination of gravitational and linear acceleration forces. In other words otoliths detect the so-called "gravito-inertial force" which is the sum of gravity and inertial force (Merfeld & Zupan 2002):

$$F_{Total} = F_{Gravity} + F_{Movement}$$

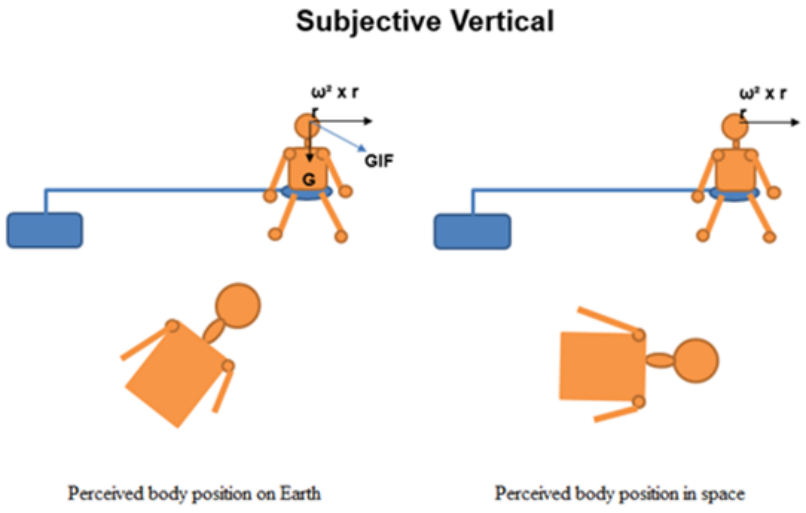

Figure 22: *Perception of body position on Earth (left), in space (right).* Draft adapted from 'Fundamentals of Space medicine' (Clément 2003, p. 100)

After spaceflight Astronauts often report a sense of translation e.g. when rolling their head. That was considered evidence to the assumption that in space the CNS interprets all otolith signals to indicate translation. This explanation model became the basic idea behind the so- called "Otolith Tilt Translation Reinterpretation" (OTTR) hypothesis (Clément 2003, p. 96). During the Neurolab mission, there have been centrifuge experiments, which showed significant changes in astronaut's perception in relation to preflight tests. On Earth, astronauts reported a 45-degree tilt of their body position, but a 90-degree tilt in space, which is a conflict to the OTTR hypothesis (Clément 2003, p. 99-100). (see Figure 22) In the figure above r is labeled as the arm length of the centrifuge, ω as angular frequency, G as the gravity acceleration vector (9,81 m/s^2 on earth) and GIF as the gravito-inertial force vector.

In 2003 Merfeld introduced the rotation otoliths tilt translation reinterpretation (ROTTR) hypothesis, which is a very interesting way of explaining postural changes and resulting problems that astronauts experience when they come back from long space flights (Merfeld 2003). However, test subjects' reports on motion perception are interesting especially during OVAR as motion perception might vary in direct correspondence to otolith-ocular responses (Wood et al. 2007).The differentiation between tilt and translational perception in OVAR was the focus of Wood, Reschke and Clément (2007). Their experimental design allowed them to compare the perception at low and high stimulus frequencies. Interestingly, subjects reported greater sensation of tilt with perceived motion along a conical path while rotating with a low number of revolutions per second, but this conical path deforms much more cylindrical. On the other hand, subjects perceived reduced tilt and increased translation along to an upright cylindrical path while rotating with higher frequency. (Wood et al. 2007) "Based on the linear interpolation between the torsional and horizontal SPV modulation at 0.2 and 0.8 Hz, the crossover of tilt and translation otolith-ocular responses appears to occur in the region of increased motion sickness susceptibility." (Wood 2002)

The differentiation of tilt translation perception by the segregation of frequency was also research subject in a number of studies done in the past (Merfeld et al. 2005a; Merfeld at al. 2005b; Wood 2007). The main inference of frequency segregation for otolith signals is that the responses will depend on the frequency of linear acceleration, i.e. the speed of rotation velocity, therefore three stimulus frequencies (15, 30 and 60°/s, CW) are recommended for future OVAR studies.

2.4.3 Orientation perception and space motion sickness

A couple of different hypotheses were made in the last couple of decades, and the conflict theory is definitely the most popular one. It says that due to the conflicting inputs the central nerve system is not able to process the information correctly which results in motion sickness (Clément 2002, p. 131-132). Due to the lack of afferent information (otoliths), changes in the perception of orientation occur in space (Panel 2004, p. 71). Another hypothesis blames the increased intracranial pressure in space (Saborowski et al. 2002). In space, body fluids of astronauts undergo distributional changes.

One of the most common symptoms reported in this context is head edema, which is the reason why astronauts often report vision problems.Kinetosis is something astronauts also suffer from, especially as rotational maneuvers are their daily duty in order to decrease the demineralization of their bones and to prevent the cardiovascular system from conditioning to microgravity. However, persons without vestibular organ functions have no susceptibility to space motion sickness (Oman et al. 1986, cited in Saborowski 2001). Space sickness is a term that describes the physical inability to cope with physiological changes while the body undergoes microgravity conditions. Approximately every second a cosmonaut suffers from such conditions. Especially in space shuttles as well as in Skylab missions test subjects reported more severe symptoms than during Apollo missions (Clément 2002, p. 134-135). Asthon Graybiel undertook the most acknowledged way of categorizing motions sickness symptoms (Dizio & Lackner 1991). Later Dizio and Lackner investigated motions sickness symptoms during parabolic flights by using Graybiels' motions sickness chart for categorizing degree of tests subjects' symptoms (Dizio & Lackner 1991). (see Table 2)

TABLE I. MOTION SICKNESS SUSCEPTIBILITY IN PARABOLIC FLIGHT, TIME CONSTANT (IN SECONDS) OF DECAY OF NYSTAGMIC SLOW PHASE VELOCITY FOLLOWING SUDDEN STOP STIMULATION (SS), AND MODIFICATION OF THE TIME CONSTANT BY HEAD MOVEMENTS (HM) AND BY GRAVITOINERTIAL FORCE LEVEL (G) EARLY AND LATE IN FLIGHT.

Subject ID	Motion Sickness Susceptibility Score	Time Constant				Change in Time Constant Relative to SS, 1G Baseline			Change in Reduction of Time Constant Early vs. Late	
		SS, 1G	SS + HM, 1G	SS, 0G	SS, 1.8G	SS + HM, 1G	SS, 0G	SS, 1.8G	SS, 0G	SS, 1.8G
1	0.0	15.7	12.2	7.6	13.6	−3.5	−8.1	−2.1	−1.3	+0.7
2	0.6	11.7	9.1	8.5	8.5	−2.6	−3.2	−3.2	0.0	−3.5
3	1.0	16.7	13.6	13.5	13.7	−3.1	−3.2	−3.0	−1.8	−1.2
4	2.7	16.0		10.1	10.5		−5.9	−5.5	+0.2	+0.4
5	6.8	12.0	8.5	10.3	11.7	−3.5	−1.7	−0.3	−1.2	0.0
6	9.9	14.7	8.4	8.4	13.3	−6.3	−6.3	−1.4		
7	11.8	17.4	12.1	12.8	15.8	−5.3	−4.6	−1.6		
8	12.9	19.1	12.4	15.4	20.9	−6.7	−3.7	+1.8		
9	13.0	16.3	10.5	12.0	15.3	−5.8	−4.3	−1.0		
10	15.3	13.7		7.4	12.2		−6.3	−1.5		
11	19.6	26.4	15.6	16.2	17.9	−10.8	−10.2	−8.5	+0.4	+0.3
12	20.1	12.7		9.5	10.3		−3.2	−2.4		
13	22.4	21.1		17.6	20.3		−3.5	−0.8		
14	25.5	17.1	10.4	8.9	11.3	−6.7	−8.2	−5.8		
15	27.9	18.6		12.1	15.9		−6.5	−2.7		
$\bar{X}$		16.6	11.3	11.4	14.1	−5.4	−5.3	−2.5	−0.6	−0.6
S.D.		3.79	2.33	3.22	3.62	2.44	2.35	2.51	0.93	1.59

Table 2: *Categorization of Motion Sickness Symptoms*. Chart taken from 'Motion Sickness Susceptibility in Parabolic Flight and Velocity Storage Acitivity.' (Dizio & Lackner 1991)

Parabolic flight maneuvers offer an effective way to experience 20 to 30 sec of microgravity conditions. Mittelstaedt and Glasauer postulated that in microgravity most test subjects experience standing straight or in a 180-degree upside-down body position. Interestingly, these perception reports also showed that the perception of environment is independent from the own body perception, which means that some test persons have the feeling they stand straight and their environment is upside-down and vice versa. Glasauer and Mittelstaedt explained this phenomenon with a gravity acceleration independent bias factor affected by somatic and vestibular gravity receptors (Mittelstaedt & Glasauer 1993, cited in Saborowski 2001). Interesting experiments testing the estimation of objects stability could provide a better understanding how and which parameters effect the perceived SV (Barnett-Cowan et al. 2011). In both military and civil aviation accidents, pilots often reported inverted surroundings; therefore, Mittelstaedt and Glasauer further postulated that the SV is the result of the physical vertical and the so-called idiotropic vector (z-axis). Both vectors and their relation to each other are the reason for an inverted perception (Mittelstaedt & Glasauer, cited in Saborowski 2001). However, during the last couple of years there have been experimental designs used to predict and analyze the neurophysiological mechanisms that lead to motion sickness symptoms. Most of these models go back to the so-called reafference principle (Holst & Mittelstaedt 1950, cited in Saborowski 2001). As assumed, there is a difference in the perception of active and passive rotational movements. If the expected rotational motion is in conflict with the 'efferent copy', a conflict might occur (Young 1984, p. 1030).

3 Conclusion

The present thesis has shown that the SPV vector during rotational head movements can possibly be predicted (Raphan & Cohen 1988), but that it is still unclear how otolith- canal interactions exactly modulate 3-D eye movements (Haslwanter et al. 2000). According to the research mentioned in sections 3.3 and 3.4 a relevant experimental question could be: "How will the OVAR nystagmus be modulated under changing gravity conditions?" It is expected that the varying Gz forces during a parabola modulate primarily the slow phase velocity (SPV) of the VOR in tilted position (Dizio & Lackner 1991), this could provide unrevealed knowledge about the modulation effects of otolith ocular pathways especially before and after microgravity phases. Consequently, changes in the velocity storage, affecting the sensory-motor control of body orientation would be the result (Merfeld 2003). "The effective decay rates and three-dimensional organization of velocity storage are dependent upon body orientation relative to gravity and also are influenced by gravitoinertial force (G) level" (Dizio & Lackner 1992). Therefore, it is expected that changes in time constants of the 3-D eye movements during each gravity phase of the parabolic maneuver occur. Based on the present thesis the orientation of the SPV vector is expected to show changes in different g levels of the parabolic maneuver. Due to these dynamic changes, the test subject's orientation is expected to be biased as well (Dizio & Lackner 1991; Dizio & Lackner 1992), especially before and after the zero g phase (Dizio & Lackner 1991; Raphan & Cohen 1988). By making use of different gravity conditions, perception changes were reported (Dizio & Lackner 1991). Consequently the neuro-vestibular mechanisms explained in the present thesis would have to adapt (Merfeld 2003)**.** It is still not clear how the CNS processes this after OVAR. However, in correlation to changing eye movements the present thesis has shown that it is still not exactly clear how motion sickness is linked to specific characteristics of eye movements. The paper of Wood 2002 mentioned in section 4 shows one small flaw as assumptions made are based on the measurements of different test subjects (Wood 2002). By critical reading, one can that Wood's assumptions on the "crossover effect" for the investigation of motion sickness symptoms in correlation to eye movements are based on the experimental outcomes of two different test subject groups (Denise et al. 1996) and (Wood 2002). Consequently, these data are not ideal to compare therefore these results cannot be seen as representative. However using the same test subject group in a new experimental design would definitely be interesting in this context.

3.1 Orientation experiments during parabolic flight

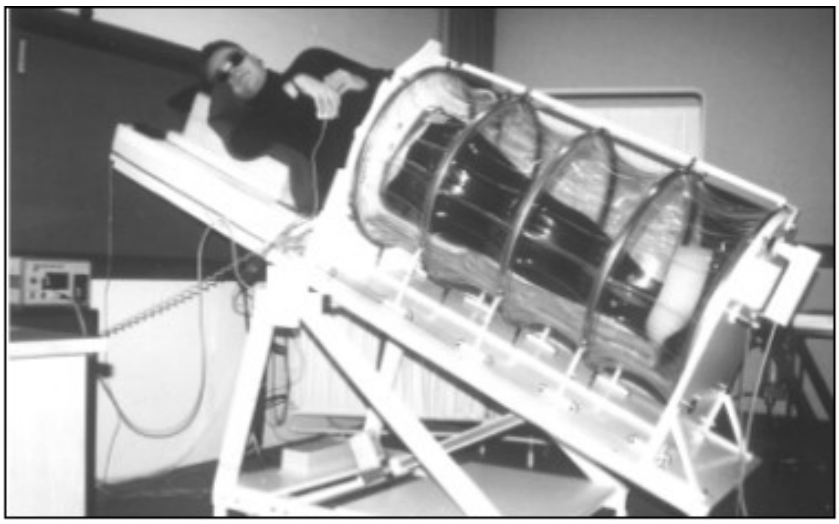

Figure 23: *Lower Body Negative Pressure (LBNP) device with test subject*. Image taken from ‚Über die Beeinflussung der Lagewahrnehmung und des visuellen Systems mittels Über- und Unterdruck auf den Unterkörper' (Saborowski 2001, p. 57)

The following experimental order introduced during parabolic flight maneuvers (see section 4) is designed to enhance our understanding of normal behavior on earth as well as in unusual force environments. By studying these environmental effects, basic mechanisms of movement and orientation, could be helpful to solve practical problems in aeronautics and astronautics (Clément 2003, p. 123-127). After bed rest, studies regaining an upright posture in man has proven to be challenging due to the change of blood distribution (Clément 2002, p. 164). In tests with lower body negative pressure (LBNP) (see Figure 23) devices, subjects have reported shifting perception of their subjective vertical position. (Saborowski et al. 2002).

Mittestaedt and Glasauer also discussed the effects of gravitoreceptors in 1993. Especially the perceptional phenomenon of an inverted surrounding (see section 2.4.3) was an important hint (Mittelstaedt & Glasauer 1993, cited in Saborowski 2001). In 1994, Gierke and Parker postulated that thoracic and abdominal gravitoreceptors stimulation in the range of 4-6 Hz could contribute significantly to kinetosis (Gierke & Parke 1994, cited in Saborowski 2001). Effects on the cardiovascular system and on orientation perception, as thoracic blood shifting, are very likely (Clément 2002, p. 131-132). Consequently, these findings indicate that perception of orientation and movement should no longer be explained with a stand-alone vestibular-brain feedback model.

There are pharmaceutical substances called scopolamine, which can be used to reduce the sickness symptoms (Clément 2003, p. 135). However, they are often connected to negative side effects, like coordination problems and hallucinations (Clément 2003, p. 135). OVAR experiments are relevant when it comes to a longer layover in space. Here it will be of interest to observe the post rotatory characteristics of 3-D eye movements in correlation to possible motion sickness symptoms. The intention is to find a physiological way to overcome the motion sickness. This could be achieved by using scientific data, like that of the proposed OVAR experiment, to create specifically adapted training programs in order to reduce the susceptibility to motion sickness of patients and astronauts. Vestibular tests are often used as tests of function for clinical diagnostics, and their purpose is to determine the effects that varying force environments have on the neural control of movement, posture and the perceived orientation of the human body. In this context, parabolic flight campaigns provide ideal conditions to investigate ambiguous information provided by the otolith organ. In order to understand how inner ear dynamics influence three dimensional eye movements, the following hypothesis would be of interest to study.

3.2 Hypothesis of OVAR parabolic flight experiments

As former investigations have mostly focused on pre/post flight tests of OVAR (Clément et al. 2007; Clément & Wood 2013), the following proposed experiments place their main focus on the OVAR nystagmus under changing gravity exposure. Especially the modulation of the SPV vector, changes in amplitude (if higher or lower especially before and after the microgravity phase of the parabolic maneuver) and changes in initial and peak of SPV could provide new information.

4 Feasibility Study

4.1 Purpose of this Study

Based on the experiments done in the past the experimental question proposed would be how the nystagmus following Off Vertical Axis rotation gets modulated in different levels of G.

- The main emphasis of this study lays on the investigation of the spatial and temporal properties of OVAR per and after-nystagmus by using three different gravity conditions during parabolic flight. Measurements include changes in the decay rate, modulation of the orientation and amplitude of the slow phase of velocity (horizontal, vertical and torsional) before and after microgravity phase. In addition, we wish to determine changes in the initial and peak SPV during per- and post-rotatory OVAR in all phases of the parabolic maneuver (1g-2g-0g-2g-1g).

- Another purpose of this study is to study the modulation of the perception due to the varying g atmospheres, around this region (0.04–0.17 Hz).

- Additionally the crossover phenomenon of the torsional and horizontal responses described by Wood in 2002 is of interest to investigate in direct correspondence to motion sickness symptoms before, during and after the parabolic flight campaign around this region (0.04–0.17 Hz).

4.2 Materials and Methods

4.2.1 Experimental Design

Test Subjects:

A collective of 15 individuals (Dizzio & Lackner 1991) who should be tested at least 8 months earlier in ground OVAR experiments around the frequency span (0.05-0.8Hz) where motion sickness is supposed to be highest (Denise et al. 1996). Since it is well known that Off Vertical Axis Rotation provokes motion sickness we recommend investigating eye parameters in two groups. Group I made of 11 individuals, aged 24±2.4 years (mean ± SD). Group II should contain five subjects, aged 26.2±5.6 years (Haslwanter 2000). Test persons are not allowed to take motion sickness pharmaceuticals like scopolamine, as they have a biasing influence on the recorded eye responses. In addition, test subjects history and ground-based testing should indicate no susceptibility to motion sickness. Due to the ESA parabolic flight criteria each test subject needs to pass an FAA Class III flight physical examination (see Appendix).

Preflight - Ground Experiments:

Based on the experimental outcomes of Wood 2002, the suggested ground test design has two main objectives:

- Select 15 test persons with no susceptibility to motion sickness during OVAR around the frequency span (0.05-0.8Hz) (Denise et al. 1996).
- Investigating torsional and horizontal OVAR responses around a frequency span of (0.05-0.8Hz) to determine if most severe motion sickness symptoms correlate with the so called “crossover effect“ (Wood 2002)

Occurring symptoms will be evaluated based on a motion sickness categorization chart (see section 2.4.3.) (Dizio & Lackner 1991).

Procedure during the parabolic maneuver

The following experimental design is based on the experimental designs chosen by Dizio and Lackner (Dizio & Lackner 1991; Dizio & Lackner 1992). A proper comparison of the nystagmus in these different parabola allows to determine whether the amplitude is higher >1g or lower <1 g in both VOR and OVAR eye movements.

Proposed Stimulation Mode

To obtain an answer to the experimental question of how the OVAR nystagmus gets modulated, a measurement of eye movements during two different experimental orders is of interest. The first part of the experiment requires subjects to rotate around an earth-vertical axis (VOR) and then get stopped. Every time they rotate with a constant speed (of 15, 30 and 60°/s) in one direction e.g. clockwise (CW). In the second experimental order, the same subject rotates at a constant velocity with a 20° tilt (15, 30 and 60°/s, CW) about an earth-horizontal axis and is then stopped. The intention behind the chosen experimental design is to measure comparable data of the VOR in translated and tilted position – during per and after nystagmus with the same experimental parameters in all different phases of a parabolic maneuver.

Experimental Order

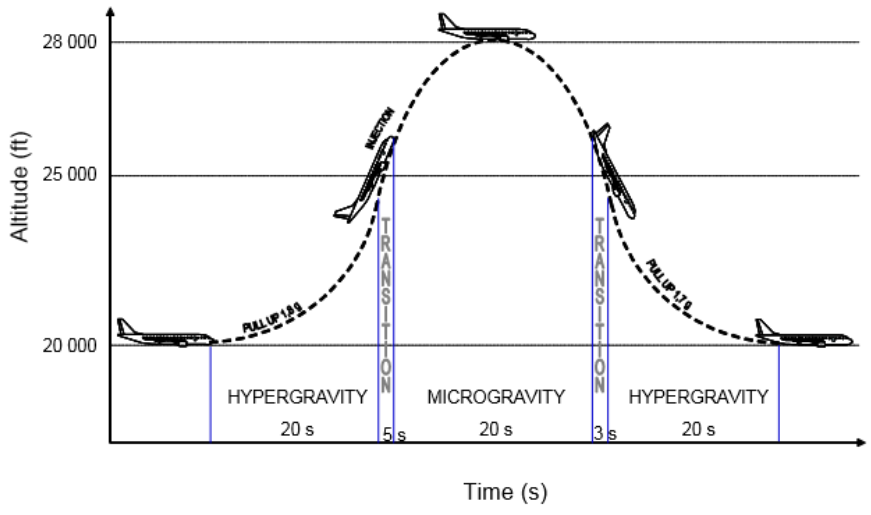

Figure 24: Illustration of a parabolic maneuver. Parabolic draft taken from 'Lung function in micro- and in hypergravity.'(Montmerle 2005, p. 14)

Our experimental order is strictly based on the four-different gravitational levels (1g, ±1.8g and 0g) during a parabolic maneuver.[2] ESA guarantees 30 parabolic maneuvers during one campaign. We suggest participating at least in three campaigns. This will be necessary to successful record eye movements during the proposed experiments.

[2] For more detailed information about the parabolic maneuver please read, ESA technical specifications, see Appendix

Stimulation Paradigm

Test persons rotate in two experimental orders:

1) VOR with a constant speed (of 15, 30 and 60°/s) in one direction e.g. clockwise (CW) in translated position.
2) same subject rotates at a constant velocity with a 20° tilt (15, 30 and 60°/s, CW) about an earth-horizontal axis and is then stopped.

A three minutes period including the stimulus should be applied as followed:

a) When flying straight and level:

a	1G	1.8G	0G	1.8G	1G
120sec. CW rotation stop	20sec. after nystagmus	20sec. after nystagmus	20sec. after nystagmus		

b) When flying straight and level, with the end of the stimulus just after the 1.8 g climb onset. This results in 60 seconds of post rotatory nystagmus, the first 20 sec at 1.8 g, the second 20 seconds at 0 g, and the last 20 seconds at 1.8 g again:

b	1G	1.8G	0G	1.8G	1G
120sec. CW rotation stop		20sec. after nystagmus	20sec. after nystagmus	20sec. after nystagmus	

c) When flying straight and level, such that the stop coincides with the onset of the 0 g period resulting in recording of 20 seconds of 0 g, 20 seconds of 1.8 g, and 20 seconds of 1 g:

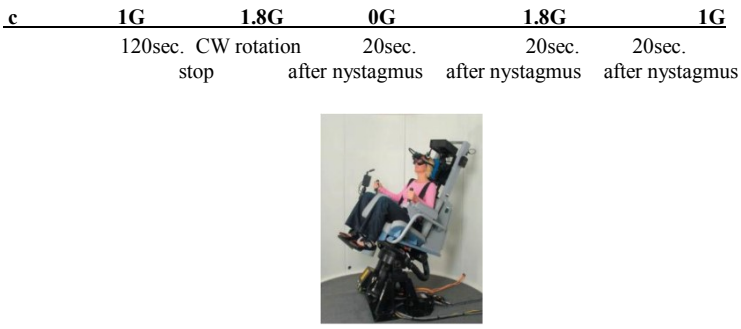

d) When flying straight and level, such that the stop coincides with the onset of the second 1.8 g period. This results in 20 seconds post rotatory nystagmus during the 1.8 g period, and 40 seconds during the 1 g period:

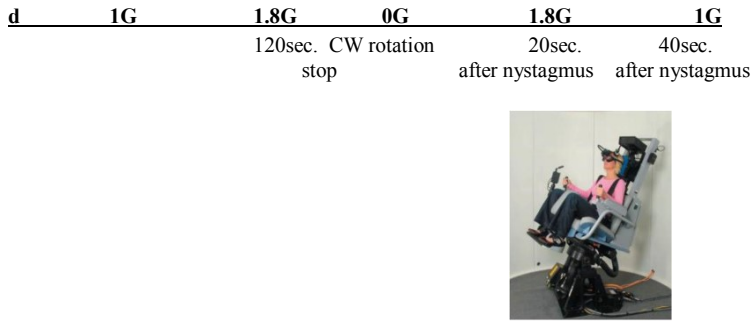

e) When flying straight and level, such that the stop coincides with the end of the parabola, resulting in recording of 60 seconds of post rotatory nystagmus:

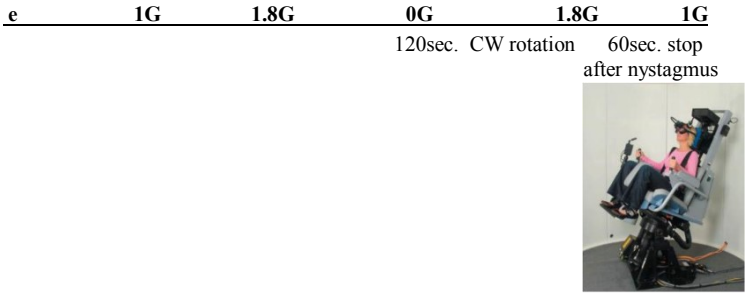

Figure 25: Own work, Illustrations a) - e). Image of test person during OVAR taken from Neuro Kinetics, Inc.

Summary of Recorded Eye Movements:

- CW VOR (tilt/translate) rotation for 120sec. (1g) and after stopping in tilt/translated position for 60 sec. (20sec. 1g – 20sec.1.8g – 20sec. 0g)
- CW VOR (tilt/translate) rotation for 120sec. (1g) and after stopping in tilt/translated position for 60 sec.(20sec. 1.8g – 20sec.0g – 20sec.1.8g)
- CW VOR (tilt/translate) rotation for 100sec (1g), 20sec (1.8g) and after stopping in tilt/translated position for 60 sec.(20sec.0g-20sec.1.8g-20sec.1g)
- CW VOR (tilt/translate) rotation for 80sec. (1g), 20sec. (1.8g) and 20sec. (0g) and after stopping in tilt/translated position for 60 sec. (20sec.1.8g – 40sec. 1g)
- CW VOR (tilt/translate) rotation for 60sec. (1g), 20sec. (1.8g), 20sec. (0g), 20sec. (1.8g) and after stopping in tilt/translated position for 60 sec.(60sec.1g)

4.2.2 Hardware systems recommended

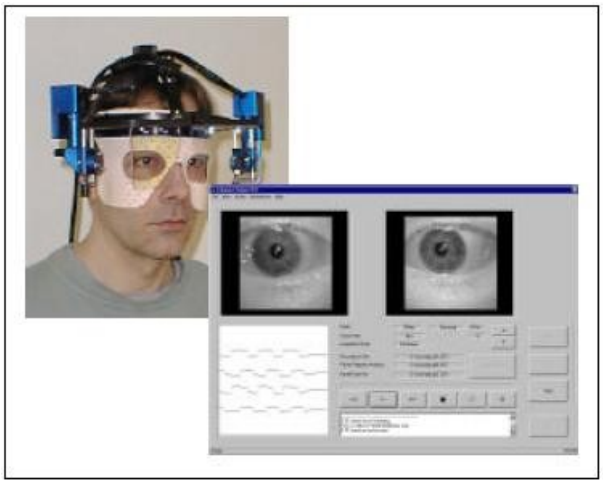

Figure 26: *Eye Tracking System*.
Courtesy taken with permission from Chronos Vison GmbH

Continuous observation of the horizontal and vertical eye movements are recorded by standard electro-oculographic techniques provided with preamplifiers and electrode checkout circuitry. The EOG signals are recorded on the PC and on the PC printer. In addition to the EOG registration, eye movements should also be recorded by means of an improved CCD sensor devise mounted in a light excluding mask worn by the test subject, thus permitting continuous observation (see Figure 26). Besides EOG tracings, three-axial and angular accelerations together with actual and nominal chair velocity are recorded in order to permit continuous observation.

Rotatory Device

OVAR devices are usually bulky because there has to be a substantial restraint system to prevent the subject from flopping around, this should not be a problem in the microgravity phase but the hyper-g phase would require even sturdier restraints than on earth. In addition, an OVAR device usually requires more electrical power than a vertical axis rotator because the load (body plus restraint system) is not necessarily balanced, which creates periodic torques for which the motors must compensate in order to maintain the commanded angular velocity. A technical support team has to ascertain whether aircraft power is sufficient for the device, we propose to use (see appendix). The recommended rotation chair is not a standard Barany rotation chair[3] as used for medical diagnostics (see Figure 27). The electro motor, which rotates the chair, is controlled by an axis-integrated tachometer. This rotation chair is specifically designed; this means that the number of revolutions per minute where increased to overcome the moment of inertia during the parabola. In other words during the two g phase there are usually a problem that has to be faced, which is obtaining the constant rotation. Therefore, we use a chair that should be tested before, and which needs the power to overcome even the lateral forces of 4 G (x-y-z). (see also Appendix chapter 11)

Figure 27: *Rotatory chair system*. Image taken with permission from EKIDA GmbH

[3] All Hardware Systems have to match ESA technical specifications, see Appendix

4.3 Limitations and Constrains

Gravito-Inertial Force Vector

Figure 28: *Forces acting on aircraft.* Illustration adapted from 'The dynamics of parabolic flight: flight characteristics and passenger percepts.' (Karmali & Shelhammer 2008, p. 14)

The illustration beside describes the four main forces acting on a plane (Karmali & Shelhammer 2008). (see beside Figure 28) During a parabolic maneuver, thrust and lift have to be adjusted appropriately in order to achieve a perpendicularly oriented gravito-inertial force vector ($\overrightarrow{GIF}$) relative to the aircraft's floor (Karmali and Shelhammer 2008). (see next page Figure 29) In this context, Karmali and Shelhammer recently published a detailed description on forces acting during a parabolic flight maneuver. As discussed in their paper, the GIF is what the otolith senses (see later in this chapter), and it is usually perpendicular to the floor of the plane, but sometimes it is tilted slightly forward and backwards (Karmali & Shelhammer 2008). However, previous rotatory chair experiments also led to the assumption that both the GIF magnitude and the orientation of the GIF varies significantly during parabolas, relative to the aircraft frame. This happens not only during transitions between GIF levels but also during the supposedly steady hypo- and hyper-GIF periods" (Prof. P Dizio 2015, pers.comm., 11 April). In this case, the angle between the rotation axis and the GIF, which is a critical variable in OVAR experiments, will be very difficult to control in parabolic flight because the rotator is fixed to the aircraft frame while the GIF angle fluctuates relative to the frame. Nevertheless, when interviewed on 11 April 2015, Professor P Dizzio confirmed that this does not entirely rule out well-controlled OVAR experiments in parabolic flight, but it does require knowing the magnitude and 3-dimensional direction of the GIF and careful planning to obtain and verify the desired stimulation pattern. This intention is of special interest during preflight test procedures. (see also appendix chapter 9)

Draft of the Gravito-Inertial Force Vector:

$\vec{a}\ (x)$ Acceleration vector x – aircraft's longitudinal Axis

$\vec{a}\ (z)$ Acceleration vector z- aircraft's vertical Axis

To describe a position of the plane during the parabola a tangent line is drawn thorough the aircraft's mass point marked as the point **(P)**. This tangent line shows the planes' flying direction during the described moment. As a result, the plane has two acceleration components. The direction of acceleration along $\vec{a}\ (x)$_plane longitudinal axis. The vector along $\vec{a}\ (z)$ indicates the acceleration vector of the aircraft's vertical axis. By adding these two acceleration vectors $\vec{a}\ (x) + \vec{a}\ (z)$ we get $\vec{a}\ (sum)$ as the sum vector.

$\overrightarrow{GIF} = \overrightarrow{(G)}$ (Gravity Acceleration-Vector) + $\vec{a}\ (sum)$

$\overrightarrow{GIF}$ is perpendicular to the aircraft's floor

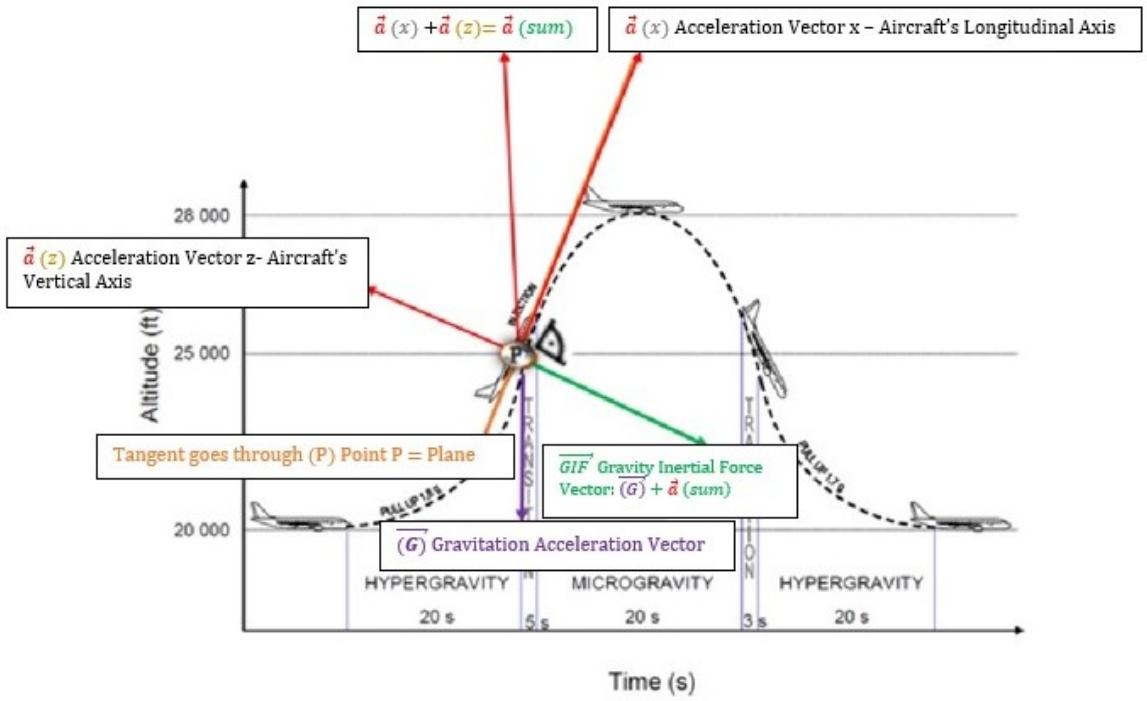

Figure 29: Own work, *description of the GIF-Vector during a parabolic maneuver.* Parabolic draft taken from 'Lung function in micro- and in hypergravity.'(Montmerle 2005, p. 14)

Forces acting on test subjects and otoliths during a parabolic maneuver

The figure below shows different force vectors acting on test subjects during the descending part of a parabolic maneuver. In this illustration, the plane axes (x and z-axes of the aircraft) were adapted to a co-ordinate system. Θ is the pitch angle between the longitudinal axis of the aircraft and the earth's horizontal axis. The force (W) indicates the weight of a person and is the sum vector of the projections Wz and Wx. Acting forces between the feet of a test person and the plane's floor are labeled as Nx and Nz in the illustration beside. Additionally net accelerations projected along the longitudinal and vertical axes of the aircraft are titled ax and az (see Figure 31). A Parabolic flight maneuver has the aim to keep Nz and az near zero during the microgravity phase (0 g). This is just achievable when minimizing Nx and ax (Karmali & Shelhammer 2008). (see above Figure 30) In this respect, the flight precision of the parabolic trajectory as well as experience and skills of the commanding pilot are crucial in order to achieve microgravity conditions (Nz and az near zero) for a time span of 20-25 seconds (Dr. V. Pletser 2004, pers.comm., 23 May). However, the force vectors described above have major influence, on the validity of the experiments proposed. Consequently, a performance evaluation of the suggested rotatory chair device is necessary (see also appendix, chapter 9 and 11).

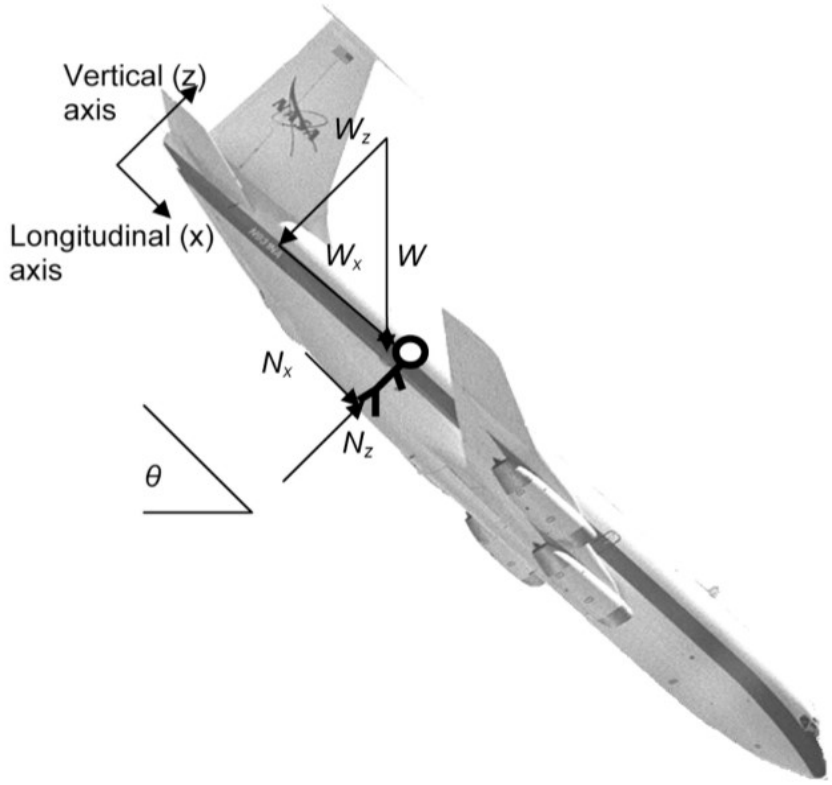

Figure 30: *Forces acting on test subjects during a parabolic flight maneuver.* Illustration taken from 'The dynamics of parabolic flight: flight characteristics and passenger percepts.'
(Karmali & Shelhammer 2008, p. 12)

Otolith-organ mechanics

In order to understand acceleration forces acting on the otoliths, the otolith organ was modelled as a spring-damper-mass system (see Figure 31). The following mechanical extrapolations are based on the assumption that the temporal bone moves in direct correspondence to the body and is in a translated position with respect to the plane; therefore, both head and plane have the same pitch angle with respect to earth (Karmali & Shelhammer 2008).

Net accelerations: ax **and** az**:**

(For graphical illustration, see Figure 31)

Accelerations projected along the longitudinal axis of the plane *(ax)*

Accelerations projected along the vertical axis of the plane *(az)*

g---gravity acceleration 9,81 m/s^2

Θ--- Head and aircraft pitch angle with respect to earth

$$ax = g \cdot sin\Theta$$

In 1.8g $$az = (1.8 - cos\Theta) \cdot g$$

In microgravity $$az = cos\Theta \cdot g$$

Forces acting on Otolith

(For graphical illustration, see Figure 31)

Weight of the otolith *(Wo)*

g---gravity acceleration 9,81 m/s^2

mo---mass of otolith

$$Wo = g \cdot mo$$

Projections of otolith sensed forces acting along vertical axis is below.

Force of the otolith projected along vertical axis (Foz):

g---gravity acceleration 9,81 m/s^2 in 1g

We assume g in the formula below as state of gravity during the parabola 1±1.8 or 0 g

Woz---Weight of otolith projected along vertical axis

mo-----Mass of otolith

aoz--- Accelerating force acting on otolith along vertical axis

Θ--- Head and aircraft pitch angle with respect to earth

$$\sum Foz = mo \cdot aoz = Woz = Wo \cdot cos\Theta = mo \cdot g \cdot cos\Theta = g \cdot cos\Theta$$

Projections of otolith sensed forces acting along longitudinal axis is below.

Force of the otolith projected along longitudinal axis (Fox):

g---gravity acceleration 9,81 m/s^2 in 1g

We assume g in the formula below as state of gravity during the parabola 1±1.8 or 0 g

Wox---Weight of otolith projected along *longitudinal* axis

mo-----Mass of otolith

aox--- Accelerating force acting on otolith along *longitudinal* axis

Θ--- Head and aircraft pitch angle with respect to earth

$$\sum Fox = mo \cdot aox = Wox = Wo \cdot sin\Theta = mo \cdot g \cdot sin\Theta = g \cdot sin\Theta$$

Acceleration difference between temporal bone (net accelerations ax and az) and acceleration acting on otolith (aox and aoz), produces a hair cell deflection:

g---gravity acceleration 9,81 m/s^2 in 1g

We assume g in the formulas below as state of gravity during the parabola 1±1.8 or 0 g

Θ--- Head and aircraft pitch angle with respect to earth

Force projected along x-axis is canceled

$$ax - aox = g \cdot sin\Theta - g \cdot sin\Theta = 0$$

Forces Acting along z-Axis

In 1.8 G level: $az - aoz = 1.8g$

In 0 G level: $az - aoz = 0g$

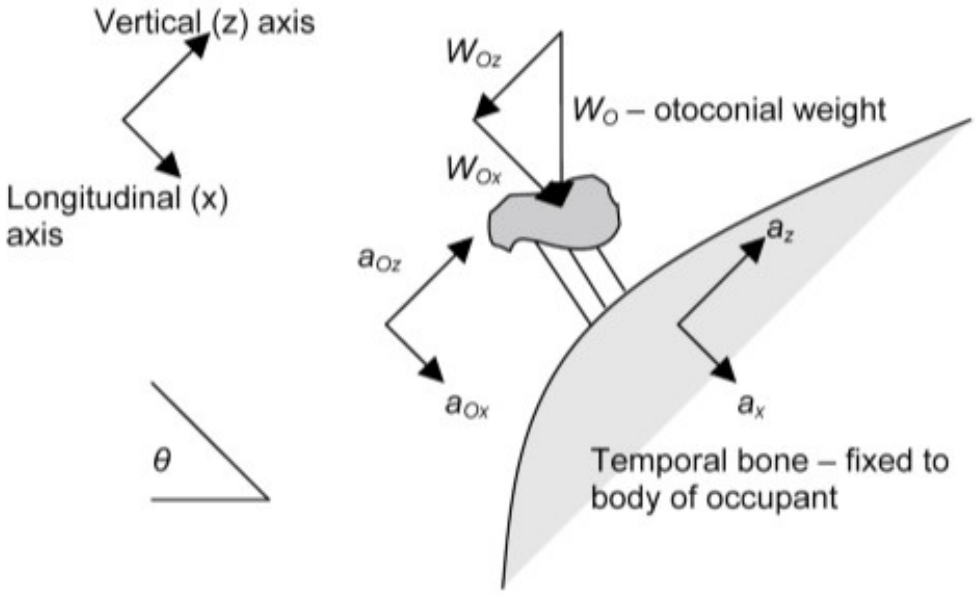

Figure 31: Forces acting on otolith during a parabolic flight maneuver. Illustration taken from 'The dynamics of parabolic flight: flight characteristics and passenger percepts.' (Karmali & Shelhammer 2008, p. 13)

4.4 Expected Results

Based on the hypothesis postulated and the experimental outcomes mentioned before following results are expected.

1. The SPV of both the VOR and OVAR is expected to be quicker in 1.8g and 0g than in 1g (Dizio & Lackner 1992).

2. The decay rate of both the VOR and OVAR could be shortened due to the magnitude of (G) (Dizio & Lackner 1991; Dizio & Lackner 1992).

3. Formerly test persons reported cylindrical rotation perception during OVAR experiments (Cléments 2002; Wood et al 2007). Due to different rotational frequencies (0.04–0.17 Hz) as well as to the varying G levels (±1.8g and 0g) test persons are expected to report dimensional changes. Therefore, perception reports could also show significant difference between pre- and post-flight-tests**.**

4. Post-rotatory VOR after nystagmus as well as OVAR post-rotatory eye movements could show a shortened decay rate in 1.8 and 0g than in 1g. (Dizio & Lackner 1992)

5. OVAR post-rotatory perception of head positions (nose down, ear down) are expected to show changes due to the oscillating G levels of the parabolic maneuver (Clément 2002).

6. During 1g phase, torsional and horizontal eye movements are expected to occur in the rotational frequency span of (0.05-0.08) in correspondence with the highest report on motion sickness symptoms (Denise et al. 1996; Wood 2002). This region could show changes due to stimulation frequencies during ±1.8g and 0g, as a result this region could shift especially when comparing data of torsional and horizontal eye movements to those of the pre- and post-flight-tests.

5 References

Angelaki, D.E., Wei, M.I.N., Merfeld, DM., 2001. Vestibular Discrimination of Gravity and Translational Acceleration. The Vestibuar Labyrinth in Health and Disease, (314), pp.114–128.

Backous DD, Minor LB, Aboujaoude ES, Nager GT 1999, Relationship of the utriculus and sacculus to the stapes footplate: anatomic implications for sound- and/or pressure induced otolithic activation. Ann Otol Rhinol Laryngol; 108(6):548-553.

Baloh, R., Honrubi, V., Kerber, K.A. 2011, Clinical Neurophysiology of the Vestibular System. In Oxford University Press, pp. 77–207.

Barnett-Cowan, M., Fleming R.W., Singh, M., Bülthoff, HH 2011, Perceived object stability depends on multisensory estimates of gravity. PloS one, 6(4), p.e19289. Available at: http://www.pubmedcentral.nih.gov/articlerender.fcgi?artid=3083421&tool=pmcentrez&rendertype=abstract [Accessed March 15, 2015].

Basta D, Todt I, Eisenschenk, Ernst A. 2005, Vestibular evoked myogenic potentials induced by intraoperative electrical stimulation of the human inferior vestibular nerve. Hear Res; 204(1-2):111-114.

Benson AJ 1974, Modification of the response to angular accelerations by linear accelerations. In: Kornhuber HH (Hrsg.) Handbook of Sensory Physiology, Vol VI/2: Vestibular System. Springer, New York, S 281-320.

Bertolini, G. et al., 2008. Do humans show velocity-storage in the vertical rVOR ? Brain Research, (171), pp.207–210.

Bertolini, G., Stefano R., Bockisch CJ, Marti S, Straumann D, Palla, A 2012, Is vestibular self-motion perception controlled by the velocity storage? Insights from patients with chronic degeneration of the vestibulo-cerebellum. PloS one, 7(6), p.e36763. Available at: http://www.ncbi.nlm.nih.gov/pubmed/22719833 [Accessed March 15, 2015].

Bickford RG, Jacobson JL, Cody DTR 1964, Nature of average evoked potentials to sound and other stimuli in man. Ann N Y Acad Sci; 112:204-23.

Bisdorff, A., Von Brevern M.,Lempert, T, Newman-Toker D 2009, Classification of vestibular symptoms: towards an international classification of vestibular disorders. Journal of vestibular research : equilibrium & orientation, 19(1-2), pp.1–13. Available at: http://www.ncbi.nlm.nih.gov/pubmed/19893191 [Accessed February 11, 2015].

Bockisch, C. J., Straumann, D., & Haslwanter, T. 2005, Human 3-D aVOR with and without otolith stimulation. Experimental Brain Research, 161 (3), 358–67.

Brandt, T., Dieterich, M. & Strupp, M. 2012. Vertigo - Leitsymptom Schwindel. In Vertigo - Leitsymptom Schwindel. Springer, pp. 26–29.

Brantberg K, Fransson PA, Bergenius J, T.A., 1996. Tilt suppression, OKAN, and head-shaking nystagmus at long-term follow-up after unilateral vestibular neurectomy. Journal of Vestibular Research, 6((4)), pp.235–41.

Büttner U, Waespe W 1981, Vestibular nerve activity in the alert monkey during vestibular and optokinetic nystagmus. Exp Brain Res. 41(3-4):310-5.

Cazals Y, Aran J, Erre J, Guilhaume A, Aurousseaou 1983, Vestibular acoustic reception in the guinea pig: A saccular function?. Acta Otolaryngol; 95(3-4): 211-217 McCue

Clarke, AH. 1995, Neuere Aspekte des vestibulo-okulären Reflexes. Available from: <http://www.mbfys.ru.nl/staff/j.vangisbergen/endnote/endnotepdfs/labyrinthectomy/Clarke_review_vestibulair.pdf>. [08 February 2015].

Clarke AH, Engelhorn A. 1998, Unilateral testing of utricular function. Exp Brain Res. 121(4):457-464.

Clarke AH, Schonfeld U, Hamann C, Scherer H. 2001, Measuring unilateral otolith function via the otolith-ocular response and the subjective visual vertical. Acta Otolaryngol Suppl 545:84-7.

Clément, G., 2003, Fundamentals of Space Medicine. In Fundamentals of Space Medicine. Dordrecht: Springer Netherlands, pp. 1–241.

Clément, G., Pierre Denise, Millard F. Reschke, Scott J. Wood 2007, Human ocular counter-rolling and roll tilt perception during off-vertical axis rotation after spaceflight. Journal of Vestibular Research, 17 (5-6), pp. 209–215.

Clément, G., & Wood, SJ 2013, Eye movements and motion perception during off-vertical axis rotation after spaceflight. Journal of Vestibular Research, 23 (1), pp. 13–22.

Cody DTR, Bickford RG 1969, Averaged evoked myogenic responses in normal man. Laryngoscope; 79(3):400-416.

Cohen B, Suzuki JI 1963, Eye movements induced by ampullary nerve stimulation. Am J Physiol 204:347-5.

Cohen B 1974, The vestibilo-ocular reflex arc.In: Kornhuber HH (ed) Handbook of sensory physiology. Vestibular system. Springer, Berlin-Heidelberg-New York, pp 477-540.

Cohen B, Maruta J, Raphan T 2001, Orientation of the eyes to gravitoinertial acceleration. Ann N Y Acad Sci. 942:241-58.

Cohen, B. & Gizzi, M., 2002. The physiology of the vestibulo-ocular reflex. In L. M. Luxon et al., eds. A Textbook of Audiological Medicine Clinical Aspects of Hearing and Balance. CRC Press, pp. 701–716.

Colebatch JG, Halmagyi GM. 1992, Vestibular evoked potentials in human neck muscles before and after unilateral vestibular deafferentation. Neurology, 42:1635-1636.

Colebatch JG, Halmagyi GM, Skuse NF 1994, Myogenic potentials generated by a click evoked vestibulocollic reflex. J Neurol Neurosurg Psychiatry; 57(2):190-197.

Colebatch JG, Rothwell JC 2004, Motor unit excitability changes mediating vestibulocollic reflexes in the sternocleidomastoid muscle. Clin Neurophysiol; 115(11):2567-2573.

Curthoys, I. S., Vulovic, V. & Manzari, L 2012, Ocular vestibular-evoked myogenic potential (oVEMP) to test utricular function: neural and oculomotor evidence. Acta Otorhinolaryngologica Italica: Organo Ufficiale Della Società Italiana Di Otorinolaringologia E Chirurgia Cervico-Facciale, 32 (1), pp. 41–5. Available from: <http://www.pubmedcentral.nih.gov/articlerender.fcgi?artid=3324959&tool=pmcentrez&rendertype=abstract>. [Accessed March 15, 2015].

Dai, Mingjia, Sofroniou Sofronis, Kunin Mikhail, Raphan Theodore and Cohen, Bernard 2010, Motion sickness induced by off-vertical axis rotation (OVAR). Experimental Brain Research, 204(2), pp.207–222.

Darlot, C. & Denise, P. 1988, Nystagmus induced by off-vertical rotation axis in the cat. Experimental Brain Research, 73(1):78-90.

Darlot C, Denise, P Droulez, J, Cohen B & Berthoz A 1988, Eye movements induced by off-vertical axis rotation (OVAR) at small angles of tilt. Experimental Brain Research, Exp Brain Res. 1988;73(1):91-105.

Denise, P, Etard, O, Zupan L and Darlot, C 1996, Motion sick- ness during off-vertical axis rotation: prediction by a model of sensory interactions and correlation with other forms of motion sickness, Neurosci. Lett., 203 183–186.

Dizio, P & Lackner, JR 1991, Motion Sickness Susceptibility in Parabolic Flight and Velocity Storage Acitivity. Aviat. Space Enivron. Med., 62, pp. 300–307.

Dizio, P & Lackner, JR 1992, Influence of gravitoinertial force level on vestibular and visual velocity storage in yaw and pitch. Vision Research, 32 (1), pp. 111–20.

Dieterich M, Brandt T 1994, Vestibular syndromes in the roll plane: topographic diagnosis from brainstem to cortex. Ann Neurol: 36 (3):337-47.

Fanghänel, J, Pera F, Anderhuber F, Nitsch R 2003, Waldeyer, Anatomie des Menschen. In Waldeyer, Anatomie des Menschen. pp. 461–519.

Fernández C, Goldberg GM 1971, Physiology of peripheral neurons innervating semicircular canals of the sqiurrel monkey II. Response to sinusoidal stimulation and dynamics of peripheral vestibular system. J Neurophysiology 34: 661.

Furman, JM, Schor RH, Schumann TL 1992, Off-vertical axis rotation: a test of the otolith-ocular reflex. Ann Otol Rhinol Laryngol.;101(8):643-50.

Furman, JM, Schor RH, Kamerer DB 1993, Off-vertical axis rotational responses in patients with unilateral peripheral vestibular lesions. Ann Otol Rhinol Laryngol; 102(2):137-43.

Furman, JM, Koizuka, I. & H. Schor, R 2000, Characteristics of secondary phase post-rotatory nystagmus following off-vertical axis rotation in humans. Journal of vestibular research, 10, pp.143–150.

Geisler CD, Frishkopf LS, Rosenblith WA 1958, Extracranial responses to acoustic clicks in man. Science; 128:1210-1211.

Gerathewohl, SJ 1959, Work proficiency in the space cabin simulator. Aerospace Medicine, 30, pp. 722–35.

Gierke, von, HE & Parker, DE 1994, Differences in otolith and abdominal viscera gravicep- tor dynamics: Implications for motion sickness and perceived body position. Aviation, Space, and Environmental Medicine, 65, 747-751.

Glasauer, S 1992, Interaction of semicircular canals and otoliths in the processing structure of the subjective zenith. Ann NY Acad Sci 656: 847-849.

Goldberg, JM, J Wilson, V, Cullen, KE, Angelaki, DE., M. Broussard, D., Buttner-Ennever, J., Fukushima, K., Minor, LB 2012, Vestibular system, A Sixth Sense. Scholarpedia (Vol. 3). Oxford University Press, pp. 4-275.

Graybiel A, Wood CD, Miller EF, Cramer DB 1968, Diagnostic criteria for grading the severity of acute motion sickness. Aerosp Med.39(5):453-5.

Harris, LR, Barnes, GR 1987, Orientation of vestibular nystagmus is modified by head tilt. In: Graham MD, Kemink JL (eds) The vestibular system: neurophysiologic and clinical research. Raven, New York, pp 539–548.

Harris, LR 1987, Vestibular and optokinetic eye movements evoked in the cat by rotation about a tilted axis. Experimental Brain Research; 66(3): 522-32.

Harris, LR 1988, The contribution of the horizontal semicircular canals to the response to off-vertical-axis rotation in the cat. Experimental Brain Research, 71(1):147-52.

Haslwanter, T., 2000. Computational and Experimental Aspects of Rotatory Eye Movements in Three Dimensions 2000. , pp.1–88. Available at: <http://work.thaslwanter.at/PDFs/Theses/haslwater_habil.pdf> [Accessed January 20, 2015].

Haslwanter, T, Jaeger R, Mayr S & Fetter M 2000, Three-dimensional eye-movement responses to off-vertical axis rotations in humans. Experimental Brain Research, 134 (1), pp. 96–106.

Heinemann, I 2014, Aus der Klinik für Hals-Nasen-Ohren-Heilkunde der Medizinischen Fakultät der Charité – Universitätsmedizin Berlin. pp. 6-8.

Hess BJ, Dieringer N 1990, Spatial organization of the maculoocular reflex of the rat: responses during off-vertical axis rotation. Eur J Neurosci 2:909–919.

Hess BJ, Dieringer N 1991, Spatial organization of linear vestibuloocular reflexes of the rat: responses during horizontal and vertical linear acceleration J Neurophysiol 66(6): 1805-18.

Hess, BJM, Jaggi-Schwarz ,K & Misslisch, H 2005, Canal-otolith interactions after off-vertical axis rotations. II. Spatiotemporal properties of roll and pitch postrotatory vestibuloocular reflexes. Journal of Neurophysiology, 93 (3), pp. 1633–46.

Highstein, SM, Fay RR & Popper AN 2004, The Physiology of the Vestibuloocular Reflex (VOR). Chapter: The Vestibular System. pp. 235–285.

Holst E, Mittelstaedt H 1950, Das Reafferenzprinzip. In Naturwissenschaften 37 pp.464-476.

Huang TW, Young YH, Cheng PW 2004, Eliciting constant and prominent waves n34-p44 of vestibular-evoked myogenic potentials. Acta Otolaryngol; 124(9):1022-1027.

Jenkinson, N & Miall, RC 2010, Disruption of saccadic adaptation with repetitive transcranial magnetic stimulation of the posterior cerebellum in humans. Cerebellum (London, England), 9(4), pp.548–55. Available at: <http://www.pubmedcentral.nih.gov/articlerender.fcgi?artid=2996540&tool=pmcentrez&rendertype=abstract> [Accessed January 20, 2015].

Johst, U., 2001. Zur klinischen Bedeutung der exzentrischen vertikalen Rotation zum Nachweis von Otolithenfunktionsstörungen beim Menschen. Albert-Ludwigs-Universität Freiburg. pp.1-36.

Karmali, F. & Shelhamer, M., 2008. The dynamics of parabolic flight: flight characteristics and passenger percepts. Acta. Astronautica, 63(410), pp.594–602.

Klinke, R & Silbernagl, S 2001, Lehrbuch der Physiologie. In R. Klinke & S. Silbernagl (Eds.), Gleichgehwichts -, Lage- und Bewegungssinn / Sensomotorische Systeme: Körperhaltung, Bewegung und Blickmotorik 3. ed., pp. 562, 595–603, 669–685.

Kushiro, K, Zakir M, Ogawa, Y, Sato, H 1999, Saccular and utricular inputs to sternocleidomastoid motoneurons of decerebrate cats. Exp Brain Res; 126(3): 410-416.

Kushiro, K, Dai, M, Kunin, M., Yakushin, SB, Cohen, B & Raphan, T 2002, Compensatory and orienting eye movements induced by off-vertical axis rotation (OVAR) in monkeys. Journal of Neurophysiology, 88 (5), pp. 2445–62.

Lackner, J.R. & DiZio, P., 2009. Angular displacement perception modulated by force background. Experimental Brain Research, 195(2), pp.335–343. Available at: http://link.springer.com/10.1007/s00221-009-1785-6.

Lewis, RF., Priesol, AJ., Nicoucar, K, Lim, K & Merfeld, DM 2011a, Abnormal motion perception in vestibular migraine. The Laryngoscope, 121 (5), pp. 1124–5.

Lewis, RF, Priesol, AJ., Nicoucar, K, Lim, K & Merfeld, DM 2011b, Dynamic tilt thresholds are reduced in vestibular migraine. Journal of Vestibular Research: Equilibrium & Orientation, 21 (6), pp. 323–30.

Lim, CL, Clouston, P, Sheean G, Yiannikas ,C 1995, The influence of voluntary EMG activity and click intensity on the vestibular click evoked myogenic potential. Muscle Nerve; 18(10):1210-1213.

Luft, B. 2011, Die anatomische Lokalisation des VEMP-Reflexes im Hirnstamm. Medizinischen Fakultät der Friedrich-Schiller-Universität Jena, pp.11-15.

Luxon, L. et al., 2002. A Textbook of Audiological Medicine: Clinical Aspects of Hearing and Balance. In A Textbook of Audiological Medicine. CRC Press, pp. 701–715.

McCue MP, Guinan JJ 1994, Acoustically responsive fibers in the vestibular nerve of the cat. J Neurosci; 14(10): 6058-6070.

McCue MP, Guinan JJ 1995, Spontaneous activity and frequency selectivity of acoustically responsive vestibular afferents in the cat. J Neurophysiol 74:1563-1572.

Merfeld, DM., Laurence R. Young 1990, Spatial orientation in the squirrel monkey: An experimental and theoretical investigation. Annals of Biomedical Engineering March/April 1993, Volume 21, Issue 2, p 186.

Merfeld, DM., Zupan, L., Peterka, R., 1999. Humans use internal models to estimate gravity and linear acceleration. Nature, (398), pp.615–618.

Merfeld, DM., 2003, Rotation otolith tilt-translation reinterpretation (ROTTR) hypothesis: a new hypothesis to explain neurovestibular spaceflight adaptation. Journal of neurophysiology, 13, pp.309–320.

Merfeld, DM, Park, S, Gianna-Poulin, C, Black, FO., Wood, S. & Black, O 2005a, Vestibular Perception and Action Employ Qualitatively Different Mechanisms. I . Frequency Response of VOR and Perceptual Responses During Translation and Tilt. J Neurophysiol, 94, pp. 186–198.

Merfeld, DM., Park, S, Gianna-Poulin, C, Black FO., Wood S., Daniel, M. & Owen, F, 2005b. Vestibular Perception and Action Employ Qualitatively Different Mechanisms. II . VOR and Perceptual Responses During Combined Tilt & Translation. J Neurophysiol 94, pp. 199–205.

Mittelstaedt, H, Glasauer, S 1993, Illusions of verticality in weightlessness. Clinical Investigator, 71, 732-739.

Mittelstaedt H, Glasauer, S 1993, Crucial effects of weightlessness on human orientation. J Vestib Res.3(3):307-14.

Mittelstaedt, H 1999, The Role of the Otoliths in Perception of the Vertical and in Path Integration. May 28; 871:334-44.

Murofushi T, Curthoys IS, Topple AN, Colebatch JG, Halmagyi GM 1995, Responses of guinea pig primary vestibular neurons to clicks. Exp Brain Res; 103(1):174-178.

Murofushi T, Halmagyi GM, Yavor RA, Colebatch JG 1996, Absent vestibular evoked myogenic potentials in vestibular neurolabyrinthitis. An indicator of inferior vestibular nerve involvement?. Arch Otolaryngol Head Neck Surg; 122(8):845-848.

Murofushi T, Curthoys IS 1997, Physiological and anatomical study of click-sensitive primary vestibular afferents in the guinea pig. Acta Otolaryngol; 117(1):66-72.

Nieuwenhuys R, Voogd J, Huizen van C 1991, Das Zentralnervensystem des Menschen. Springer, Berlin Heidelberg New York Tokyo.

Oman, C.M., Lichtenberg, BK, Money, KE & McCoy, RK 1986, M.I.T./Canadian vestibular experiments on the Spacelab-1 mission. 4. Space motion sickness: symptoms, stimuli,and predictability. Experimental Brain Research, 64, 316-334.

Planel, H. 2004, Space and Life. An Introduction to Space Biology and Medicine pp. 69–81. CRC Press.

Raphan T, Cohen B, Matsuo V 1977, A velocity storage mechanism responsible for optokinetic nystagmus (OKN), optokinetic afternystagmus (OKAN) and vestibular nystagmus. In: Baker N, Berthoz A (eds) Control of gaze by brainstem neurons: Elsevier, Amsterdam, pp. 37-47.

Raphan T, Matsuo V, and Cohen B 1979, Velocity storage in the vestibulo-ocular reflex arc (VOR). Exp Brain Res 35: 229-248.

Raphan T, Cohen B, Henn V 1981, Effects of gravity on rotatory nystagmus in monkeys. Ann NY Acad Sci 374:44–55, 1981.

Raphan, T. & Cohen, B 1988, Organizational principles of velocity storage in three dimensions. Ann N Y Acad Sci, (545), pp.74–92.

Saborowski, R 2001, Über die Beeinflussung der Lagewahrnehmung und des visuellen Systems mittels Über- und Unterdruck auf den Unterkörper. Available at <http://geb.uni-giessen.de/geb/volltexte/2001/434/pdf/d010036.pdf> [Accessed March 15, 2015].

Saborowski, R, Vaitl, D., Stark, R 2002, Perception of posture and cerebral blood flow. International Journal of Psychophysiology: Official Journal of the International Organization of Psychophysiology, 43 (2), pp. 167–75.

Sato H, Imagawa M, Isu N, Uchino Y 1997, Properties of saccular nerve-activated vestibulospinal neurons in cats. Exp Brain Res; 116(3):381- 388.

Scherer H 1997, Das Gleichgewicht. 2. Auflage Springer-Verlag Berlin;: 15-523.

St George, RJ, Day, BL & Fitzpatrick, RC, 2011. Adaptation of vestibular signals for self-motion perception. The Journal of Physiology, 589(4), pp.843–853. Available at: <http://doi.wiley.com/10.1113/jphysiol.2010.197053> [Accessed March 15, 2015].

Straumann, D, Haslwanter, T, Hepp-Reymond, M-C & Hepp, K 1991, Listing's law for eye, head and arm movements and their synergistic control. Experimental Brain Research; 86(1):209-15.

Straumann, D. & Klinik, N. n.d.. Der vestibulo-okuläre Reflex (VOR) und seine klinische Bedeutung. Available at: <http://slideplayer.com/slide/1341039/> [Accessed March 03, 2015].

Townsend, GL, Cody,DTR. 1971, The averaged inion response evoked by acoustic stimulation: Its relation to the saccule. Ann Otol Rhinol Laryngol; 80(1):121-131.

Uchino, Y, Suzuki, S. 1983, Axon collaterals to the extraocular motoneuron pools of inhibitory vestibuloocular neurons activated from the anterior, posterior and horizontal semicircular canals in the cat. Neurosci Lett 37(2):129-35.

Uchino, Y, Sato H, Sasaki, M, Imagawa, M, Ikegami, H, Isu, N, Graf, W 1997, Sacculocollic reflex arcs in cats. J Neurophysiol; 77(6):3003-3012.

Udo de Haes Schöne H 1970, Interaction Between Statolith Organs and Semicircular Canals on Apparent Vertical and Nystagmus. Acta Otolaryngol (Stockh) 69, 25-31.

Waespe, W., Cohen, B. & Raphan, T., 1985. Dynamic modification of the vestibulo-ocular reflex by the nodulus and uvula. Science, 228(4696), pp.199–202. Available at: http://www.sciencemag.org/cgi/doi/10.1126/science.3871968.

Waespe W, Schwarz U 1986, Characteristics of eye velocity storage during periods of suppression and reversal of eye velocity in monkeys. Exp Brain Res 65(1):49-58.

Waltmann, K 2004, Die Dreidimensionalität der Okulomotrischen Reizantwort bei thermischer Prüfung des Gleichgewichtsorgans unter besonderer Berücksichtigung der tonisch torsionalen Deviation. , pp.1–20. Available at: <http://www.diss.fu-berlin.de/diss/receive/FUDISS_thesis_000000001386>. [Accessed March 03, 2015].

Welgampola MS, Colebatch JG 2001, Characteristics of tone burst-evoked myogenic potentials in the sternocleidomastoid muscles. Otol Neurotol; 22(6):796-802.

Wood, SJ 2002, Human otolith-ocular reflexes during off-vertical axis rotation: effect of frequency on tilt-translation ambiguity and motion sickness. Neuroscience Letters, 323 (1), pp. 41–44.

Wood, SJ, Reschke, MF, Sarmiento, LA & Clément, G 2007, Tilt and translation motion perception during off-vertical axis rotation. Experimental Brain Research, 182 (3), pp. 365–377.

Wu HJ, Shiao AS, Yang YL, Lee GS 2007, Comparison of short tone burst-evoked and click evoked vestibular myogenic potentials in healthy individuals. J Chin Med Assoc; 70(4):159-163.

Young, LR 1984, Perception of the body in space: mechanisms. Comprehensive Physiology. 1023–1066.

6 Reference of Figures

Figure 1: Clément, G., 2003, Fundamentals of Space Medicine. In Fundamentals of Space Medicine. Dordrecht: Springer Netherlands, p. 91, Note: Sensory Systems.

Figure 2: Baloh, R., Honrubi, V., Kerber, K.A. 2011, Clinical Neurophysiology of the Vestibular System. In Oxford University Press, Note: Illustration of Rotational Axis

Figure 3: Straumann D. Skull base location of the vestibular organ, taken from presentation: Der vestibulo- okuläre Reflex (VOR) und seine klinische Bedeutung, slide 11. Originally taken from Ferner & Straubesand 1982.
Available from http://slideplayer.org/slide/1341039/. [08 February 2015]

Figure 4: Clément, G., 2003, Fundamentals of Space Medicine. In Fundamentals of Space Medicine. Dordrecht: Springer Netherlands, p.99

Figure 5: Haslwanter, T., 2013. Physiology & Computer Simulations., p.123. Note: The otholith organs are responsible for sensing linear acceleration. The utricle (left) is approximately horizontally oriented; the saccule (center)

Figure 6: Scherer H 1997, Das Gleichgewicht. 2. Auflage Springer-Verlag Berlin, p. 16.
Note: Interaction of the vestibulo-ocular reflex (VOR) and the vestibulospinal reflex (VSR), Scherer 1997, p. 16.

Figure 7: Goldberg, JM, J Wilson, V, Cullen, KE, Angelaki, DE., M. Broussard, D., Buttner-Ennever, J., Fukushima, K., Minor, LB 2012, Vestibular system, A Sixth Sense. Scholarpedia (Vol. 3). Oxford University Press, p.6.
Note: Shows the communication pathways of the vestibular nuclei, Taken from The Vestibular System A Sixth Sense Jay M. Goldberg et al.s, 2012, p.6.

Figure 8: Shows test subject in experimental Situation (VOR), taken with permission from company EKIDA

Figure 9: Klinke, R & Silbernagl, S 2001, Lehrbuch der Physiologie. In R. Klinke & S. Silbernagl (Eds.), Gleichgehwichts -, Lage- und Bewegungssinn 3. ed., p. 692 Note: Arc of the VOR

Figure 10: Clarke, AH. 1995, Neuere Aspekte des vestibulo-okulären Reflexes. Available from: <http://www.mbfys.ru.nl/staff/j.vangisbergen/endnote/endnotepdfs/labyrinthectomy/Clarke_review_vestibulair.pdf>. [08 February 2015], p. 14.
Note: Central processing pathways vestibular organ, nuclei and eye muscles, taken from Clarke A. 1995, p.14

Figure 11: Anastasio T.J.. 2010, Tutorial on Neural System Modeling. The velocity storage adapted from, p. 44

Figure 12: Luft, B. 2011, Die anatomische Lokalisation des VEMP-Reflexes im Hirnstamm. Medizinischen Fakultät der Friedrich-Schiller-Universität Jena, p. 13.
Note: Shows the vestibular nuclei and their integrative functions. Adapted from Luft 2011, p.13 (originally taken from Schünke et al., 2006).

Figure 13: Kerber, KA & Baloh, RW, 2011. The evaluation of a patient with dizziness Available_from: <http://www.lookfordiagnosis.com/mesh_info.php?term=Head+Impulse+Test&lang=1>. [28 June 2015]
Note: The head trust test shows the physiological response (A) and the pathologic correction saccades (B).

Figure 14: Chiarovano E, Darlington C, Vidal P.P, Lamas G, de Waele C, 2014, The Role of Cervical and Ocular Vestibular Evoked Myogenic Potentials in the Assessment of Patients with Vestibular Schwannomas.
Availablfrom: <http://journals.plos.org/plosone/article?id=10.1371/journal.pone.0105026>. [29 June 2015], p. 2.
Note: Cervical VEMPs (saccular function) are induced by air-conducted sounds e.g. 500 Hz short-tone bursts (AC STB) or clicks. Ocular VEMPs (utricular function) are evoked by AC STB, bone-conducted vibration AFz (AFz BCV) or at the mastoid (mastoid BCV) taken from Chiarovano et al 2014, p. 2

Figure 15: Demonstration of the "tilt suppression" phenomenon. Notice the nystagmus in (A) shows the VOR per - an afternytagmus (head translated position). (B) When head tilts post-rotatory time constant is shortened (VOR suppression) compared to the post-rotator. Own work.

Figure 16: Shows test subject in experimental Situation (OVAR), taken from company DIFRA. <http://www.difra.be/eng/Balance-systems/Rotary-Chairs/MegaTorque> [16 April 2015]

Figure 17: Wilson-Pauwels, Akeson & Stewart Cranial nerves 3 ed. 20 'Right eye movements around the "X", "Y", and "Z" axes.
Available from <http://images.frompo.com/22bf444ed11eeda458a09350cc2c1b05> [16 April 2015]

Figure 18: Haslwanter, T, Jaeger R, Mayr S & Fetter M 2000.'Three-dimensional eye-movement responses to off-vertical axis rotations in humans.' Experimental Brain Research, 134 (1), pp. 98. Note: OVAR Nystagmus horizontal decay, persistent vertical and torsional components.

Figure 19: Haslwanter, T, Jaeger R, Mayr S & Fetter M 2000.'Three-dimensional eye-movement responses to off-vertical axis rotations in humans.' Experimental Brain Research, 134 (1), p. 98. Note: Horizontal, vertical and torsional eye movements generated by Off-Vertical Axis Rotation

Figure 20: Kushiro, K, Dai, M, Kunin, M., Yakushin, SB, Cohen, B & Raphan, T 2002, Compensatory and orienting eye movements induced by off-vertical axis rotation (OVAR) in monkeys. Journal of Neurophysiology, 88 (5), pp. 2447.
Note: Horizontal, vertical, and roll eye positions (A–C) taken from Kushiro et al. 2002, p.2447.

Figure 21: Wood, SJ 2002, Human otolith-ocular reflexes during off-vertical axis rotation: effect of frequency on tilt-translation ambiguity and motion sickness. Neuroscience Letters, 323(1),p.42.
Note: **"**Otolith–ocular responses and motion sickness as a function of frequency. The response amplitude and phase shift (positive is leading) for torsion (squares) and horizontal SPV (circles) are shown as a function of frequency (mean 1 SEM). Note how the peak of motion sickness susceptibility (dashed line) during OVAR at the same tilt angle (adapted with permission from [5]) occurs in the region where torsional and horizontal SPV modulation responses crossover. "(Wood 2002, p.42) Human otolith-ocular reflexes during off-vertical axis rotation, taken from Wood SJ 2002, p.42.

Figure 22: Clément, G., 2003, Fundamentals of Space Medicine. In Fundamentals of Space Medicine. Dordrecht: Springer Netherlands, p. 100
Note: Perception of body position on Earth (left), in space (right). Draft Based on Gilles Clément Fundamentals of Space medicine 2003, p.100

Figrue 23: Saborowski, R 2001, Über die Beeinflussung der Lagewahrnehmung und des visuellen Systems mittels Über- und Unterdruck auf den Unterkörper., p. 57 Available from http://geb.unigiessen.de/geb/volltexte/2001/434/pdf/d010036.pdf. [Accessed March 15, 2015].
Note: Lower Body Negative Pressure (LBNP) device with test subject, taken from Saborowski 2001, p.57.

Figure 24: Illustration of a parabolic maneuver. Parabolic draft taken from Montmerle, S., 2005. Lung function in micro- and in hypergravity,.p.14 Available from: <http://www.ssu.ac.ir/cms/fileadmin/user_upload/Moavenatha/MBehdashti/TebKar/PDFs/Fitness_for_Duty_in_Hazardous_Occupations.pdf > [Accessed 29 May 2015].

Figure 25: Own work, Illustrations a) - e). Image of test person during OVAR taken from Neuro Kinetics, Inc.

Figure 26: Eye Tracking System, courtesy taken with permission from Chronos Vison

Figure 27: Rotatory chair system, courtesy taken with permission of company EKIDA

Figure 28: ESA-Zero-G Airbus A300 for parabolic flights, 2007 Available from: http://www.esa.int/var/esa/storage/images/esa_multimedia/images/2007/11/zero-g_airbus_a300_for_parabolic_flights/9988895-2-eng-GB/Zero-G_Airbus_A300_for_parabolic_flights.jpg [Accessed 6 March 2015]
Note: Force acting on aircraft adapted from (Karmali & Shelhammer 2008).

Figure 29: Own work: Vector description. Parabolic draft taken from Montmerle, S., 2005. Lung function in micro- and in hypergravity,.p.14 Available from: <http://www.ssu.ac.ir/cms/fileadmin/user_upload/Moavenatha/MBehdashti/TebKar/PDFs/Fitness_for_Duty_in_Hazardous_Occupations.pdf > [Accessed 29 May 2015].
Note: Own work: Description of the GIF-Vector during a parabolic maneuver. Parabolic draft adapted from Montmerle 2005, p.14

Figure 30: Karmali, F. & Shelhamer, M., 2008. 'The dynamics of parabolic flight: flight characteristics and passenger percepts.' Acta. Astronautica, 63(410), p.12.
Note: Forces acting on test subjects during a Parabolic Flight maneuver, taken from (Karmali & Shelhammer 2008).

Figure 31: Karmali, F. & Shelhamer, M., 2008. 'The dynamics of parabolic flight: flight characteristics and passenger percepts.' Acta. Astronautica, 63(410), p.12. Note: Forces acting on otolith during a Parabolic Flight maneuver, taken from (Karmali & Shelhammer 2008)

7 Reference of Tables

Table 1: Baloh, R., Honrubi, V., Kerber, K.A. 2011, Clinical Neurophysiology of the Vestibular System. In Oxford University Press, p. 75.
Note: Shows activated and inhibited eye muscles in correspondence to the stimulated Semicircular Canal, adapted from Baloh et al. 2011, p.75.

Table 2: Dizio, P & Lackner, JR 1991, Motion Sickness Susceptibility in Parabolic Flight and Velocity Storage Acitivity. Aviat. Space Enivron. Med., 62, p. 302.
Note: Categorization of Motion Sickness Symptoms, taken from Dizio & Lackner 1991, p. 302.

8 Appendix I

Parabolic Flight Campaign with A300 ZERO-G

The following sections were taken from the User Manual of the ESA Parabolic Flight office or online: http://web.mit.edu/~wilken/www/Neptunas/Novespace_User_Manual.pdf

User's Manual

(Edition 5., July 99)

Table of Content

List of Figures

8.1 A300 Zero-G Parabolic Flight Technique

8.1.1 Obtaining microgravity

A reduced gravity environment is obtained by flying a specially modified Airbus A300 Zero-G through a series of parabolic maneuvers, which result in approx. twenty-two seconds periods of « 0g » acceleration (actually around 10^{-2} g). Each parabola is initiated with a 1.8 g pull up and terminated with a 1.8 g pull out. A normal mission lasts two to three hours and consists of thirty parabolic maneuvers.

8.1.2 Obtaining microgravity

-Description of the Parabolic Maneuver-

Starting from a steady normal horizontal flight, the aircraft takes a 1.8 g load factor, nosing up to 45° and climbing to 23 000 Ft over an interval of about twenty seconds. This is the entry pull-up phase.

Then the engine thrust is considerably reduced, to the point where it just overcomes the aerodynamic drag, and the pilot kills the lift. This transitory phase of "injection" separating the 1.8 g pull-up from the zero g parabola lasts fewer than five seconds.

The aircraft is then in microgravity phase for some twenty-five seconds. A symmetrical 1.8g pullout phase is then executed on the down side of the parabola to bring the aircraft back to its steady horizontal flight in about 20 seconds. There is an interval of two minutes between two parabolas.

8.1.3 Acceleration Levels and Piloting Techniques

During the 20 to 25 seconds of the parabolic maneuver, the residual gravity level for any apparatus attached to the aircraft structure oscillates between - $5*10^{-2}$ and + $5*10^{-2}$ g (z-axis) and between - 10^{-2} and + 10^{-2} g (x- and y-axis).

A small object free floating in the cabin may benefit from a higher quality of weightlessness (microgravity less than 10^{-4} g) for a period of five to ten seconds, i.e. until it touches the walls of the aircraft. This is called the free-float technique necessitating at least one person from the safety crew as additional assistance.

The piloting techniques may be, up to a technically realizable degree, adapted to the needs of the experimenters.

The different techniques are:

a) Standard technique where the crew is trying to obtain a level of microgravity as close to zero as possible (in average and in amplitude) and as long as possible.

b) The procedure to minimize negative microgravity values, called soft procedure.

c) The procedure to keep a residual gravity (of low or high value).

d) The free-float procedure where the piloting is done with respect to keeping an object free-floating in the middle of the cabin (visible for the pilots on a video screen).

The application of procedures which are not standard ones may result in parabolas of minor quality, i. e. of reduced duration. As these techniques might necessitate a special training or material (especially the last two ones, c and d) and therefore generate additional cost for the user, the interested experimenters are highly recommended to contact Novespace early before a campaign to express their needs.

8.2 Experimentation Area Description

In this chapter we present the resources of the aircraft. These resources (room availability, electric power, venting...) are to be *shared* by different experiments. Although it seems obvious, we would like to emphasize the fact that unless the entire aircraft is commissioned by one single company, all experimenters are obliged to share the aircraft resources. Hence, the aircraft will not be entirely at one's disposal. In a standard campaign, 10 to 15 different experiments share global resources.

8.2.1 Cabin dimensions (See Figures 2, 3, and 4)

The testing cavity is 20 meters in length, 5 meters in width, and 2.3 meters in height (see figures 2, 3, and 4). The second front door, through which equipment is loaded, is 1.93 m high by 1.07 m wide. An experiment being larger than the door may be loaded by being taken apart. The total volume of the cabin is 300 m^3.

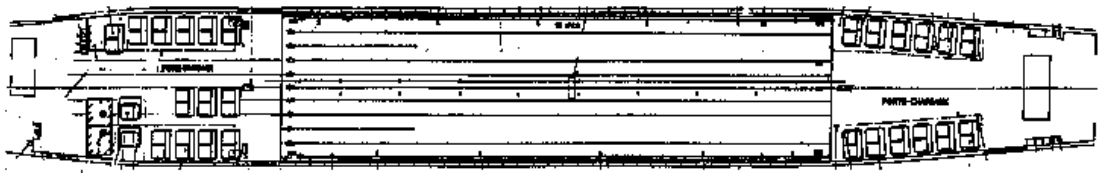

Fig. 1: Upper View of the cabin

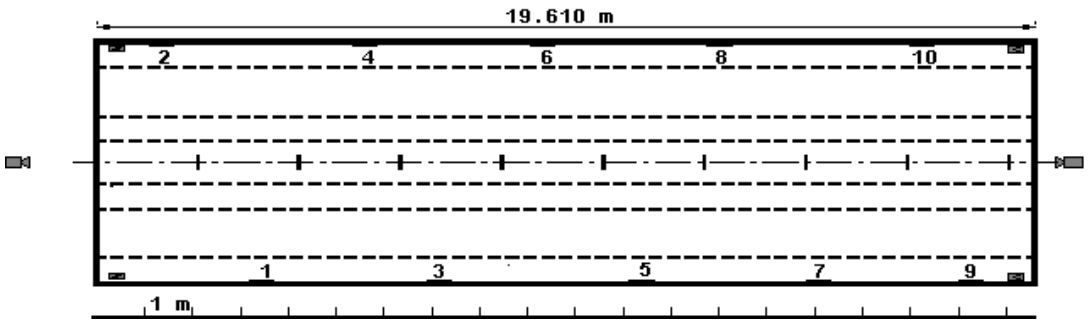

Fig. 2: Bi- Section of Aircraft cabin

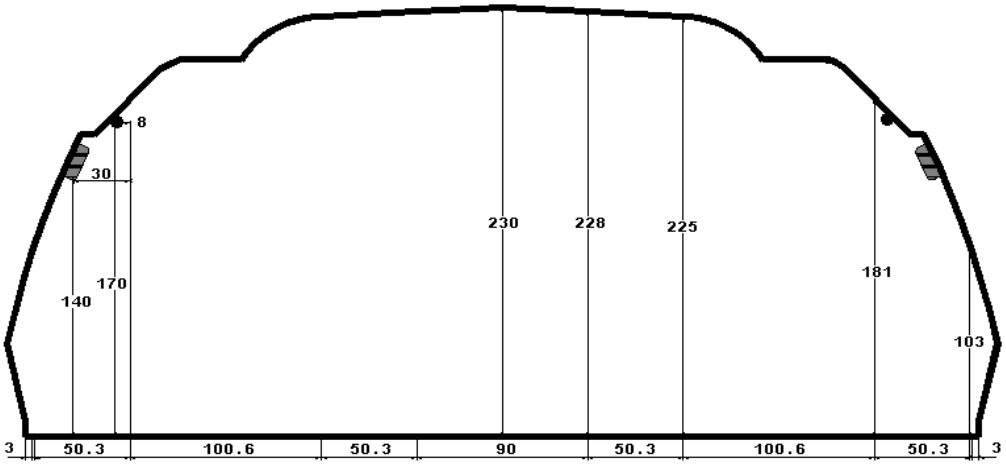

Fig. 3: Cross Section of Aircraft Cabin- position of attachment rails

8.3 User Procedures

8.3.1 Safety Policy

The A300 Zero-G parabolic flight programme is operated in accordance with stringent safety procedures established by the French "Centre d'Essais en Vol". The exploitation in microgravity is done under an exceptional "Laisser-Passer" signed by the General Direction of Civil Aviation in France.

The flights are regarded as test flights and as such fall under the rules for test flights, under the authority of the "Centre d'Essais en Vol". Due to the critical nature of this programme, a multi-stage review and approval procedure has been developed to ensure flight safety. Approval from multiple authorities is required prior to flight.

In particular, the test experimenter must submit to Novespace relevant documents at different stages of the project (including experiment description and hazard analysis). In addition, all test personnel must follow Novespace requirements and attend a final safety review and

safety visit prior to flight. These items are described in the following chapters. The degree of detail, rigor, and formality required in the development and conduct of a reduced gravity test depends on the complexity, hazards, and uniqueness of a test. Communications with Novespace are required early and often to eliminate any last minute surprises which might cause delays. Relevant personnel will review and comment on preliminary drawings and plans at all stages of development. It should be noted that a flight will be conducted only after Novespace and CEV have been assured that a safe, well organized, and productive flight can be achieved. During the flights, all personnel on board the aircraft will be under the direction of the aircraft flight crew and test directors for the entire duration of a campaign. The aircraft commander is the final authority for all operations from boarding to deplaning.

Strict adherence to the authority of test personnel will be rigidly enforced. Any deviation from the flight-test plan must be discussed with Novespace before its implementation.

8.3.2 Documentation requested

Three months prior to flight, the test experimenter should forward to Novespace a document containing general information. This package should contain:

1. Test Objectives
2. Brief description of the test and associated test equipment (Please note if test is fixed or free-floating)
3. Dimensions of equipment
4. Total weight
5. Electrical consumption
6. Number of flights requested (1, 2 or 3)
7. Number of test personnel required for flight and detail of each person's function on board
8. Special support required (personnel, equipment, etc..) or special constraints (temperature, pressure, ground support, etc..)
9. Preliminary Hazard Analysis identifying hazards and controls (any format is acceptable)
10. Names, addresses, and phone number of points of contacts

Two months prior to flight, the test equipment data package must be submitted to Novespace, who will review the proposed test with CEV qualified experts, if need be. This package should contain the following:

1. Experiment title and Principal Investigators names and address

2. Test objectives

3. Test description

4. Equipment description (narrative, drawing, schematics, photographs, block diagrams, etc.)

5. Structural load analysis (please indicate the position of each structure)

6. Weight of each structure (measured, not estimated!)*

7. Electrical consumption (maximum and average) of each part of experiment (measured, not estimated!)*

8. Proof of mechanical resistance of each structure (see Appendix 2)

9. Pressure vessel certification (if applicable, see Appendix 3)

10. In flight test procedures (checklist form, please)

11. In the case of experiments on humans, detailed protocol in French and insurance certificate complying with French Huriet law (protecting persons in biomedical research).

12. Test support requirements (flight and ground) and constraints

13. Data acquisition system description

14. Test operation limits or restrictions, specific requirements

15. Hazard Analysis in accordance with Appendix 1 including Material Safety Data Sheet (MSDS) for Materials.**

16. Information and liability waiver forms for each flying individual, signed by each experimenter and his/her employer (see appendix 7 and 8), including assistant personnel on the ground.***

* It is really important that the weights and electrical consumptions are measured (the latter with a multimeter) and not estimated. Under- or over-estimation are both considered as not trustable and experiments in this case will not be allowed to fly.

** The Hazard Analysis is compulsory, in the form of appendix 1 of the manual.

*** The list of personnel including ground personnel must be known at least four weeks before the first flight. No personnel will be allowed to enter the airport area unless he or she is on the list.

8.3.3 Safety visit

The Safety Visit is the final review prior to flight. It includes a complete review of supporting analyses and documentation, an inspection of the test equipment, and a final verification of flight readiness.

A safety visit is required for all new and modified test articles. A list of modifications to already-flown equipment and changes to any test procedures must be provided.

During the safety visit the test equipment will be either approved, or approved after pending corrections have been implemented, or denied for flight. An unanimous decision is required for flight approval. Test equipment which has not been approved due to lacking conformity with any rules subject to the flight may be scheduled for a subsequent review when deficient areas have been corrected.

8.3.4 Medical Certificates

In order to obtain clearance to fly, personnel must obtain a Federal Aviation Administration (FAA) Class III physical test and pass a hypobaric chamber test. The medical visit is not a routine visit, and personnel can be denied clearance should they be found unfit for flight. This test can be performed by any qualified medical services affiliated with Aeronautic Medicine. Please contact Novespace if you would like the physical exam and altitude test to be conducted in a registered centre in France. A medical visit is valid for a year and the hypobaric chamber is valid for five. A copy of the physical exam results (NOT just the medical certificate) and the physiological training record for each person must be received at Novespace at least three weeks prior to the flight date.

8.3.5 Pre-Flight Briefing

A precise schedule for the week before and the week of flights will be delivered by Novespace one month before flight. A security briefing will take place the day before or the morning of the first flight. This briefing is mandatory for all experimenters. A schedule of the flight, advice concerning the flight, and a security procedure and rescue exposé will be presented.**Novespace will verify, if each experimenter has passed the necessary tests (medical and hypobaric chamber test) and has been present at the security briefing.**

8.3.6 Biomedical experiments with human subject

All investigations involving test on human subjects must include a specific protocol in French, complying with Huriet law (protecting subjects of biomedical experiments). This protocol shall be submitted to CCPPRBB (biomedical research "ethic" commission, composed of eighteen members including medical doctors, psychiatrists, social workers, etc..), which will review each protocol (they charge a fee for it).
The "promotor" of experiment (usually the PI) should provide a insurance certificate, complying with French law (exact wording and minimum guarantee can be asked to Novespace), covering his liability in case of injury linked to the experiment. Special procedures apply to the experiment subjects (forms to be signed, listing in a national subjects file, etc...). Novespace can assist the PI's in complying with these requirements if necessary, PI's must contact Novespace as early as possible.

8.4 Test Equipment- Fabrication Requirements

Before manufacturing an experiment, designers should contact Novespace to get first approval on the design. Thereby experimenters can implement necessary changes, if required, already before start of construction.

8.4.1 Structural Requirements

All equipment must be designed and manufactured to withstand the following loads during take off and landing.

X axis 9 g forward

1.5 g backward

Y axis 3 g left or right

Z axis 4.2 g upward

7.3 g downward

The X, Y and Z directions are referenced to the main aircraft reference system.

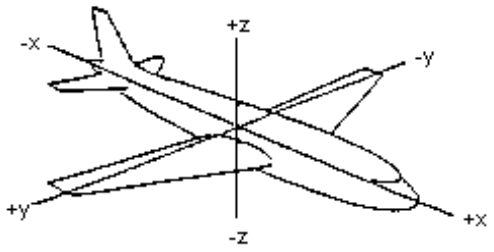

Fig 4:Aircraft Reference Axes

Structural calculations for the take off and landing configuration should be based on the yield strength of the hardware. The in-flight test configuration should be designed for a possible 2.5-g force at maneuver entry and exit. Free-float test articles should be designed for a possible 2.5-g force from any direction due to possible recovery on an end or side of the airplane after a maneuver.

Each structural analysis must at least include :

1. Structural drawing or diagram

2. Stress calculations results (if in table form, at least one sample calculation must be given)

3. Component weights and positions

4. Material properties

Structural calculations must be delivered with the description of the experiments.

The equipment must also be designed to withstand vibrations and compression/de-compression cycles corresponding to normal operation of the cabin pressure system, as well as a sudden decompression resulting from a pressure system failure. In case of doubt, it is recommended that the equipment be tested in an altitude chamber.

The simple model calculation in Appendix 2 can be used to demonstrate the strength of the structures. In case the safety coefficients resulting from this simple calculation do not exceed 1, the experiment is not accepted unless the strength of the structures are demonstrated with a complete structural calculation. If this calculation still leads to a safety coefficient of less than 1, the structure has to be strengthened.

8.4.2 Aircraft Rail Loading

The position of the experiments in the airplane is determined by Novespace and agreed by the "Centre d'Essais en Vol". Aircraft rails, in other aircraft used to fasten seats to aircraft floor, are used in A300 ZERO-G to fasten experiments to the floor by means of specially designed interfaces. As the complete specifications may not be described here, a basic rule is: The load on a rail should not be higher than 100 kg per linear meter.

As an example, if an experiment with four attachment points is heavier than 200 kg, two attachment points on the same rail are to be located more than one meter one from the other.

It is recommended to consult Novespace in advance if an experiment is to be build-up. In most cases the experiments comply with rail loading specification. But, if one or several of the items below are fulfilled it is mandatory to contact Novespace in advance:

- experiment weighs more than 200 kg
- the center of gravity of experiment is higher than 670 mm
- the distance between two fastening points on one rail is less than 508 mm (20 inches)
- the experiment is longer than three meters.

Maximal loads for each fixation point in the different directions are:

In x 2250 daN, in y 900 daN, in +z 1330 daN (direction to the ceiling) in -z 1750 daN (direction to the ground).

8.4.3 Equipment Attachment

The base of any experimental equipment must be drilled with 12 mm holes so that it can be fastened to the attachment interfaces by means of H-head M10 screws provided by Novespace. The screw holes should be in positions easily accessible so that the screws may be fastened by Sogerma personal having the skills to tighten the screws.

The distance between two holes on the same rail (X-axis) must be a multiple of one inch (25.4 mm).

Two holes in line on two different rails (Y-axis) must be 503 mm or 1006 mm apart (when checking the distance between holes, be sure to check also the diagonals). The actual distance will be confirmed by Novespace.

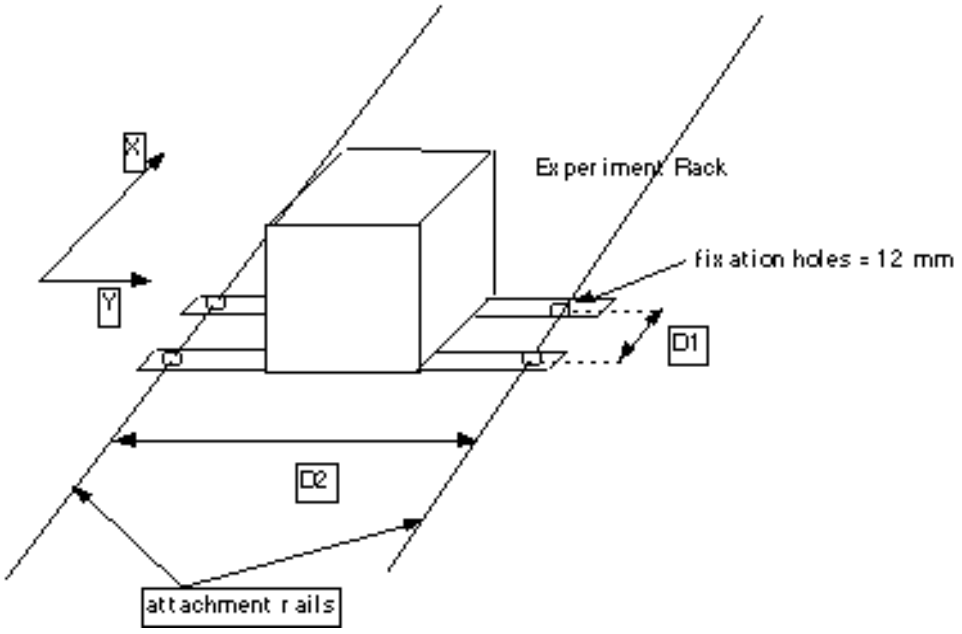

Fig 5: Equipment Attachment

8.5 Flight Campaign Organization

8.5.1 Campaign Order

It is best to plan a parabolic flight campaign at least six months in advance to ensure free choice of flight date and location. At the very latest, an order must be submitted 12 weeks before the requested flight date.

8.5.2 On-Board Support

Well-trained safety personnel will be on-board the aircraft to support experimenters. When flying an experiment requiring extra support from Novespace safety personnel, this personnel will be included in the customer's totally available personnel seat count. The necessity of Novespace safety personnel will be decided upon during the safety review (one month before the flight) by attending safety experts. Please Note: a normal strapped-down experiment does not require extra safety personnel, but a free-floating experiment usually does.

8.5.3 Data Recording and Accelerometers

After the campaign, Novespace provides a set of data recorded during the flight which includes acceleration levels. On request, and if available, Novespace can also provide accelerometers which can be directly connected to the experiment equipment.

Experiment Timeline

- Two months prior to flight:
  - Provision of detailed documentation (hardware and procedures)
  - Provision of description, hazard analysis
- Six weeks prior to flight:
  - Security review

One week prior to flight:

  - Hardware reception at Bordeaux

- Hardware mounting and assembly
- Experimental ground testing

- One week to one day prior to flight:
  - Loading, bolting, and electrical connecting

- One day prior to flight:
  - Security visit

- **FLIGHT DAY(S)**

- Last flight day (afternoon) - unloading

8.5.4 Test Personnel Timeline

- Five years to three weeks prior to flight:
  - Hypobaric chamber test training

One year to three weeks prior to flight:

- Medical aptitude exam
- One month prior to flight:
  - Detailed information on each person flying

One week prior to flight:

- Parental authorization for personnel (if applicable)
- Waiver of liability signed by company and personnel

One day prior to flight :

- Pre-flight briefing

FLIGHT DAY(S)

Novespace will deliver, one month prior to flight, a precise schedule for the week before and the week of flights.

9 Appendix II

The following sections were selected form a technical guideline manual. Like the user manual in Appendix I, this document “GUIDELINES FOR EXPERIMENT DESIGN AND BUILDING”, is also available at the ESA Parabolic flight Campaign office.

-GUIDELINES FOR EXPERIMENT DESIGN AND BUILDING-

Table of Content

List of Figures

9.1 Experimental Area General Description Of A300 Zero-G

This section describes the experimental area inside the A300 ZERO-G. It provides the reader with information on cabin area and its setup.

9.1.1 Cabin overview

Cabin of the A300 ZERO-G is divided in 3 main parts:

- The front seats area
- The experimental area
- The back seats area

At the front of the cabin is the cockpit. Access to the aircraft is available through 6 doors, 2 at the front of the front seats area, 2 at the back of the same area and 2 at the rear of the back seats area.

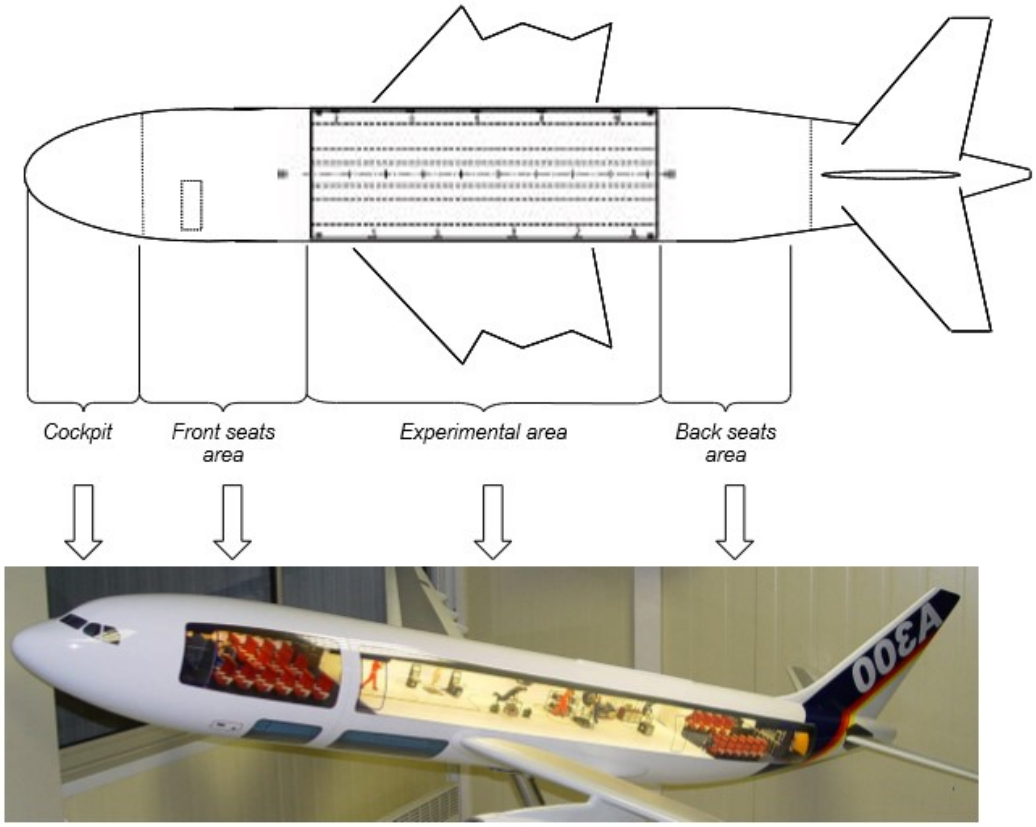

One of the 6 access doors is used to enter the experiments inside the aircraft, this door is generally the right one at the back of the front seat area.The maximum dimensions (projection on a flat plan) of this door are: Height: 1.93 m Width: 1.07 m

9.1.2 Experimental area presentation

The experimental area is 20 meters in length, 5 meters in width, and 2.3 meters in height. This is in this area, and only in this one, that the experiments can be performed.

Fig.1-2-1 Picture of experimental area with experiments

The experimental area is fitted with protection nets at the front and at the rear and is fully covered with foam paddings (i.e. the floor, the ceiling and the walls). This area is equipped with 10 electrical panels, 4 vent-line connections and fixation rails for experiments.

Fig.1-2-2 Experimental area

Fig.1-2-3 Exp. area w/o floor padding

The main dimensions of the experimental area section are detailed in the following schematic:

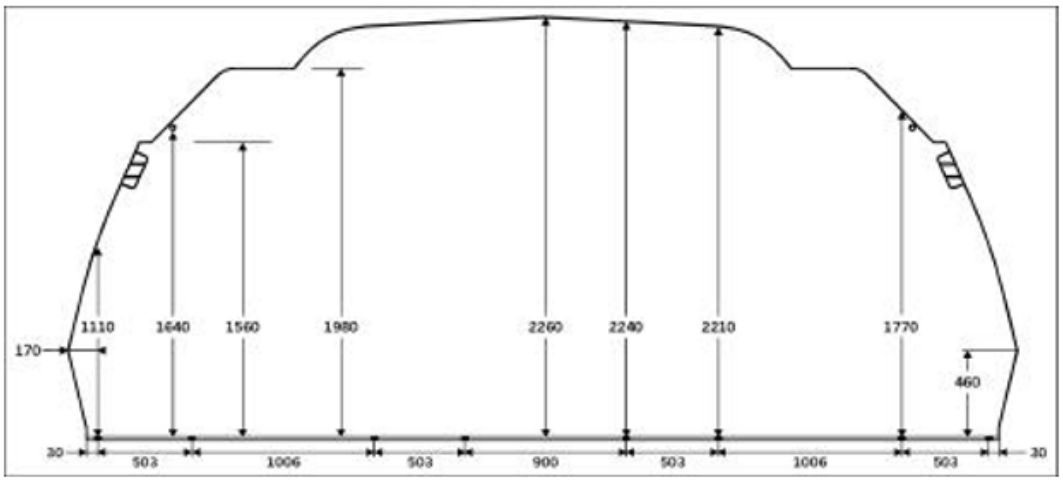

Fig.1-2-4 Cross section of aircraft cabin

All along this area on both sides is fixed a steel tube handle bar at the head level, another handle strap is fixed in the centre of the area at the ceiling level.

9.1.3 Environment

Cabin pressure is maintained at approximately 820mb from beginning to end of parabolic maneuvers. This pressure is obtained after 10 to 20 minutes after take-off. Normally, cabin temperature varies from 18 to 25 degrees Celsius in flight. The temperature in the cabin is not controlled while the airplane is on the ground.

9.1.4 Mechanical interfaces

Experiments are fixed in the experiment area using rails usually used to fix seats. These rails are in the longitudinal axis of the aircraft, and the distance between 2 rails is either 503 mm or 1006 mm.

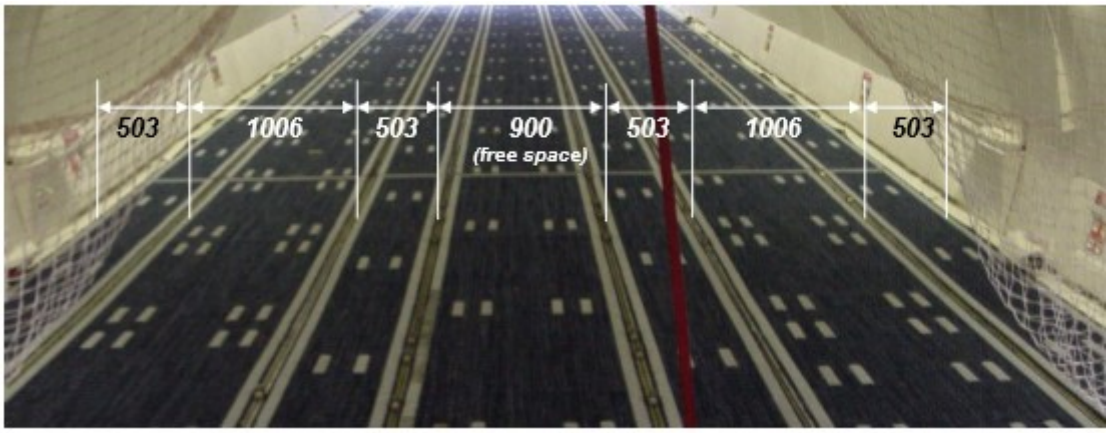

Fig.1-4-1 Picture with distance between fixation rails

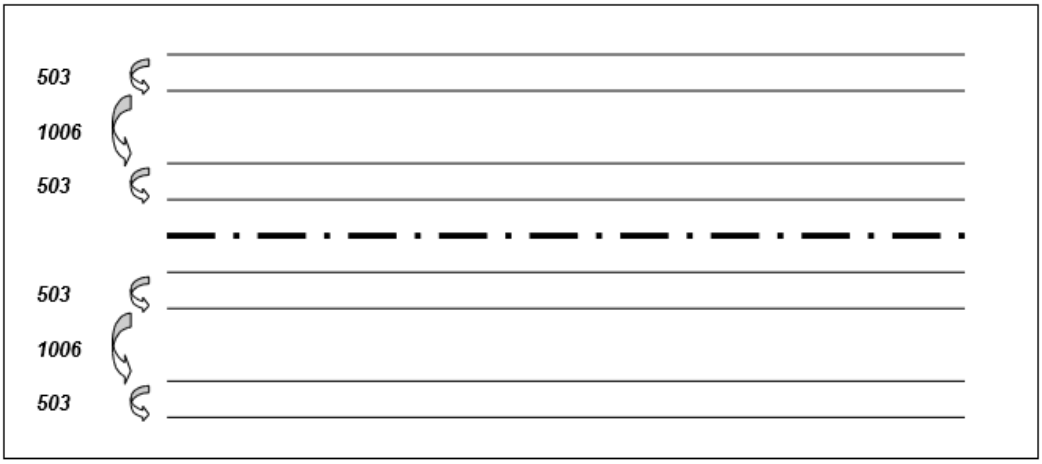

Fig.1-4-2 Top view of experimental area with distance between fixation rails

Steel blocks called “interfaces” are used between aircraft rails and experiments base plate. These interfaces are fixed on the rails with a pitch of 1’’ in the longitudinal axis (from the rear to the front of the cabin).

9.2 Experiment Design and Building: Advices and Rules

Requirements for 0g experiments in A300 ZERO-G are obviously different from those for laboratory experiments. This section presents operational and safety requirements and try to provide experimenters with some advice, rules and recommendations for designing and building an experiment. Most of recommendations are based on NOVESPACE experience. In following pages, advice on experiment design and building are there as general proposal covering 90% of experiment need. These are not strict rules but more good sense advice. Mainly, the experiment design should be based on experiment risk analysis. This important analysis, in addition to operational need, should drive the experiment design. Such risk analysis is introduced in NOVESPACE "User's Manual".
The sections dealing with mechanical and electrical parts are applicable to all experiments: 2.1 Mechanical constraints 2.2 Mechanical design and building 2.3 Electrical design and building
In the following section, the topics have to be selected upon needs. It presents most of systems commonly used in A300 ZERO-G. This section is not an exhaustive one. 2.4 Systems and specific design for experiment fitted with specific system, experimenters should contact NOVESPACE with an appropriate risk analysis.

9.2.1 Mechanical constraints

This section is dedicated to mechanical limitations. This topic is mainly the most specific to the A300 ZERO-G and has its own section.

9.2.2 Reference axis

Before to start with the description of the mechanical requirements, let us have a look on the aircraft reference axis.

Fig.2-1-1: aircraft reference axis

The aircraft reference system is not a direct one.

9.2.3 Structural requirements

As described in §1.3 all experiments are attached to the aircraft floor. Obviously, the requirements between an experiment into a laboratory and an aircraft are different. For instance, aircraft structure and equipment should be able to withstand the aircraft certification crash load. This rule is also applicable to experiment loaded in the A300 ZERO-G. Others limitations are also defined in this section (e.g. loads on the seats/experiments rails, material allowed aboard,….).

This section is summarising and explaining all mechanical limitations.

Crash loads

All experiment structure and item used for equipment fixation should be designed to withstand the following loads during take-off and landing:

X-axis	9g forward 1.5g backward
Y-axis	3g left or right
Z-axis	4.2g upward 7.3g downward

Fig.2-1-2: crash load for designing experiment

An analysis should demonstrate that the experiment structure and all item used for equipment fixation remain within the yield strength of every part. It means that the material, the shape and the strength of all structural items should be known.

• Flight loads

During parabolic flight, all experiments undergo twice -1.8g on Z-axis per parabola. The experiment should be able to withstand this acceleration repeated during all the flight.

• Linear loading on aircraft rails

EADS, manufacturer of A300 ZERO-G, has defined load limitations on seat/experiment rails. Rails, fixed to the floor along the aircraft X-axis, are used for the fixation of experiment.

The basic rule is that the maximum load on 1 linear meter (X-axis) should be less than 100 kg. In that case account should be taken of the experiment weight, number of fixation points, number of rails on which the experiment is attached and distance between fixation points on X-axis. For instance an experiment of 200kg (or up to 400kg), located on 2 rails, fixed with 4 fixation points should have a distance between fixation points on X-axis higher than 1m (equal or higher than 40 inches). This basic rule is only applicable for experiment with a Centre of Gravity (CoG) lesser than 670mm on Z-axis and a minimum distance of fixation points of 508mm (20 inches).

IMPORTANT NOTE: in this paragraph, when fixation point's distance is mentioned, the rail load rule applies to fixation points for a rack and between racks. For experiment, made of several racks, the loading rule and minimum distance between fixation points are also applicable between racks. So, whatever the number of racks, on one linear meter the weight on fixation points should be less than 100 kg.

Extension of the basic rules: - Experiment with a CoG > 670mm. In that case, the rail loading is decreased as shown below: RL < 67 000 / H Where, RL is the maximum authorised loading on 1 linear meter H is the height of CoG on Z-axis. And the distance between fixation points in the same rack and between all around racks should at least 508mm (20") - Experiment with fixation points distance less than 508mm (20"). In that case the rail loading is also decreased as shown below RL < 23 000 / H for fixation points distance between 8" and 20" RL < 8 733 / H for fixation points distance between 3" and 7" And the CoG should be less than 670mm.

If one criteria of the extension is not respected, then the basic rule should be applied.

Table summarising the maximum rail load: H (mm) (1) D (mm) (2)

H (mm) (1)	D (mm) (2)	maximum rail loading on 1 linear meter (kg)
<670	20" and more	<100 kg
<670	Between 8 and 20"	< 23 000 / H
<670	Between 3 and 7"	< 8 733 / H
>670	20" and more	67 000 / H

(1): represents the height of CoG on Z-axis.

(2): represents the distance between two adjoining fixation points on the same rack and between different racks.

• Maximal loads for each interface

There are also some loading limitations on interfaces used for fixing the experiment on the aircraft rails. Based on the crash load value, defined before, each interface should withstand a force lesser than:

Axis	Direction	Value (daN)
X	+ or -	2 250
Y	+ or -	900
Z	+	1 330
	-	1 750

maximum load on interface

Note: these loads are covered by linear loading and are there only for information

9.2.4 Mechanical design and building

This section introduces instructions and rules with regard to mechanical design and building. 2.2.1. Fixation base on aircraft interfaces This part is presenting the proper mean to attach an experiment to the aircraft floor.

The base of the experiment should be an Aluminium base plate with a thickness of 10mm. Fixation holes (min. of 4) should be drilled in it as mentioned below - The distance between fixation holes on Y-axis should be either 503 or 1006 mm. The choice of this distance should be agreed with NOVESPACE. - The distance between fixation holes on X-axis should be a multiple of one inch. Please refer to section

9.2.5 Structural requirements

(Linear loading) for determining the minimum distance between fixation holes The distances between fixation holes should have been carefully checked on the base plate. Important remark: Diagonals made by fixation holes should be equal.

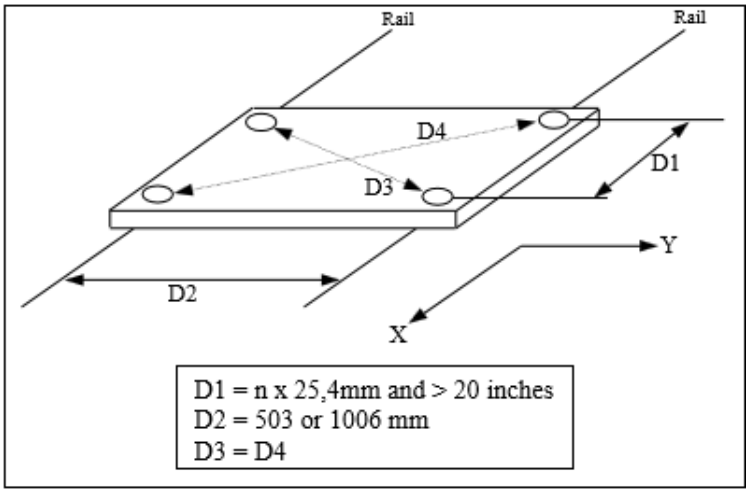

Fig.2-2-1: base plate and fixation holes

Each fixation hole should have a diameter of 12mm and without any tapping.

NOVESPACE will provide screws for fixing the base plate to aircraft interfaces and torque it as request by aircraft manufacturer.

For experiment using several racks, it is recommended to use several base plates.

Fig.2-2-2: multi-rack experiment

For light experiments, Aluminium or Steel bars could be used instead of base plate. But the bars (e.g. strut profiles, Al bars) should be able to withstand torque load (35 Nm). The use of wide washer is mandatory there to distribute the torque load on the bar and to avoid its bending. It is also possible to use a base plate with a thickness of 5mm but the experiment/rack weight should be below 50kg.

The second function of the base plate is to fix the experiment structure. The base plate is fixed on interface on rails. Between rails, the aircraft floor is fitted with padding. The base plate bottom should be completely flat as shown in the figure below. This is the only authorised way to attached structure or equipment on the base plate. The base should not incorporate thread!

9.2.6 Equipment fixing

The fixation of equipment is ruled by crash load conditions. All equipment should be able to withstand crash load in all main aircraft axis. Important note: equipment should not be stacked-up! For most of equipment (electrical equipment, acquisition unit, monitor, …), the following method is usually sufficient: the equipment is locked on X and Y-axis by Aluminium L-profiles. Then, the relative movement on Z-axis is stopped by using cloth straps. This straps should be able to withstand the load of the equipment weight under 9g acceleration.

Fig. 2-2-9: equipment fixation

The plate, where the equipment is set-up, should have two oblong holes for the strap. Oblong holes edge should be protected with tape to reduce friction between aluminium edge and the strap. Light equipment with weight less than 1kg could be attached to the structure using Tyraps (RS reference: 321-0086).

10 Specifications of rotatory chair for parabolic flight experiments

As part of the ESA Parabolic flight campaign hardware evaluation process, proposed experimental systems have to be examined. This technical specifications section created in cooperation with Dipl.-Phys. Franz Dankwart refers to the NYDIAK 500 rotary chair system of company EKIDA, and confirms its suitability for the proposed experiments.

To perform parabolic maneuvers an Airbus 300 aircraft has been modified for this purpose. The freight cabin – length 20m, width 5m, height 1,93 m (maximum height 2,3 m) is used as the test section where all experiments have to be set up.
A standard campaign consists of 3 flights of thirty parabolas on three consecutive days. Each parabola consists of a 1,8 g pull-up phase and a phase of "0" gravity. During the 0-gravity phase the remaining gravity is in the order of ± 0,05 g. The 0-gravity phase lasts for approx. 22 s, the time between two parabolic maneuvers is set to approx. 2 min. and the time between the 1,8 g and the 0-g-phase is less than 5 seconds.

10.1 Rotary chair

The rotary chair is used to investigate the behavior of the vestibular and related systems, which maintain the steady posture of the human body. During the parabolic flight, the rotary chair has to be ably to a constant speed of up to 90°/sec constant. The rotary chair is mounted on a tilting platform, which can tilt the rotary chair up to 20° in respect to the airplane's floor. Additionally to these requirements, the system has to be able to withstand the forces during take-off and landing as described in the paragraph structural requirements (see also "guidelines for experimental design and building"). In the following paragraphs, the specifications of the rotary chair are described according to these guidelines, and how these specifications can be met by the rotary chair system NYDIAK 500 which is manufactured by EKIDA GmbH, Helmstadt, Germany. A similar system has already been built for the university hospital in Maastricht, The Netherland. The only difference to the proposed parabolic flight system is the additional excenter on the Maastricht system (used for ex-centric stimulation to investigate the otolith system) and some modification as described below.

10.2 System setup

The required rotary chair consists of:

- rotary chair drive
- Seat incl. safety belt, head-fixation, etc.
- tilting platform
- control unit including PC and monitor

The rotary chair NYDIAK 500 meets the requirement, which are sketched above. The torque motor, which drives the chair, can generate more than 300 Nm continuous torque and up to 1100-peak torque. The maximum velocity is set to 500°/s. At this velocity, the motor can provide sufficient torque to compensate for load changes and maintain constant speed. However, it is possible to exceed 500°/s in cases where only small load changes are expected. During parabolic flights, major load changes will be experienced, but the required constant speeds of up to 90°/s can be easily maintained by the NYDIAK 500 system.

10.3 System height, weight, COG, power supply

a) Height

The head room in the aircraft's test section measures 2,28 m and 2,30 m in the centre respectively. The central area with 900mm width should be let as free as possible. Next to this, an area 503 mm wide is provided at each side. Here the headroom is still 2, 20 m. the following 1006 mm area can be used up to 1, 93 m.

The motor part of the rotary chair is approx. 65 cm high (from bottom of the motor part to the surface of the seat). The back of the seat adds another 80 cm and the tilting platform 20 cm. The total height therefore adds up to 1,65. Large test persons however can be larger than the back of the seat. Additionally we have to keep another 5 cm in mind, if the rotary chair is tilted. This would lead to the following calculation:

Total height = 30 cm + 40 cm * sin α+ 150 cm * cos α

where α = tilting angle,

40 cm = distance between hinge of the tilting platform and centre of the rotary chair,

150 cm = height of rotary chair measured from the top of the tilting platform to the test person's head, assuming the top of the test person's head is 15 cm above the seat' back.

The available 1,93 m is just sufficient for the chair's height. However it is recommended to mount the chair closer to the center of the test section, e.g. to the 503 mm rails, or even better right in the centre. This means that the rotary chair occupies the centre of this part of the aircraft's test section partly or even fully.

b) Weight

The rotary chair the tilting platform and the test person (100kg) weighs approx. 350 kg. The safety requirement during the parabolic maneuver demand a well-designed system, which provides the sufficient strength under loads (test person) of at least 100 kg (135 kg according to IEC requirements). During the 1,8 g phase the forces to the chair amount to 1800 N @ 100 kg. A safety factor of 2 is demanded according to IEC regulations. The drive, seat, tilting platform etc. have to be able to withstand these forces without any structural problems. In addition, the acceleration described in the paragraph, "structural requirements" have to be met.

c) Center of gravity (COG)

The COG should be below 67 cm. This is met as long as no test person is seated on the chair. The test person's COG lies just above his hip, i.e. it is approx. 1m above the floor when he is sitting on the rotary chair. This of course lifts the total COG of the system. Depending on the patient's weight, the total COG can rise above 67 cm; detailed calculations still have to be performed.

d) Power supply

The motor draws the major part of the system's power. Although the motor is a high efficiency device it still can draw up to 5 kW from the mains power. Under normal circumstances during a parabolic maneuver the power drawn will be much lower. If turbulent air can be expected which shakes the aircraft, the rotary chair system experiences higher peak g-forces and thus the motor has to draw higher peak power to compensate for the accelerating forces. To avoid unstable rotation of the chair, the power line should be able to deliver at least 5 kW.

10.4 Structural Requirements

Requirements:
X-axis: 9 g forward, 1,5 g backwards
Y-axis : ± 3 g
Z-axis: 4,2 g upwards, 7,3 g downwards

The rotary chair NYDIAK 500 needs to be slightly modified for these forces (seat flange, back of the seat and locks for upwards forces). The structural requirements apply to the take-off and landing phases of the aircraft. During these phases, the tilting platform has to be in 0° position. The rotary chair is locked and the test person has left the seat. If the test person remains seated on the rotary chair, the system would have to be able to withstand additional downward forces up to 7300 N. It is possible to fulfil this requirement but this would further increase the system's weight.

10.5 Regulatory Requirements

The manufacturer of the NYDIAK 500 system, EKIDA GmbH, fulfils the requirements of ISO 9001 and EN 14385. The rotary chair is CE-marked. The necessary modifications can be performed by EKIDA (total quality management system).

10.6 Summary

The NYDIAK 500 rotary chair system fulfils (after some modifications to the standard system) the required specifications. The above-mentioned restrictions (see structural requirements) must be followed and a suitable fixation of the equipment to the aircraft rails has to be worked out.

11 Collaborators and Supporters

Daniel Merfeld, Ph.D. / Boston, USA

Professor of Otology and Laryngology
Investigates sensory processing of motion cues and sensorimotor integration, with physiological and psychophysical measures as well as computational neuroscience techniques such as dynamic systems modeling.

Univ.-Prof. Dipl.-Ing. Dr.techn Eugen Gallasch / Graz, Austria

Professor of Physiology
Former Principle Investigator at the Austro-MIR Space Program.
Researches included Physiological tremors in different load conditions on the musculo-skeletal system. Ground studies and space studies on motor control.

Dr. Bernard Cohen / New York, USA

Professor of Neurology

Research on humans and primates in micro-gravity conditions.
Space Program with both NASA and the Russians. Effects of adaptation and habituation on the three-dimensional vestibulo-ocular reflex are determined in trained animals and humans.

Prof. Dr.-Ing. Stefan Glasauer / Munich, Germany

Professor of Sensorimotor Physiology

Modelling of 3D eye movements (VOR, pointing movements; in patients and in healthy subjects). Developed simulations of computational and mechanical processes.
Measurement of eye movements with video-based systems. Studies on microgravity influences on human balance system.

Prof. Laurence Young, / Boston, USA

Professor of Health Sciences and Technology

Research engineer and neuroscientist at the Massachusetts Institute of Technology in Boston. Co-founder of the Man Vehicle Laboratory in MIT's Center for Space Research. Studies of physiological and cognitive limitations of humans in aircraft and spacecraft.

Prof. Gilles Clément / Strasbourg, France

Professor of Space Life Sciences in International Space University (ISU), Strasbourg, France. Prior to this position, he was Director of Research from the French National Center for Scientific Research (CNRS), Toulouse, France. Research in space life sciences has been his primary focus with experiments on eye movements, spatial orientation, and cognition in humans.

Dr. Wim Bles/ Delft, **Netherlands**

Former Head Engineer, TNO
Research interests: Main topics of interest are motion sickness, spatial (dis)orientation, motion sickness and postural stabilization. TNO Human Factors develops knowledge that is focused on human behavior and performance in demanding environments.

Dr. Thomas Haslwanter/ Austria

UAR Austria /University Clinic Zürich /DLR
Design & development of 3D eye tracker (designated by NASA for the Intl Space Station) Vestibulo-ocular reflex and the control of eye-movements in three dimensions. Simulation of the underlying computational and mechanical processes. Measurement of eye movements with video-based systems. Perception of orientation and movement in space. (VOR, pointing movements; in patients and in healthy subjects)

Prof. Andrew H. Clarke / Berlin, Germany

Prof. of Biomedical Engineering

Former Director of the vestibular lab at the Benjamin Franklin Medical Center (UKBF) Research of the three-dimensional aspects of the vestibulo-oculomotor system. Vestibulo-oculomotor research in micro-gravity. Design & development of 3D eye tracker (designated by NASA for the Int. Space Station)